

The Synthesis of N-Containing Heterocyclic Compounds from Isocyanides using Continuous Flow Chemistry and Fluorous Technologies



By

Ashlie Butler

A thesis submitted to the University of Sheffield as partial fulfilment of the requirements for the degree of Doctor of Philosophy

Declaration

The work contained within this thesis was undertaken at the University of Sheffield between September 2010 and July 2014 under the supervision of Professor B. Chen. Unless specifically stated, all work was conducted by the author and has not been submitted, in whole or part, for any degree at any other educational institution.

Ashlie Butler (July 2014)
Department of Chemistry,
Dainton Building,
Brook Hill,
Sheffield,
S3 7HF.

Abstract

Continuous flow chemistry has garnered a great deal of interest since its conception in 1997. Since then the systems have been consistently improved with a number of research groups and pharmaceutical companies now embracing the technology. Fluorous solid phase extraction (F-SPE) allows for an ease of separation of products similar to solid-phase synthesis. The optimisation and combination of these two relatively novel technologies will allow for a more efficient drug development process.

The work in this thesis describes the synthesis of a novel fluorous isocyanoacetate derivative. The reaction conditions were optimised and the final product was found to have a yield of 23% over two steps. The low yield and instability of the final product led to the use of known fluorous benzaldehyde derivatives in further reactions.

The optimum continuous flow conditions, including residence time, reactor temperature, and catalyst loading, were determined for the multicomponent reaction (MCR) of benzaldehyde, Walborsky's reagent, and 2-aminopyrimidine. The conditions were found to be 10 mol% $ZrCl_4$ catalyst loading at 80 °C over 50 mins to give a 61% yield after isolation of the product. The product shows a mixture of isomers with the ratio of 2-amino isomer to the 3-amino isomer being 20:1 in favour of the 3-amino isomer. This is a vast improvement in the regioselectivity when compared to batch conditions, with the ratio being 5:1 in favour of the 3-amino isomer. A small library of compounds were synthesised and the regioselectivity was consistently in favour of the 3-amino isomer, in some cases the evidence for the synthesis of the 2-amino isomer could not be found. Yields ranged from 27-61% of the isolated products, including two products made from aliphatic aldehydes starting materials, which could not be synthesised under batch conditions in the same reaction.

The fluorous benzaldehyde derivative described above was used in the optimised conditions for the synthesis of 4-(3-(2,4,4-trimethylpentan-2-ylamino)imidazo[1,2-

a]pyrimidin-2-yl)phenyl perfluorooctane-1-sulfonate giving a yield of 64%. The regioselectivity remained high for the 3-amino isomer, with no characteristic evidence that the 2-amino isomer was formed under the conditions. The fluororous tag was successfully removed by a palladium catalysed cross-coupling reaction with thiophenol to give a product yield of 46% utilising microwave conditions.

The synthesis of 2-oxazolines was performed under continuous flow conditions. The conditions of the reaction were optimised and found to be 70 °C reactor temperature over 20 mins without the presence of a catalyst. A small library of 2-oxazolines was synthesised to determine the versatility of the conditions. Yields ranged from 67-86%. The diastereoselectivity for the *trans* isomer of the reaction was found to be comparable with those synthesised under batch conditions. The synthesis of the 2-oxazoline with the fluororous benzaldehyde derivative under the continuous flow conditions provided the product with a yield of 92% and a diastereoselectivity of *trans/cis* of 91/9. However, the fluororous tag was not successfully removed using palladium catalysed cross-coupling reactions or by a method using Cs₂CO₃.

The continuous flow synthesis of pyrroles using an adaption of the Barton-Zard method of pyrrole synthesis was optimised. The optimum conditions were found to be 70 °C over 10 mins. A small library of nitroalkenes were synthesised as starting materials for further continuous flow synthesis. The yields of the products ranged from 67-88%, including that of an aliphatic example. The small library of pyrroles was formed from the synthesised nitroalkenes and the yields ranged from 75-86%. This did not include the synthesis of a pyrrole using the aliphatic starting material. No product was found for this reaction. The synthesis of fluororous nitrostyrene derivative was tried using several methods. Most methods were unsuccessful. One method provided inconclusive ¹H NMR data, and so the crude mixture was used in the continuous flow conditions determined for pyrrole synthesis. The resulting reaction mixture showed no presence of the desired pyrrole determined by ¹H NMR spectroscopy and LC-MS.

Acknowledgements

There are a number of people I would like to thank for the time and patience that have allowed me to carry out this work.

Firstly I would like to thank Prof. Beining Chen for opportunity to read for this PhD and for her time and effort in helping me to complete the course.

It is best to start at the beginning and so I would like to acknowledge all the teachers at Lancaster Girls' Grammar School. In particular I would like to thank Miss Keogh whose enthusiasm for chemistry rubbed off and made me enjoy a subject I had previously barely noticed. Following the education theme, I would like to thank all the lecturers at the University of Sheffield for their help and guidance through my undergraduate and postgraduate studies.

A special thank you has to go to all the technicians in the chemistry department, particularly Harry Adams for working magic with quite terrible crystals, Rob Hanson for many hours of HPLC help, and Jenny Louth for sorting out so many things that had gone wrong.

Thank you to everyone who has read through parts of this thesis in their own time, namely, Dr. Claire Rye (also thank you for your wonderful cooking), Dr. Mark Thompson, Dr. Andrew Reeder, and, Dr. Simon Jones. You all have my eternal gratitude.

I would like to thank all members of the Chen group, both past and present. Dr. James Newby and Dr. Edd Rab deserve a special mention as without them I don't think I would have survived the first few months of postgraduate life. I definitely would not have survived postgraduate life without the help (both personal and technical) of Dr. Matthew Jackson. Introducing me to referencing software and captioning is genuinely the best thing anyone has ever done for me, and he makes a great brew.

The past and present members of the Harrity group also deserve acknowledgement for encouraging my attendance at their group problem sessions and for the help the sessions provided. Everyone in E26 over the years

has been great. I am really going to miss Friday evenings in Interval with you all. In particular, Dr. Matt Connolly for all the geeky chats, Party Steve for the reasons his name implies, and Andy Brown for letting me stay in his house for the last few weeks in Sheffield.

Everyone on E-floor of the Richard Roberts building has made my postgraduate studies enjoyable. Dr. Alexa Cleasby, Dr. Mat Pringle and Dr. Iain Barlow have listened to me moan over countless cups of tea and for that I am eternally grateful. Also thank you to Zeyed for providing so much comfort food.

Two further people in the chemistry department must be singled out. Ahmet Cankut has been my housemate and good friend throughout the entirety of my PhD. Thank you for the great cooking and countless entertaining evenings. Jonny Simmons, you know how much I'll be struggling to write all this but you have genuinely helped me get through the stress of the last few months and I can't thank you enough.

It is my genuine belief that my friends outside of chemistry are responsible for the keeping of my sanity. To all my friends through undergraduate life in Sheffield, thank you for making it so much fun that I wanted to stay a student forever. It is those I have known since school age that I am most grateful to. Zoe, Gen, Heather and Harriet, what on earth would I do without you all? Thanks for being such great friends for such a long time. And someone who has been around for even longer, Marc you don't know how grateful I am for everything.

The Barker family, Yasmin, Mike, and Freya, deserve a special mention for constantly reminding me that there is a life outside of science and a lot to look forward to. Plus the copious amounts of wine and Yorkshire Puddings are extremely appreciated. I promise they will be repaid when I am no longer a student.

Finally, most importantly, I would like to thank my family. My parents, brother and sister, without whom I would not have been able to get this far and have been amazing throughout. My grandparents and aunt have also done so much for me over the years and together, everything you have all done for me is greatly appreciated.

Abbreviations

9-BBN	9-Borabicyclo[3.3.1]nonane
ADME	Absorption, distribution, metabolism and excretion
CDI	Carbonyldiimidazole
CDTP	Candidate drug target profile
DBU	1,8-diazabicycloundec-7-ene
DCC	<i>N,N</i> -dicyclohexylcarbodiimide
DIPEA	<i>N,N</i> -diisopropylethylamine
DMA	<i>N,N</i> -dimethylaniline
DMAP	4-Dimethylaminopyridine
DMF	<i>N,N</i> -dimethylformamide
dppf	1,1'-Bis(diphenylphosphino)ferrocene
ee	Enantiomeric excess
EI	Electron ionisation
EOF	Electroosmotic flow
ES	Electrospray
EWG	Electron withdrawing group
FC-72	Perfluorohexane
FEP	Fluorinated ethylene propylene
F-HPLC	Fluorous high performance liquid chromatography
F-SPE	Fluorous solid phase extraction
FTI	Fluorous technologies inc.
^F TMSE-OH	Fluorous (trimethylsilyl)ethanol
GABA _A	γ-aminobutyric acid receptor
HPLC	High performance liquid chromatography
HRMS	High-resolution mass spectrometry
IR	Infrared
LC-MS	Liquid chromatography-mass spectrometry
MCR	Multi-component reaction
MS	Molecular sieves
NMO	<i>N</i> -methylmorpholine- <i>N</i> -oxide
NMR	Nuclear magnetic resonance

NOE	Nuclear overhauser effect
PEP	Prolyl endopeptidase
PFA	Perfluoroalkoxy alkane
PTFE	Polytetrafluoroethylene
PTSA	<i>p</i> -Toluenesulfonic acid
PyBOP	benzotriazol-1-yl-oxytripyrrolidinophosphonium hexafluorophosphate
R _f	Retardation factor
r-F-SPE	Reverse fluoruous solid phase extraction
SPE	Solid phase extraction
TBAF	Tetra-n-butylammonium fluoride
TBD	Triazabicyclodecane
TFA	Trifluoroacetic acid
THF	Tetrahydrofuran
TLC	Thin layer chromatography
TM	Transition metal
UV	Ultra violet

Contents

Abstract	1
Acknowledgements	3
Abbreviations.....	5
List of Schemes	11
List of Figures.....	14
List of Tables	16
1. Introduction.....	19
1.1 Drug Discovery and Development Process	19
1.2 Continuous Flow Chemistry	21
1.2.1 Development of continuous flow chemistry	23
1.2.2. Important reactions under continuous flow conditions.....	25
1.2.3 Advantages and Limitations.....	29
1.3 Fluorous Technologies	31
1.3.1 Fluorous Solid Phase Extraction (F-SPE)	32
1.3.2 Limitations and Technical Challenges.....	36
1.4 Isocyanides	39
1.4.1 Synthesis of Isocyanides	40
1.4.2 Multicomponent reactions of Isocyanides	41
1.4.3 Isocyanoacetate	42
1.4.4 Conclusion.....	44
1.5 Vapourtec R-Series Continuous Flow Reactors.	45
1.6 Project Aims.....	47
2. Fluorous Tags.....	51
2.1 Variations of Fluorous Tags	51
2.1.1 Thiol Tags.....	51
2.1.2 FluoMar TM	52
2.1.3 Fluorous (Trimethylsilyl)ethanol (^F TMSE-OH)	53
2.1.4 Alcohol Tags.....	55
2.2 Fluorous Tag Synthesis.....	58
2.3 Fluorous Tagged Isocyanoacetate Synthesis	64
2.3.1 Coupling Reaction of Fluorous Alcohol and <i>N</i> -Formyl Glycine	64

2.3.2	Coupling Reaction under Continuous Flow Conditions.....	67
2.3.3	Synthesis of the Isocyanide by Dehydration of the Fluorous Tagged <i>N</i> -formyl Ester.....	69
2.4	Synthesis of Fluorous Tagged Benzaldehyde.....	71
2.5	Conclusions.....	72
3.	Synthesis of Imidazo[1,2- <i>a</i>]pyrimidines.....	75
3.1	Introduction.....	75
3.2	Optimisation of Reaction Conditions.....	79
3.3	Library Synthesis.....	84
3.4	Use of Fluorous Technologies in Imidazopyrimidine Synthesis.....	87
3.5	Removal of the Fluorous Tag.....	89
3.6	Conclusions.....	90
4.	Synthesis of Oxazolines.....	93
4.1	Introduction.....	93
4.1.1	Uses of oxazolines.....	93
4.1.2	Base catalysed synthesis of oxazolines.....	94
4.1.3	Transition metal catalysed synthesis of oxazolines.....	96
4.2	Oxazoline Synthesis under batch conditions.....	99
4.3	Optimisation of continuous flow reaction conditions.....	101
4.4	Library Synthesis.....	105
4.5	Fluorous tagged oxazoline synthesis.....	107
4.6	Removal of the fluorous tag.....	109
4.7	Conclusions.....	111
5.	Synthesis of Pyrroles under continuous flow conditions.....	113
5.1	Introduction.....	113
5.1.1	Synthesis of pyrroles from isocyanoacetate derivatives.....	114
5.2	Pyrrole synthesis under continuous flow conditions.....	117
5.2.2	Nitrostyrene synthesis.....	120
5.2.3	Library synthesis.....	122
5.3	Fluorous tagged pyrrole synthesis.....	124
5.3.1	Fluorous nitrostyrene synthesis.....	124
5.3.2	Fluorous pyrrole synthesis.....	127
5.4	Conclusion.....	129
6.	Conclusions and future work.....	131

6.1 Chapter 2 conclusions.....	131
6.2 Chapter 3 conclusions.....	132
6.3 Chapter 4 conclusions.....	134
6.4 Chapter 5 conclusions.....	135
7. Experimental Data	139
7.1 Experimental Data for Chapter 2	140
7.2 Experimental Data for Chapter 3	146
7.3 Experimental Data for Chapter 4	158
7.4 Experimental Data for Chapter 5	163
References	169
Supplementary Data.....	177

List of Schemes

Scheme 1. The reaction of <i>p</i> -nitrobenzenediazonium tetrafluoroborate 1 and DMA 2	23
Scheme 2. The [2+2] photocycloaddition reaction of maleimide 4 and 1-hexyne.	24
Scheme 3. [5+2] photocycloadditions of maleimides.	25
Scheme 4. Multi-phase carbonylation under continuous flow conditions.	29
Scheme 5. Thermal allylations of aldehydes with a fluoros allylstannane.	33
Scheme 6. Allylations of perfluoroalkyl iodides.	35
Scheme 7. Two step reaction with reverse F-SPE purification.	35
Scheme 8. The synthesis of isocyanides using Burgess Reagent.	40
Scheme 9. Isocyanide formation by the dehydration of formamides under microwave conditions.	41
Scheme 10. The Passerini reaction.	42
Scheme 11. The Ugi reaction.	42
Scheme 12. The synthesis of 3-aminoimidazo[1,2- <i>a</i>]pyrimidines under continuous flow conditions.	47
Scheme 13. The synthesis of oxazolines under continuous flow conditions.	47
Scheme 14. Nitrostyrene synthesis followed by pyrrole formation under continuous flow conditions.	48
Scheme 15. Use of thiol fluoros tags in displacement reactions.	52
Scheme 16. The synthesis of FluoMar™.	52
Scheme 17. A scheme to show the peptide coupling performed using 3-(perfluorooctyl)propanol 60 as the fluoros tag component.	54
Scheme 18. Synthesis of fluoros (trimethylsilyl)ethanol.	55
Scheme 19. Fluoros synthesis of hydantoin and thiohydantoin.	56
Scheme 20. Microwave assisted fluoros synthesis of aryl sulfides.	57
Scheme 21. The synthesis of vinyl(dimethyl)(3-(perfluorooctyl)ethyl)silane 55 and allyl(dimethyl)(3-(perfluorooctyl)ethyl)silane 56	58
Scheme 22. The reaction of 1-iodo-1 <i>H</i> ,1 <i>H</i> ,2 <i>H</i> ,2 <i>H</i> -perfluorodecane with chloro(dimethyl)vinylsilane and allylchlorodimethylsilane to form the vinyl and allyl precursors.	59
Scheme 23. The general reaction scheme for the hydroboration and oxidative workup of vinyl(dimethyl)(3-(perfluorooctyl)ethyl)silane.	60
Scheme 24. Diol formation and subsequent diol cleavage to form the fluoros alcohol.	61
Scheme 25. The ozonolysis and subsequent reduction to form the alcohol fluoros tag.	62
Scheme 26. Peterson rearrangement ⁶⁰	63
Scheme 27. Formylation of glycine. ⁶¹	64

Scheme 28. The formylation of glycine followed by the coupling of <i>N</i> -formylglycine to the commercially available fluorous alcohol.....	66
Scheme 29. The proposed reaction scheme for the synthesis of <i>N</i> -formylglycine fluorous ester 87 from Fmoc-protected glycine.	67
Scheme 30. Coupling reaction of Fmoc protected glycine to fluorous alcohol. ..	68
Scheme 31. The synthesis of fluorous isocyanoacetate 79	70
Scheme 32. The synthesis of fluorous aldehyde.	71
Scheme 33. The synthesis of fluorous vanillin derivative 81	71
Scheme 34. The Groebke-Blackburn three-component approach to imidazo[1,2- <i>a</i>]pyrimidines.....	76
Scheme 35. Mechanistic rationale for the formation of a product mixture in the multicomponent reaction with 2-aminopyrimidine.	76
Scheme 36. Dimroth rearrangement to the thermodynamically stable product. .	77
Scheme 37. Reaction of 2-aminopyrimidine, benzaldehyde and Walborsky's reagent using 2.5 mol% of Sc(OTf) ₃ to form a mixture of isomers used to form the calibration curves for reaction optimization.	79
Scheme 38. The reaction of 2-aminopyrimidine, 4-chlorobenzaldehyde and Walborsky's reagent to form a mixture of isomers used to create calibration curves for the timed experiment.	80
Scheme 39. The continuous flow synthesis of fluorous tagged 4-(3-(2,4,4-trimethylpentan-2-ylamino)imidazo[1,2- <i>a</i>]pyrimidin-2-yl)phenyl perfluorooctane-1-sulfonate 103a	87
Scheme 40. The palladium cross coupling reaction of the fluorous tagged imidazopyrimidine and thiophenol.	89
Scheme 41. Base catalysed synthesis of 2-oxazolines.....	95
Scheme 42. The synthesis of <i>threo</i> -4,4,4-trichlorothreonine <i>via</i> oxazoline synthesis.....	95
Scheme 43. The synthesis of oxazolines using catalytic bases 119	96
Scheme 44. Transition metal catalysed reaction of isocyanoacetates and aldehydes to form oxazoline.	97
Scheme 45. Formation of oxazolines under Kirchner's conditions. ⁹⁴	99
Scheme 46. The reaction of 2-fluoro-6-chlorobenzaldehyde with ethyl isocyanoacetate to form the corresponding oxazoline.....	101
Scheme 47. The reaction of fluorous tagged vanillin derivative and ethyl isocyanoacetate to form a fluorous tagged oxazoline product under continuous flow conditions.	107
Scheme 48. Suzuki reaction of fluorous oxazoline under microwave conditions.	109
Scheme 49. Deprotection of the aryl sulfonate.	110
Scheme 50. Formation of pyrroles <i>via</i> the Michael adduct.....	115
Scheme 51. Reaction of isocyanoacetates with activated alkynes.....	115
Scheme 52. Barton-Zard synthesis of pyrroles.	116
Scheme 53. Pyrrole formation from <i>trans</i> -β-methyl-β-nitrostyrene with ethyl isocyanoacetate.....	117

Scheme 54. Synthesis of nitrostyrenes.	120
Scheme 55. The reaction cascade for the synthesis of (<i>E</i>)-1-(2-nitroprop-1-enyl)-3-methoxy-4-perfluorooctylsulfonyloxybenzene 166	124
Scheme 56. The attempted synthesis of (<i>E</i>)-1-(2-nitroprop-1-enyl)-3-methoxy-4-perfluorooctylsulfonyloxybenzene.	125
Scheme 57. Synthesis of (<i>E</i>)-2-nitroallylic alcohol.	126
Scheme 58. Synthesis of α -nitro acrylates and cinnamates.	126
Scheme 59. The synthesis of fluorous tagged pyrroles under continuous flow conditions.	127
Scheme 60. Functionalisation of the amino group to synthesise an extensive library using fluorous technologies and continuous flow conditions.	133
Scheme 61. Synthesis of β -hydroxyamino acid followed by the removal of the fluorous tag.	134

List of Figures

Figure 1. Modern drug discovery process ²	19
Figure 2. The Vapourtec R-Series system used for this project.	21
Figure 3. Schematic of the FEP flow reactor	24
Figure 4. Simplified schematic view of the O-Cube reactor. ¹¹	27
Figure 5. Gas-solid-liquid carbonylation system.	29
Figure 6. FluoroFlash®	34
Figure 7. Fluorous solid-phase extraction. Left: a standard fluororous solid-phase extraction; Right: reverse fluororous solid-phase extraction.	36
Figure 8. General resonance structures of isocyanides.	39
Figure 9. Reactivity profile of α -isocyanoacetate derivatives.	43
Figure 10. Pharmaceutically active compounds that can be synthesised from isocyanoacetate derivatives.	44
Figure 11. The Vapourtec R-Series system.	45
Figure 12. Schematic of Rheodyne valve.	45
Figure 13. General structure of fluororous tags where X is 17-25, Y is 8-12 and Z is the functional group used to attach the tag to the molecule of interest.	51
Figure 14. The fluororous analogue of Marshall Resin, FluoMar™	53
Figure 15. ^F TMSE-OH.	58
Figure 16. The commercially available 1 <i>H</i> ,1 <i>H</i> ,2 <i>H</i> ,2 <i>H</i> -perfluorodecan-1-ol	63
Figure 17. The effect of temperature and time on the coupling reaction.	66
Figure 18. A graph to show the trend between the varying concentrations of fluororous Fmoc glycine ester samples and the area under the peak obtain by HPLC.	68
Figure 19. Commonly seen fused imidazo-systems in pharmacological relevant ligands.	75
Figure 20. Examples of pharmaceutically viable candidates containing the imidazo[1,2- <i>a</i>]pyrimidine structure.	75
Figure 21. Yields of 2-phenyl- <i>N</i> -(2,4,4-trimethylpentan-2-yl)imidazo[1,2- <i>a</i>]pyrimidine-3-amine (91b) and 3-phenyl- <i>N</i> -(2,4,4-trimethylpentan-2-yl)imidazo[1,2- <i>a</i>]pyrimidin-2-amine (91a) with varying residence times at 70 °C using 10 mol% ZrCl ₄	79
Figure 22. Yields of 2-(4-chlorophenyl)- <i>N</i> -(2,4,4-trimethylpentan-2-yl)imidazo[1,2- <i>a</i>]pyrimidine-3-amine (93b) and 3-(4-chlorophenyl)- <i>N</i> -(2,4,4-trimethylpentan-2-yl)imidazo[1,2- <i>a</i>]pyrimidine-2-amine (93a) over time using traditional batch conditions and 10 mol% ZrCl ₄	81
Figure 23. A graph to show the yield of 2-phenyl- <i>N</i> -(2,4,4-trimethylpentan-2-yl)imidazo[1,2- <i>a</i>]pyrimidine-3-amine (91b) and 3-phenyl- <i>N</i> -(2,4,4-trimethylpentan-2-yl)imidazo[1,2- <i>a</i>]pyrimidin-2-amine (91a) with varying temperature using 50 mins residence time and 10 mol% ZrCl ₄	81

Figure 24. A graph to show the varying yield of 2-phenyl- <i>N</i> -(2,4,4-trimethylpentan-2-yl)imidazo[1,2- <i>a</i>]pyrimidine-3-amine (91b) and 3-phenyl- <i>N</i> -(2,4,4-trimethylpentan-2-yl)imidazo[1,2- <i>a</i>]pyrimidine-2-amine (91a) with varying Lewis acid catalyst and loadings under both batch and continuous flow conditions. Batch conditions; 45 °C for 24 hours. Continuous flow conditions; 80 °C for 50 mins.....	82
Figure 25. X-ray crystal structure of 98a for regioisomer assignment.	85
Figure 26. Isomers of the oxazoline heterocycle.	93
Figure 27. Antibiotics containing the β -hydroxyamino acid moiety.....	94
Figure 28. Ferrocenylphosphine ligand synthesised by Hayashi <i>et al.</i>	98
Figure 29. Calibration curve for oxazoline synthesis.	101
Figure 30. The optimisation of temperature under continuous flow conditions.	103
Figure 31. The optimisation of the residence time under continuous flow conditions.	104
Figure 32. Basic structure of pyrroles.....	113
Figure 33. Porphobilinogen.	113
Figure 34. Naturally occurring antibiotics containing the pyrrole moiety.	114
Figure 35. Calibration curve for pyrrole synthesis.	117
Figure 36. The yield of pyrrole formation over a variety of temperature at 5 mins residence time.	118
Figure 37. The yield of pyrrole formation with variation of residence time at 70 °C.	119
Figure 38. Mechanism of nitrostyrene synthesis <i>via</i> Henry reaction.	120

List of Tables

Table 1. Fluorination of 1,3-dicarbonyl substrates. ⁸	26
Table 2. Summary of the results obtained for the evaluation of Pd EnCat TM catalysed Suzuki cross-couplings, performed under batch and continuous flow conditions. Purity (%) shown in brackets with yield.	28
Table 3. The reagents and conditions used for hydroboration optimisation.....	60
Table 4. The coupling reagents used for the coupling of fluorous alcohol to <i>N</i> -formyl glycine.	64
Table 5. The varying molar ratios of reagents used for optimisation of the coupling reaction.....	65
Table 6. The reaction residence times and temperatures used to determine the optimum conditions for the coupling reaction of Fmoc protected glycine and fluorous alcohol.....	69
Table 7. Library of compounds synthesised by the continuous flow adaption of the Groebke-Blackburn reaction with 2-aminopyrimidine.	84
Table 8. Batch synthesis of oxazolines.	99
Table 9. The variation of products formed under the optimised continuous flow conditions and the yields obtained.	106
Table 10. The yields and products obtained in the synthesis of nitrostyrenes. .	121
Table 11. The yields of pyrroles synthesised under continuous flow conditions.	122
Table 12. Reagents used in nitrostyrene synthesis reaction.	125

1. Introduction

1.1 Drug Discovery and Development Process

The process of bringing a drug to market from an initial concept requires a great deal of time (12-14 years) and money (\$500 million to \$2 billion¹). The challenge is to reduce the time taken and cost of drug development without cutting any ethical and legal corners.

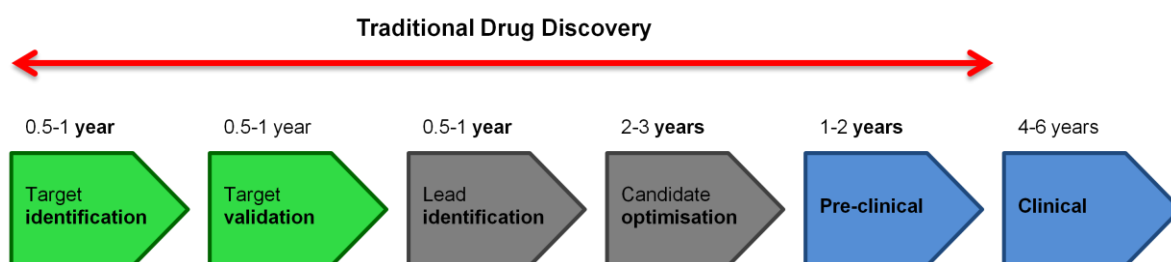


Figure 1. Modern drug discovery process²

The first stage of the drug discovery process is target identification during which specific biological targets are selected. Targets are proteins, either extracellular or intracellular, such as receptors, enzymes or transporter proteins. The second stage, target validation, is to provide experimental evidence of the relevance of the target for the disease in question. Primary and secondary screens are established to validate the selected target.³ A relevant biological assay containing tens or even hundreds of thousands of compounds is then screened for active compounds. The hits are assessed as part of the lead identification stage. The candidate optimisation phase is essentially the fine tuning of the molecule to the different parameters of the target profile using a clear structure-activity relationship and the examination of the compounds physical properties. The candidate drug target profile (CDTP) can be defined as, potency in animal disease models, *in vivo/in vitro* pharmacokinetic parameters (half-life, percentage absorbed, etc) and physical properties (solubility, molecular weight, etc.).³ The aim is to simultaneously optimise all the parameters in a single compound, the candidate drug.

Pre-clinical trials involve the testing of efficacy and toxicity in animal models. The pharmacodynamic, pharmacokinetic, ADME and toxicity data obtained allows the researchers to allometrically estimate the initial safe dosage of the drug for progression into human clinic trials. The clinical trials start with Phase I trial, where the drug is tested on healthy volunteers using a gradually increasing quantity of the drug to determine a well-tolerated dose and toxicity. The tests then progress to a small number of patients suffering from the condition in Phase II trial. Around 100-300 patients are given the candidate drug to establish an accurate dose for phase III clinical trials. Phase III involves the treatment of a large number of patients (300-3000) in multicentre trials. This phase often includes a double-blind experiment: neither the patient nor the physicians are told whether the drug or a placebo is used in treatment. A timeline of drug discovery and development process is shown in Figure 1.

The stages that are viable, both legally and ethically, for cost and time reductions are target identification through to candidate optimisation as well as the post launch scale-up. Essentially, focusing on the formation of the compound libraries is the best way to reduce the cost of the drug discovery process.

Organic synthesis generally consists of three main steps: reaction, separation, and analysis. The major problems with synthesis are low yields due to the formation of unwanted by-products through side reactions and the separation process as most products are in the same phase as the reactants. It is due to these problems that new methodologies have been developed. Optimising the yield of the reaction is of constant importance when discussing the reduction of cost (fewer starting materials wasted) in the drug discovery pipeline.

1.2 Continuous Flow Chemistry

A continuous flow system pumps reagents into a controlled reactor to produce a continuous supply of product. The pumps used are generally HPLC pumps as they are reliable and accurate as well as offering a large range of flow rates. The injection loops and the tubing inside the coiled reactor are made from inert substances such as glass, stainless steel and stable polymers. The reactors come in a number of varieties including; UV photochemical reactor, PFA coil reactor, column reactors for use with solid phase reagents and gas/liquid reactors. The casing of the reactor is an insulated glass manifold inside which heated or cooled air is circulated and the temperature measured therefore control is exceptionally accurate. The whole system is controlled manually or by the use of the appropriate computer software.



Figure 2. The Vapourtec R-Series system used for this project.

Solutions of reagents are pumped through separate tubes until coming into contact at a junction where the tubes meet. It is from this point where a reaction starts to take place in a continuous stream as opposed to a batch process. The

whole process occurs within a reactor where the pressure, temperature and residence time of the reaction can be precisely regulated.

In materials which are not solid there is a random movement of particles so that they become evenly spread over a specific volume. This is called Brownian motion. The time it takes a particle to travel, one-dimensionally, over a distance is directly proportional to the square of that distance.⁴ When the diffusion occurs over long distances the timescale is generally large enough so that it becomes negligible when considering mass transport. However, when mixing occurs on the micro-scale (such as within micro-reactors), diffusion has a significant impact on reaction timescales. The residence time (the amount of time the reagents are exposed to the reaction conditions, e.g. heating or cooling) is therefore generally less than the time required for the reaction to go to completion in large-scale batch conditions.

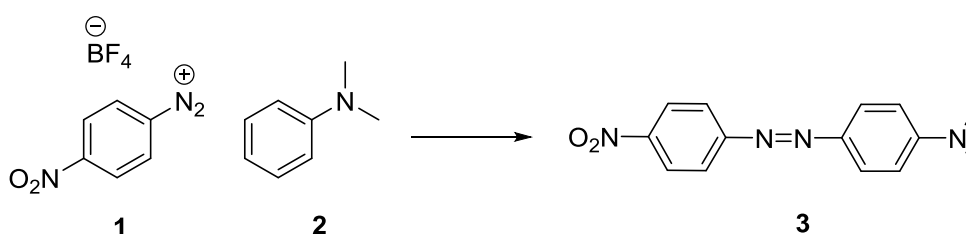
Further benefits of continuous flow chemistry can be derived from the high surface area to volume ratio of the reactor, which allows for precise control over reaction temperature as the heat can be easily applied or removed. The reaction temperature may also be raised above that of the boiling point of the solvent using back pressure regulators. This technique is therefore not only efficient, cost effective and safe, but also reduces the operator dependency as a standard operating procedure can be employed.

Continuous flow chemistry provides an efficient and practical solution for scale-up of organic reactions. In drug discovery and development processes, scale-up of a chemical reaction normally involves small scale laboratory optimised reactions (gram scale) being recreated in a pilot plant first (kilogram scale) and then transferred to a production plant (tons scale). However, a major flaw in this scale-up process is that each stage of the scale-up may require significant modifications to the original reaction, which tend to change the thermal and mass transportation properties of the reaction.⁵ This means that at each stage of production re-optimisation may be needed causing a time consuming and costly route to production where some products may fail to be formed at the industrial scale required. When a reaction is performed using flow technology the scale up

only involves operating multiple reactors in parallel and therefore reaction parameters remain unchanged, i.e. the same reaction conditions that are employed from small scale laboratory stage right through to the production stage. The risks and costs related to reaction transfer are largely mitigated.

1.2.1 Development of continuous flow chemistry

There has been a significant increase in the interest of performing reactions under continuous flow conditions since the revolutionary work of Harrison *et al.* in 1997.⁶ The work describes an organic phase reaction *p*-nitrobenzenediazonium tetrafluoroborate (**1**) and *N,N*-dimethylaniline (DMA, **2**) (Scheme 1) in a microfabricated glass chip, with fluid pumping and control driven by electroosmotic flow (EOF).⁶ The reaction was carried out in both a protic solvent (methanol) and an aprotic solvent (acetonitrile). The authors chose a reaction that was relatively fast and produced a product that could be monitored by absorbance detection. The detector was placed 5 mm from the reaction mixing point which was determined to give a reaction time of 4.1 s for methanol and 2.4 s for acetonitrile. The relative reaction efficiency was shown to be 22% and 37 % in acetonitrile and methanol respectively on-chip when the absorbencies were compared to a reaction time of 10 mins off-chip.



Scheme 1. The reaction of *p*-nitrobenzenediazonium tetrafluoroborate **1** and DMA **2**.

The microreactor technology has been advanced since this point to the development of continuous flow reactors. The aim of the development of continuous flow chemistry was to make microfluidics more amenable for organic chemists, who at this stage had not fully embraced the technology. In 2005, Booker-Milburn *et al.*⁷ developed a flow reactor for continuous organic

photochemistry. Prior to the work by this group photochemistry was generally not used for large scale synthesis due to limitations in irradiation. The authors devised a system (Figure 3) powered by conventional HPLC pumps, where the flow rate controlled the reaction time. The reagents were carried through a UV-transparent polymer, fluorinated ethylenepropylene (FEP), which was wound around a water immersion well.

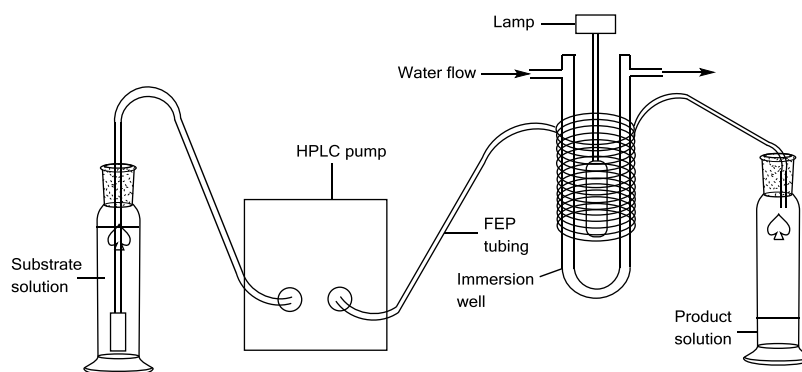
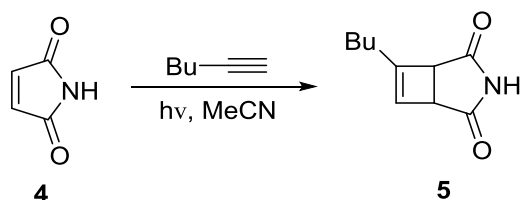


Figure 3. Schematic of the FEP flow reactor

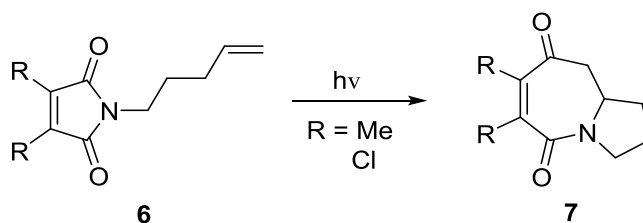
The group demonstrated the utility of the system by performing the [2+2] photocycloaddition reaction of maleimide **4** and 1-hexyne to form the cyclobutene **5** (Scheme 2). After optimisation of the flow rate and concentration the authors found that complete conversion occurred at 0.1 M and 2 mL/min.



Scheme 2. The [2+2] photocycloaddition reaction of maleimide **4** and 1-hexyne.

The [5+2] intermolecular photocycloaddition of maleimides was also demonstrated by this technology (Scheme 3).⁷ The reaction is carried out in batch processes as a step in the total synthesis of *Stemona alkaloids* giving a yield of 66% over 30 mins of irradiation with a 125 W lamp. Degradation of the product results in a drop in yield if further irradiation is performed and only allows the production of 0.5-1 g of batch product. Using the system shown in Figure 3 at

a maximum flow rate of 10 mL/min and a concentration of 0.02 M afforded a 67% yield of isolated chloro substituted product and therefore a 24 h yield of 45 g of product. The methyl substituted product was obtained in a yield of 79 % at a concentration of 0.1 M and therefore producing 44 g over 24 h.



Scheme 3. [5+2] photocycloadditions of maleimides.

1.2.2. Important reactions under continuous flow conditions

Gases employed in synthetic reactions are generally toxic, corrosive or explosive and therefore it is common for reactions using gases as reagents to be avoided if possible in industrial scale chemistry. When carefully designed, micro fluidic systems allow the addition and manipulation of gaseous streams to be thoroughly controlled and therefore drastically reduce the risk involved so that these reactions can be adopted in industrial production.

Many commercially important pharmaceuticals and plant-protection agents owe their biological activity to the presence of a single fluorine substituent.^{8,9} This has promoted an increase in the interest of small molecules containing one or more fluorine substituents and their syntheses. Chambers *et al.*⁸ used a thin film nickel reactor to perform fluorination on several 1,3-dicarbonyl compounds (Table 1). The results showed high regioselectivity where the 1,3-dicarbonyl compounds can be selectively synthesised to produce the compound containing a single fluorine atom with only small amounts of bi-fluorinated by-products observed. The group also reported the fluorination of toluene and ethyl 2-chloroacetate, again demonstrating excellent control over conversion and regioselectivity to the mono-fluorinated compound.¹⁰

Table 1. Fluorination of 1,3-dicarbonyl substrates.⁸

Entry	R ₁	R ₂	R ₃	Yield (%)			Conversion (%)
				9	10	11	
a	OEt	H	CH ₃	71	12	3	98
b	OEt	CH ₃	CH ₃	49	11	-	52
c	-OCH ₂ CH ₂ -		CH ₃	95	4	-	66
d	-(CH ₂) ₄ -		CH ₃	78	9	-	93
e	-(CH ₂) ₄ -		OEt	76	-	na	86

A more recent use of gas-liquid reactions under continuous flow is the use of an O-Cube reactor to perform several types of important ozonolysis reactions which introduce oxygen-containing groups (alcohols, ketones, etc) to a molecule by the cleavage of a carbon-carbon double bond. Ozone is a toxic and metal corrosive gas which, when reacting with an alkene produces the potentially explosive intermediate, ozonide. This means that the current ozonolysis technologies have several safety issues leading to the technique being avoided when it is actually the faster and cleaner method for production of these types of products. The set up consists of an O₂ cylinder feeding an inbuilt O₃ generator with a maximum flow rate of 20 mL/min which is then passed through a polytetrafluoroethylene (PTFE) frit where it can mix with reagent A. The PTFE tubing is wrapped around a refrigeration unit to keep the substrate cool while it mixes with the O₃. The quenching reagent is then pumped into the mixer with the ozonide to form the product. The O-Cube reactor (Figure 4) ensures that there is only a small amount of ozonide generated and is continuously quenched. As with all continuous flow reactors the temperature is more easily controlled and therefore reduces the risk of any explosions. This technique allows safe and scalable ozonolysis reactions to be performed on a laboratory scale.¹¹

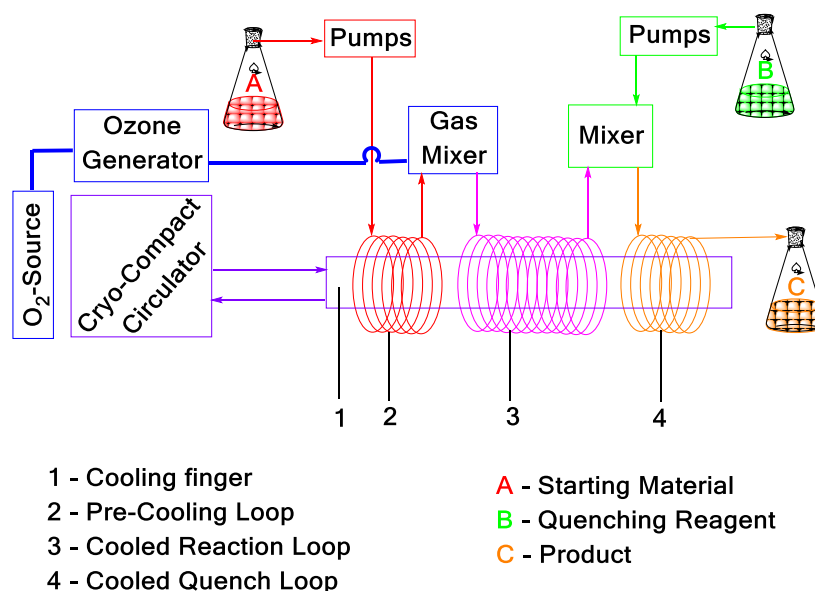
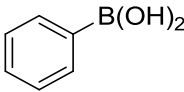
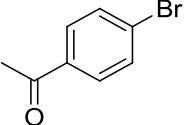
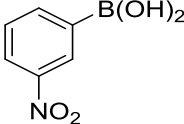
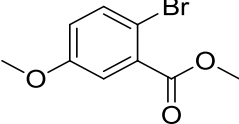
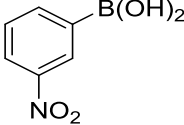
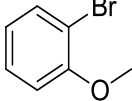
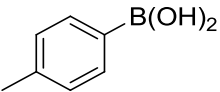
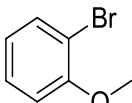
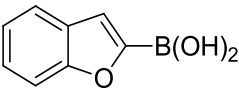
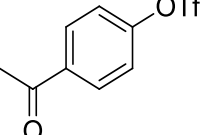


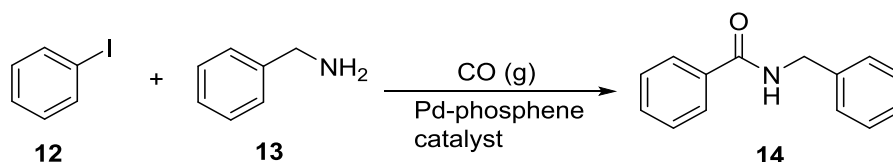
Figure 4. Simplified schematic view of the O-Cube reactor.¹¹

In addition to enhancing the reaction yields, regio/stereo selectivities^{8,12} and shortening the reaction time, reactions under flow conditions can greatly improve the reaction workups and product purifications when solid supported reagents and catalysts are used. Ley *et al.*¹³ performed microwave-assisted Suzuki cross-coupling under batch and continuous flow conditions. A U-tube flow reactor packed with microencapsulated palladium (Pd EnCat™) was placed in a microwave cavity. Aryl halide/triflate (0.07 M), boronic acid (0.07 M) and tetrabutylammonium acetate (0.14 M) were pumped through the reactor and irradiated at 50 W. After a 65 s residence time the reaction products were passed through a scavenging column to remove any excess boronic acid and tetrabutylammonium acetate. As shown in Table 2 the authors obtained an improvement in yield for most of the reactions and an increase (often exceptional) in purity in all of the reactions when performed under continuous flow conditions. Both entries **c** and **e** in Table 2 show a slight, almost negligible, decrease in yield yet a dramatic increase in purity of the product, from 54% to 92% and 30% to 91% respectively.

Table 2. Summary of the results obtained for the evaluation of Pd EnCat™ catalysed Suzuki cross-couplings, performed under batch and continuous flow conditions. Purity (%) shown in brackets with yield.

Entry	Boronic Acid	Aryl halide/triflate	% yield (% purity)	
			Batch	Flow
a			88 (98)	90 (98)
b			94 (64)	94 (98)
c			94 (54)	92 (92)
d			77 (40)	88 (94)
e			100 (30)	97 (91)

The work of de Mello *et al.*¹⁴ investigated the gas-liquid-solid reaction involving the carbonylation of an aryl halide (**12**, Scheme 4), amine (**13**) and carbon monoxide gas. The reaction was performed over a silica supported Pd catalyst which was incorporated into the fluidic system. A solution of the aryl halide and amine was mixed with the carbon monoxide gas and was then passed over the packed-bed of catalyst in the reactor. The system was maintained at 75 °C with a residence time of 12 mins as the optimal conditions. With this approach it was reported that six benzamide derivatives were synthesised. The substituted aryl halide used affected the reaction yields which ranged from 23-99%. The benzamide derivative shown in Scheme 4 (N-benzylbenzamide **14**) is formed with 46 % yield when a homogeneous catalyst is employed. However, when gas-solid-liquid continuous flow reaction conditions are employed there is an improved yield of 63%. After 18 reactions were performed there was no reduction in catalytic activity.



Scheme 4. Multi-phase carbonylation under continuous flow conditions.

As an extension of their previous work de Mello *et al.*¹⁵ investigated the incorporation of ^{11}C into the benzamide products by the on-line generation of ^{11}CO . The half life of ^{11}C is 20 mins and therefore classical batch process, taking several half lives of the species to reach completion, is known to have difficulties. However, when incorporating the system shown in Figure 5, the radiochemical yields were vastly improved, with the range of radiochemical yields being 33-79%.

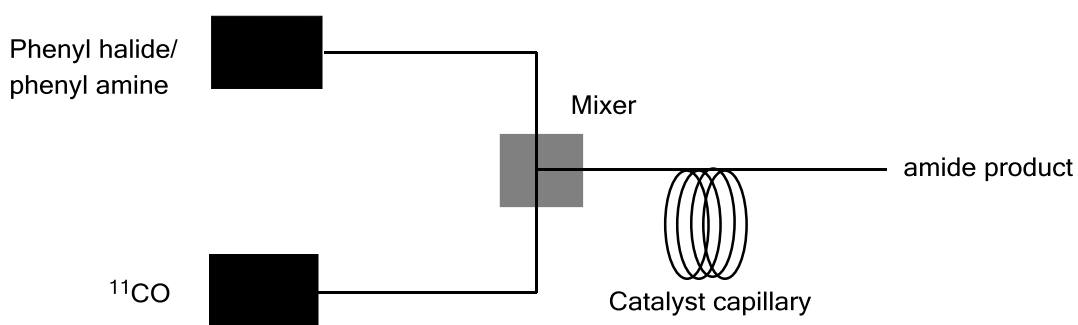


Figure 5. Gas-solid-liquid carbonylation system.

1.2.3 Advantages and Limitations

In conclusion, it has been shown by the various examples reported above that continuous flow reactors have led to a significant improvement in yield of reactions as well as improving the conditions under which the reactions are performed. The improvements in safety as well as the ease of scale-up make this technique a source of great interest. However, not all chemical reactions are suitable for continuous flow reactors. The main limitation for reactions being performed under continuous flow conditions is the relative insolubility of products and the formation of precipitates during the reaction. This means the product or side products can precipitate out of solution and cause blockages within the reactor. When the reaction is transferred from batch to continuous flow, solvent

suitability studies are required to ensure no blockages are formed. This can lead to different reaction conditions being employed in each case; hence it is recommended that all reactions are carried out using flow reactors from the start of the chemistry to save research efforts from transferring from batch conditions to flow ones. The rate at which reactions can be optimised is limited by the throughput of the analytical instrumentation employed to characterise a given process.⁵ Further development of on-line analytics can reduce this problem and allow for mainstream use of parallel flow reactors.

As with all issues in process development, headway is already being made for solutions to these issues. A number of groups have reported the use of ultrasonification¹⁶ or pulsed agitation¹⁷ to prevent the build-up of precipitates within the system; however, this does not work in every case. Also there have been several reported specifically engineered reactors that are targeted towards a particular synthesis problem. The Ley group recognised the need for a more general approach to the problem of blockages within the system and so they employed the use of the Coflore[®] agitating cell reactor (ACR) developed by AM technology. The reactor features a reaction block mounted on a laterally shaking motor.¹⁸ The reaction used was the formation of the hydroiodide salt of N-iodomorpholine by reaction of morpholine with iodine as it was known to rapidly produce a suspension when the two input streams mix. The yields produced using this method were found to be comparable with those produced by a batch process. The work concluded that the ACR opens up the opportunities for processing the slurries and solid precipitates under flow conditions.

With the development of further technologies and the increase in interest of continuous flow systems by companies such as BP, Pfizer and Glaxo Smith Kline the scope of this chemistry can only increase. The combination of continuous flow chemistry with ease of purification techniques could change the design of medicinal chemistry in the future.

1.3 Fluorous Technologies

Product separation has always been a bottleneck for conventional solution-phase batch synthesis and so methods such as resin-based solid-phase combinatorial synthesis and polymer-assisted solution-phase parallel synthesis have been increasingly employed. Fluorous technologies have been developed using fluorous alkyl chains incorporated into reagents or catalysts and fluorous solid phase extraction (F-SPE) which allow for the kinetic efficiency of solution-phase chemistry and the ease of separation of solid-phase chemistry to be combined, resulting in the ease of product separation.

Compared to solid-phase synthesis and solution-phase synthesis, fluorous synthesis has several unique features.¹⁹ Fluorous molecules can be separated by traditional methods such as chromatography and recrystallisation, as well as fluorous techniques such as fluorous solid-phase extraction. Fluorous reactions can be monitored by analytical methods such as NMR, IR, and TLC in the same manner as non-fluorous solution-phase synthesis. Reaction conditions employed in the absence of fluorous tags can be used with little or no modification. Unlike conventional solid phase support, molecules with fluorous tags are normally as soluble as their non-tagged parents. Reactions using fluorous tags are homogeneous reactions and have favourable reaction kinetics. Fluorous tags are chemically inert so they have a minimal effect on the reactivity of the molecule and are chemically stable. 'Light fluorous' molecules (17 fluorine atoms or less present in the molecule) are equally soluble in organic solvents and 'heavy fluorous' molecules (more than 17 fluorine atoms present in the molecule) can become soluble in organic solvents upon the addition of heat. The fluorous materials used can often be recovered after the fluorous separation.

During the early 1990's Zhu studied the synthetic benefits of using fluorous solvents, such as perfluoromethylcyclohexane and perfluorohexane, due to their miscibility with organic solvents at elevated temperatures.²⁰ Following this work, Horvath and Rabai investigated a fluorous biphasic system for the recovery of catalysts. They used a rhodium catalyst for the hydroformylation of alkenes and were able to extract the catalyst using phosphine ligands that were compatible

with a fluororous based biphasic system.²¹ The 'light fluororous' technique was developed by the Curran group and Fluororous Technologies, Inc. (FTI). The group used fluororous synthesis in nitrile oxide cycloadditions to fluororous labelled derivatives (silyl esters) of simple unsaturated alcohols such as allyl alcohol.²² Also performed were the Ugi and Biginelli reactions.

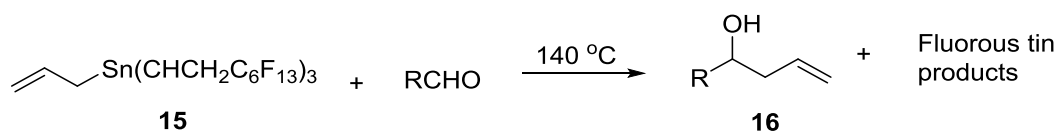
The presence of functionalised perfluoroalkyl groups within the reagents, scavengers, catalysts or substrates facilitate the process of separation in single-step reactions. For multi-step reactions fluororous tags or fluororous protecting groups can be used. Early work with fluororous tags relied on 'heavy fluororous' moieties, defined as more than 60% of fluorine by molecular weight, which underwent liquid-liquid extraction using (expensive) fluororous solvents. These solvents are primarily perfluorocarbons or perfluoroalkyl alkyl ethers. More recently, 'light fluororous' tags have been used in organic synthesis as no fluororous solvents are needed. This is due to the shorter fluororous chains (C_3F_7 to $C_{10}F_{21}$) being soluble in organic solvent reaction mediums and the development of separation techniques using 'light fluororous' tags performed using fluororous solid phase extraction (F-SPE) or fluororous high performance liquid chromatography (F-HPLC).

1.3.1 Fluororous Solid Phase Extraction (F-SPE)

F-SPE is a reliable separation technique that resembles more a filtration than a chromatographic technique.²³ The polarity of the molecule does not control the separation as with conventional chromatography, instead it depends solely on the presence or absence of a fluororous tag. There are two classes of F-SPE called standard or reverse F-SPE. The standard solid-phase extraction is much more common and involves the partitioning between a fluororous solid phase and a fluorophobic liquid phase.²⁴ The relatively novel reverse F-SPE is the opposite to standard F-SPE, i.e. it uses a fluorophobic solid phase and a fluororous liquid phase.

Standard F-SPE

The standard F-SPE method was introduced by Curran *et al.*²⁵ using a fluorous reverse phase silica gel column which selectively retains molecules containing fluorous groups when organic solvents are used to elute the column. The column can then be flushed using a fluorophilic solvent to remove the fluorous fraction. Thermal allylation of aldehydes with a fluorous allylstannane **15** was performed (Scheme 5). The crude reaction mixture was loaded onto the fluorous reverse phase silica gel and eluted with acetonitrile. This yielded the organic products of the reaction (**16**) with comparable yields and purities to the liquid-liquid phase extraction. The column was then eluted with hexane (a fluorophilic organic solvent) and evaporated to yield the fluorous fractions. The yields ranged from 55-98% crude yield (purities 83-94%) when using liquid-liquid extraction compared to 40-88% isolated yield for the method using F-SPE.



Scheme 5. Thermal allylations of aldehydes with a fluorous allylstannane.

It was found that in some cases hexane was not a strong enough eluent to remove all fluorous fractions quickly and so other solvents such as dry MeOH or THF are now more commonly used. The fluorophobic solvent was also altered to ensure all organic fractions are removed from the crude material. The organic materials move at the solvent front in the following systems: 70-80% MeOH/H₂O, 50-60% CH₃CN/H₂O or DMSO.

The fluorous solid phase extraction kit, FluoroFlash[®] (Figure 6), is commercially available from FTI and is a silica gel with a fluorocarbon bonded phase. FluoroFlash[®] SPE silica gel requires the use of either light positive pressure or light negative pressure as the particle sizes are between 40-60 μm.

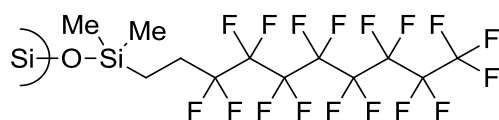


Figure 6. FluoroFlash®

An example of a typical F-SPE separation procedure is as follows:²⁶

Step 1 - Wash the new cartridge: Wash a new cartridge with 1 mL of DMF (or other loading solvent) under a vacuum or positive pressure depending on your SPE manifold. This step can be omitted with recycled cartridges.

Step 2 - Preconditioning: Pass through 6 mL of 80:20 MeOH: H₂O to condition the cartridge. Discard the preconditioning eluent.

Step 3 - Sample loading: Dissolve sample (100-300 mg) in 0.5 mL of DMF and load onto the cartridge using vacuum or positive pressure to ensure that the sample is completely adsorbed onto the cartridge.

Step 4 – Fluorophobic elution: Wash with 6-8 mL of 80:20 MeOH: H₂O to obtain the fraction containing the organic compounds.

Step 5 – Fluorophilic elution: Wash with 8 mL of MeOH to obtain the fraction containing the fluoruous compounds.

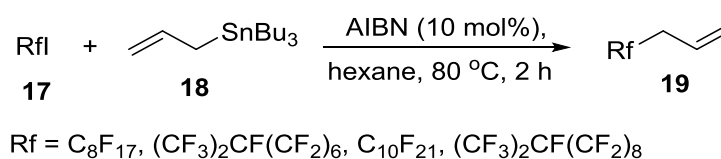
Step 6 – Regenerate the cartridge: To regenerate the SPE cartridge, wash with 6-10 mL of THF or acetone before reuse.

Reverse F-SPE

As suggested by the name, the usual roles of the solid phase and liquid phase are reversed in this method of separation. The mixture of organic and fluoruous molecules are loaded onto a polar solid phase material (standard silica gel is commonly used). The first elution is performed with a fluoruous solvent to elute the molecules containing the fluoruous tag or protecting group. The organic fraction is now left at the start of the column. The second liquid phase elution is performed using a suitable organic solvent to remove the organic fraction.

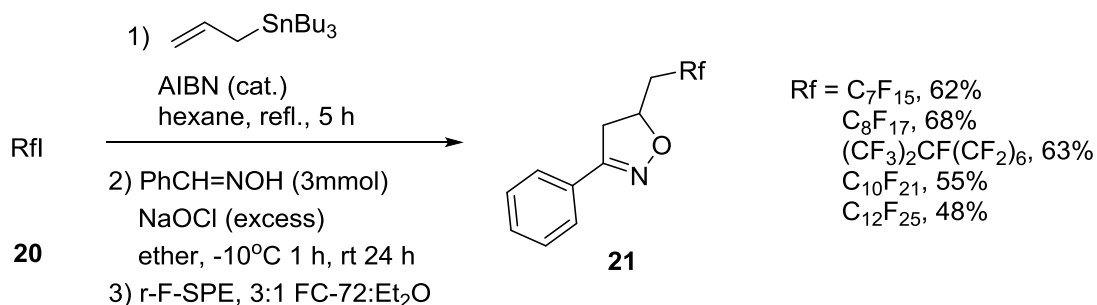
This method was introduced by Curran *et al.*²⁷ in 2004 and due to the recent nature of the technique there are limited examples and references demonstrating its use. In the past, fluoruous solvents had rarely been used in chromatography so

simple TLC experiments were run first to ensure the pairing of fluoruous solvent and polar solid phase was sufficient for separation. After testing numerous systems they found that to obtain the best separation (measured by R_f values) mixtures of FC-72:Et₂O or FC-72:hexafluoro-2-propanol were to be used (FC-72 is perfluorohexane, a derivative of hexane with all hydrogen atoms replaced with fluorine atoms, C₆F₁₄). The separations of fluoruous esters were found to be improved using this method as opposed to standard F-SPE. The group then performed a set of reactions similar to the work of Ryu *et al*²⁸ who described the allylation of perfluoroalkyl iodides (RfI, **17**) with allyl stannanes **18** to provide allyl perfluoroalkanes **19** (Scheme 6) and separated the products using standard F-SPE.



Scheme 6. Allylations of perfluoroalkyl iodides

After performing the same reaction under the same conditions Curran *et al.* separated the products from the side products using reverse F-SPE instead.²⁷ Yields ranged from 69-97% and purities were above 90% in all cases. The products were then used to synthesise isoxazolines (Scheme 7) and once again the products were purified utilising the reverse F-SPE technique. The yields over the two steps ranged between 48-68 %.



Scheme 7. Two step reaction with reverse F-SPE purification.

This technique is especially useful when the product of the reaction is the fluorinated compound. Also there is a reduction in cost due to the use of regular silica gel as opposed to the commercial FluoroFlash[®] and the fluorinated solvents used in the extraction can be reused. There is evidence that this method is useful for smaller fluorinated tags which have previously been deemed too small for standard F-SPE, such as the tag C₄F₉. Figure 7 shows the difference between standard and reverse F-SPE.

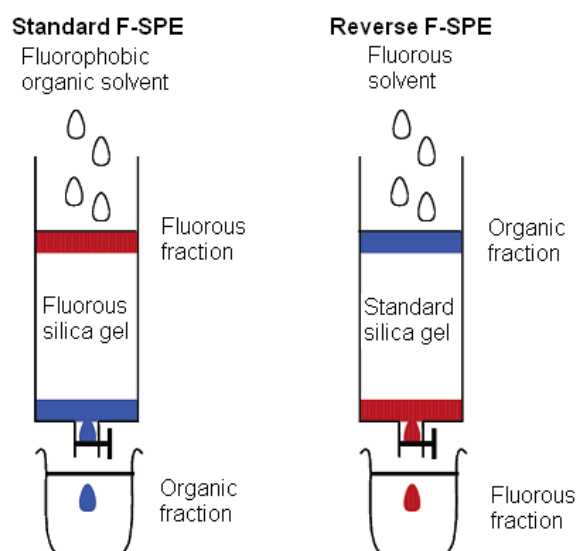


Figure 7. Fluorinated solid-phase extraction. Left: a standard fluorinated solid-phase extraction; Right: reverse fluorinated solid-phase extraction.

1.3.2 Limitations and Technical Challenges

In summary, fluorinated synthesis has the advantages of solution-phase synthesis and solid-phase synthesis with fewer of the disadvantages. In recent years there has been a vast increase in interest of using fluorinated chemistry for the development of compound libraries for drug discovery. With further development of the technique it will soon be a powerful tool for organic synthesis. The only drawback is the expense created by the separation techniques. Standard F-SPE requires FluoroFlash[®] cartridges which are expensive, however they can be reused and so the cost can be spread over a substantial period of time. Reverse F-SPE requires fluorinated solvents which are notoriously more expensive than

organic solvents. The ease of separation compared to traditional methods is, in some cases, worth the cost.

There is also a limitation to the efficiency of the method of F-SPE. The limiting reagent of the reaction must be the fluoros starting material and it must be fully consumed in the reaction or further separation techniques will be required. As stated above, F-SPE relies only on the presence of a perfluorocarbon chain and so it does not separate a mixture of fluoros compounds including isomers.

There are several issues with the standard F-SPE technique including, the loading solvents, the elution solvents and the fluoros silica gel reusability. Many solvents can be used for loading the sample onto the column; the amount of solvent that can be used depends on the fluorophilicity. Breakthrough may occur if too much of a very fluorophilic solvent is used and so the volume of solvent must be reduced. Breakthrough is when a small amount of the fluoros fraction is eluted along with the organic fraction.

The first pass of the elution needs to be fluorophobic and so water miscible solvents are the ideal choice. However, if the organic fraction has low solubility in the solvent system chosen it can lead to blockages in the column due to precipitate formation. Increasing the percentage of organic solvent used and reducing the loading mass of the crude material can mitigate the problem of precipitate formation.

Fluoros silica can be relatively expensive and so to try and reduce the cost, the cartridges of FluoroFlash[®] can be reused. The fluoros stationary phase can be cleaned by washing with fluorophilic solvents (acetone, MeCN and THF) or with a mixture of MeCN-H₂O containing 0.5% TFA.²³ Other precautionary measures can be taken such as pretreating or removing insoluble solids, large amounts of salts or strongly basic or acidic compounds before loading onto the column. The cartridges must also be preconditioned to ensure there are no air bubbles.

Reverse F-SPE also has a few issues. Although standard silica is used, which is considerably cheaper than the FluoroFlash[®] cartridges, fluoros solvents are

required. These solvents are more expensive, more environmentally persistent and are incredibly non-polar. The non-polarity of the solvents can cause issues with those fluorinated fractions that are somewhat polar.²⁹ This issue can occasionally be overcome by mixing the fluorinated solvent with an organic solvent, however, they are immiscible with many organic solvents and so the range of solvent blends is limited.

1.4 Isocyanides

Isocyanides are a class of organic compounds in which the functional group is a nitrogen-carbon triple bond that is bonded to the rest of the molecule *via* the nitrogen atom as opposed to the carbon atom, as in the case of cyanides. The fact they are isomers of cyanides gave rise to the name isocyanide. The isocyanide functional group can be described by two resonance structures (Figure 8). Isocyanides are isoelectronic with carbon monoxide and therefore the isocyanide group is linear, similar to CO in coordination complexes.

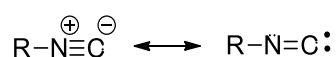


Figure 8. General resonance structures of isocyanides.

Compared to cyanides, isocyanides are substantially more volatile and easily distinguishable by their vile odours.³⁰ It has been suggested that it is these odours that have hindered the use of isocyanides, Ivar Ugi states;³¹

“The development of the chemistry of isonitriles has probably suffered...through the characteristic odour of volatile isonitriles, which has been described by Hofmann and Gautier as ‘highly specific, almost overpowering’, ‘horrible’, and ‘extremely distressing’. It is true that many potential workers in this field have been turned away by the odour.”

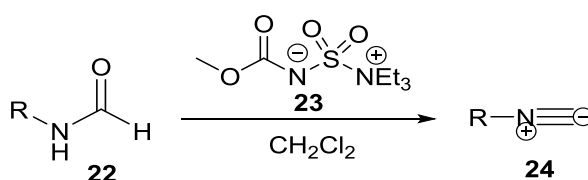
Isocyanides have even been used in nonlethal weapons due to their sufficiently obnoxious odour.³²

Due to the resonance forms of the functional group, the molecule can react as either an electrophile or a nucleophile during the course of a reaction. In strong bases, with the exception of methyl isocyanide, the isocyano group tends to be stable with only a limited number of reports in which the group reacts with bases. However, isocyanides are highly sensitive to acidic conditions. Hydrolysis of the isocyanide to the corresponding formamide occurs readily in the presence of aqueous acid.

1.4.1 Synthesis of Isocyanides

The first reported formation of an isocyanide was in 1859 by Lieke³³ who intended to use allyl iodide and silver cyanide to synthesise allyl cyanide, but allyl isocyanide was isolated instead. The progress of isocyanide chemistry seemed to halt with only a small number reported that can be synthesised by Lieke's route. A breakthrough came in 1958 when it was discovered that the dehydration of formamides is a general route to their formation. The work of Ugi *et al.*³⁴ showed that isocyanides could easily be formed from the reaction of formamides in the presence of phosphorous oxychloride with pyridine or potassium *tert*-butoxide.

Several further methods of isocyanide synthesis have been reported including the use of the Burgess reagent³⁵ **23** by McCarthy *et al.*³⁶ in 1998 (Scheme 8). Problems arose with the conventional halide reagents (phosgene, triphosgene and phosphorous oxychloride for example) when the authors attempted to dehydrate β -trialkylsilyloxyformamides. When using the halide based systems, desilylation of the substrate occurs preferably over dehydration. As the Burgess reagent is an established dehydrating reagent for alcohols³⁷ and promotes the formation of cyanates and cyanides from nitroalkenes and carboamides respectively,³⁸ the authors decided to employ this reagent in the synthesis of isocyanides.

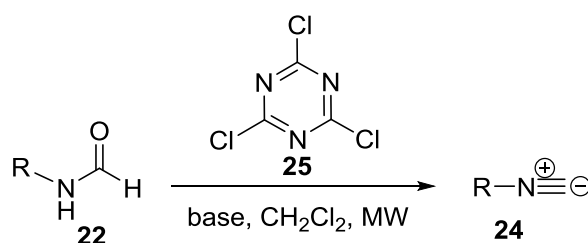


Scheme 8. The synthesis of isocyanides using Burgess Reagent.

The work showed that the reagent can be applied to prepare a range of different isocyanides, including those that underwent desilylation using conventional reagents. The reaction must take place in dry dichloromethane, as the reagent is highly moisture sensitive, and can mainly be performed at room temperature. Occasionally the reaction needs to take place under reflux. The reagent also

allowed for selective dehydration of formamido alcohols to the corresponding hydroxy isocyanide which was previously unknown.

The synthesis of isocyanides from formamides under microwave conditions has been described by Porcheddu.³⁹ The previously mentioned methods use extremely toxic or unstable reagents and can often be costly. The purification of the products has also been shown to be a problem due to the reactivity of the isocyanide itself. The authors decided to try the dehydration using a much cheaper reagent, cyanuric chloride (2,4,6-trichloro[1,3,5]triazine **25**), however the reaction provided only modest yields. Initially the authors concentrated on the production of aliphatic isocyanides and optimising the microwave conditions (Scheme 9). The reaction mixture was exposed to microwave radiation at 100 °C for 10 mins to provide the desired products in good yields (80-98%) and purities. The authors then tried this method to form aromatic isocyanides. No desired product formation was found using the protocol outlined above and so the authors investigated different conditions. It was found that by changing the base (from pyridine to triethylamine), changing the order of addition of the reagents and the microwave conditions were changed to 3 mins and 50 °C, good yields could be obtained.

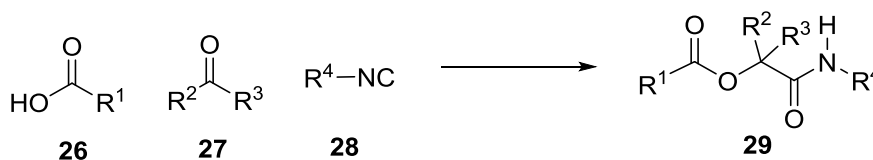


Scheme 9. Isocyanide formation by the dehydration of formamides under microwave conditions.

1.4.2 Multicomponent reactions of Isocyanides

Multicomponent reactions (MCRs) are atom efficient reactions where three or more starting materials combine to form a single product. MCRs have been known for over 150 years, with the widely accepted first MCR recorded in 1850 when Strecker synthesised α -amino acids from α -cyanides.⁴⁰ Isocyanides are

particularly useful in the context of MCRs due to their ability to react as both a nucleophile and an electrophile. In 1921 Passerini⁴¹ reported the first isocyanide-based MCR which later was named after him (Scheme 10). The reaction occurs with a carboxylic acid **26**, a ketone **27** and an isocyanide **28** to form an α -acyloxy amide **29**.



Scheme 10. The Passerini reaction.

The most famous and most utilised MCR reaction was discovered in 1959 by Ugi.⁴² The reaction is a four component MCR which involves the reaction of a carboxylic acid, an amine, a ketone or an aldehyde and an isocyanide to form a bis-amide (Scheme 11). The scaffold produced by the Ugi reaction allows for a large variation of the appendages and so the reaction has been used extensively for the formation of chemical libraries. Simply by varying the starting materials, a great number of different compounds can be formed by one standard reaction. Combining the Ugi reaction with other follow-on reactions allows for diversity of the compound backbone.



Scheme 11. The Ugi reaction.

1.4.3 Isocyanoacetate

Primary amines are used to synthesise formamides using a method called formylation. Since the discovery of the dehydration of formamides to form isocyanides, protected amino acids have been employed in these types of

reactions. Ugi, in 1961, synthesised the first α -isocyano ester (isocyanoacetate)⁴³ and now this compound and its derivatives are readily available. The isocyanoacetate molecule (**35**) contains four reaction centres⁴⁴ (Figure 9); the carbonyl group with either a protecting group or leaving group (blue), a substituent R (red) which can handle functional groups, an acidic CH fragment (green) and the isocyanide group (pink). The molecule therefore provides outstanding diversity of reactions due to the combination of these reactive centres.

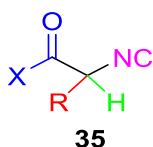


Figure 9. Reactivity profile of α -isocyanoacetate derivatives.

Isocyanoacetate derivatives are known to be building blocks for a number of natural product syntheses and in the synthesis of biologically active compounds (Figure 10). Coumermycin A **36** is a potent antibiotic isolated from *Streptomyces* that binds reversibly and with high affinity to the amino-terminal 24K subdomain of the B subunit of bacterial DNA gyrase (GyrB). Eurystatin A **37** is a natural product isolated from *Streptomyces eurythermus* as has been reported to be a potent inhibitor of the serine protease prolyl endopeptidase (PEP).⁴⁵ Vincamine **38** is used in the treatment of vascular diseases.⁴⁶ Broad varieties of peptides and peptide mimetics have been synthesised by multicomponent reactions of isocyanoacetate derivatives. They have also shown use in inorganic chemistry as coordination ligands to transition metals, and in polymer chemistry.

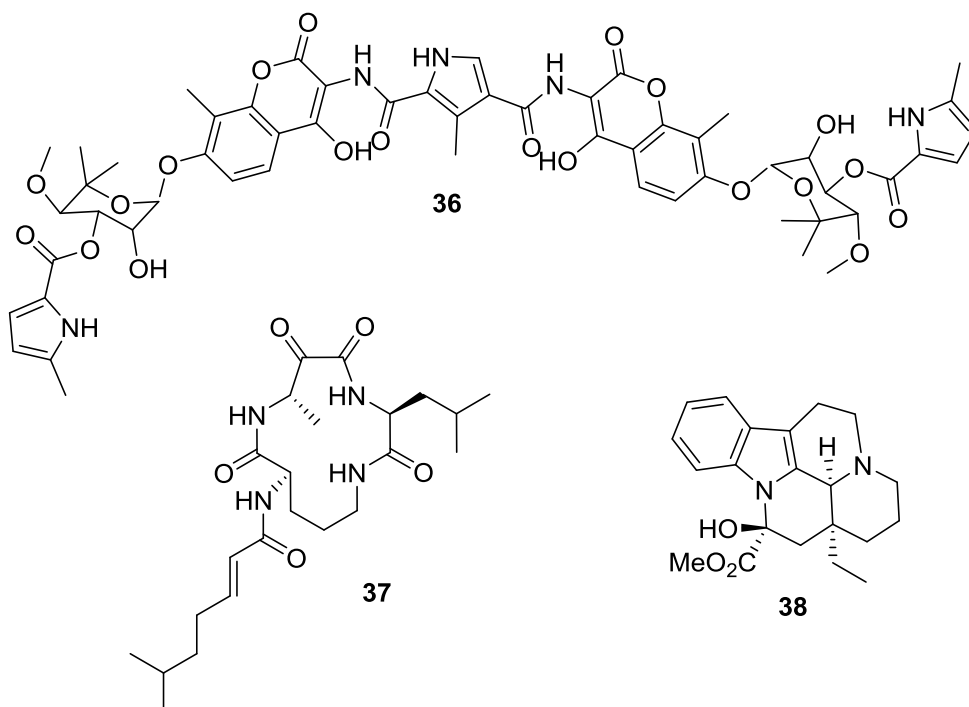


Figure 10. Pharmaceutically active compounds that can be synthesised from isocyanoacetate derivatives.

1.4.4 Conclusion

Isocyanides have specific and unique chemical profiles. Since their discovery the research with this class of compounds has been limited due to the instability of a number of the products, as well as the distinct odour being incredibly off putting. A number of methods have been developed for the synthesis of isocyanides, mainly involving the dehydration of a formamide. Isocyanoacetate derivatives have a reactivity profile which allows for several areas of reaction as discussed above. The reactivity of isocyanoacetate derivatives allows for the use of these compounds as starting materials in many natural product syntheses and in the formation of pharmaceutically active compounds, particularly in the synthesis of heterocycles. These reactions will be discussed in later chapters.

1.5 Vapourtec R-Series Continuous Flow Reactors.

The continuous flow system used in this project is the Vapourtec R-Series system which is commercially available from Vapourtec (Figure 11).



Figure 11. The Vapourtec R-Series system.

The system used includes a two channel module consisting of the R2+ module. The Knauer HPLC pump has a maximum reaction pressure of 42 bar and offers flow rates ranging from 0.01-9.99 mL/min. This module allows for reagents to be directly injected into sample loops of 2, 5 or 10 mL size or pumped through from sample reservoirs.

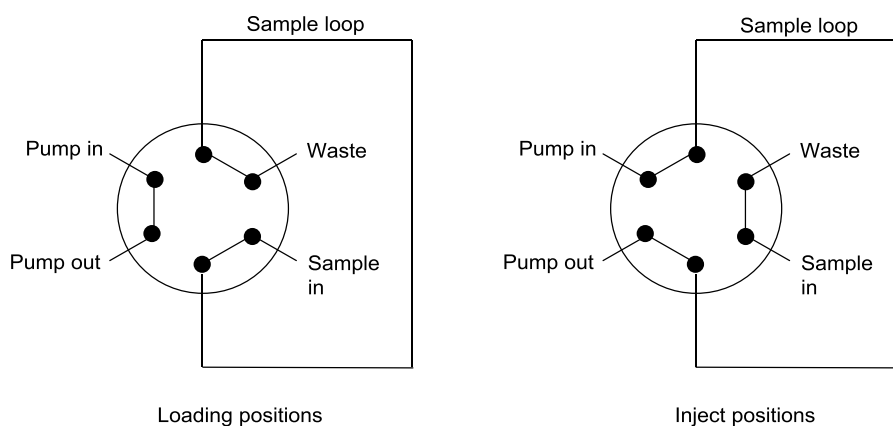


Figure 12. Schematic of Rheodyne valve.

Reagents in the sample loops are pumped through the system by an automated Rheodyne valve (Figure 12). When in the loading positions the solvent is pumped into the system and straight out to the reactor while the sample can be injected into the sample loop and any excess solution will be passed into the waste receptacle. In the inject position the solvent from the pumps is pumped through the sample loop and so the sample is pumped out of the valve and into the reactor.

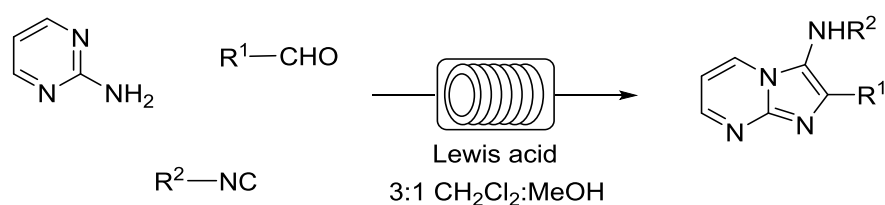
The Vapourtec R-Series platform allows up to four separate reactors or columns to be attached in any configuration. Coiled tube reactors are housed within an insulated glass manifold that can be heated to 150 °C. Air is circulated through the glass manifold and this is how the temperature control is achieved. The temperature is constantly monitored at the reactor wall by a thermocouple that is accurate to 1 °C. A standard column reactor is also available that can also be contained within a glass manifold and heated up to 150 °C in the same manner as the coiled reactor. There is also a range of back pressure regulators available that can allow solvents to be heated to above their atmospheric boiling point.

The conditions of flow rate, temperature of up to four reactors, and system pressure can be precisely controlled by using the inbuilt interface which displays the real-time parameter values. If the pressure is too high or too low the system will automatically stop the reaction conditions, flow rate and temperature. The Vapourtec software Flow Commander™ can also be used to control the entire system. The software allows all the set up and calculations to be automated and also allows for maximum data collection.

1.6 Project Aims

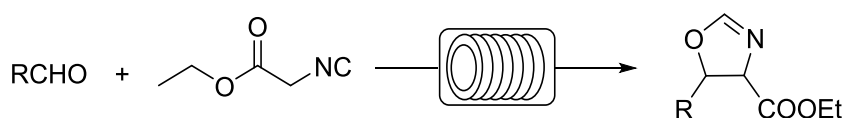
The aim of this project was to synthesise a fluororous tagged component which can be used in several heterocyclic formation reactions under continuous flow conditions.

The conditions for the synthesis of 3-aminoimidazo[1,2-a]pyrimidines using a continuous flow reactor were to be optimised, followed by the synthesis of a small library to show the scope of the reaction (Scheme 12). A fluororous tagged benzaldehyde **40** was then used to synthesise 3-aminoimidazo[1,2-a]pyrimidines to investigate the advantage of fluororous technologies with this reaction. A palladium catalysed cross coupling reaction would then be performed to demonstrate the removal of the fluororous tag.



Scheme 12. The synthesis of 3-aminoimidazo[1,2-a]pyrimidines under continuous flow conditions.

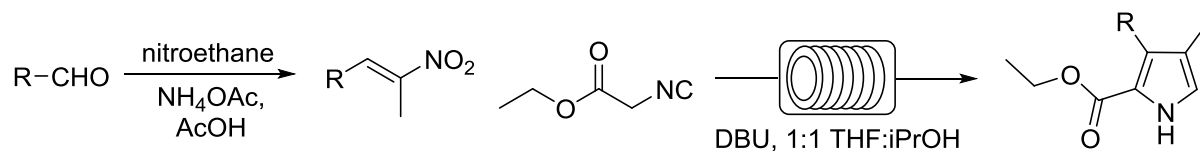
A small library of 2-oxazolines were to be synthesised under continuous flow conditions after a series of optimisation reactions are performed (Scheme 13). The reaction could then be performed using a fluororous tagged benzaldehyde and the results are to be compared. A palladium catalysed cross coupling reaction will be carried to remove the fluororous tag.



Scheme 13. The synthesis of oxazolines under continuous flow conditions.

The conditions for the Barton-Zard synthesis of tri-substituted pyrroles were to be optimised under continuous flow conditions. The synthesis of a small library of

pyrroles will be performed after the synthesis of several nitrostyrene starting materials. The next stage is using the fluororous tag technology with the optimised conditions. The reactions to synthesise several fluororous tagged nitrostyrenes and the subsequent pyrrole formation reactions under continuous flow conditions were to be studied.



Scheme 14. Nitrostyrene synthesis followed by pyrrole formation under continuous flow conditions.

2. Fluorous Tags

Fluorous tags are used in a similar way to the linkers used in solid phase synthesis. The fluorous tags are attached to the reactant, which is then used in multistep synthesis and cleaved once the final step is completed. The molecules used as tags usually contain a short aliphatic spacer to shield the molecule from the fluorous chain which is electron withdrawing and can, therefore, affect reactivity (Figure 13). The inclusion of an ethylene or propylene linker group can provide the fluorous tagged molecule with a similar reactivity to its non-fluorous analogue.⁴⁷

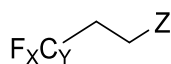
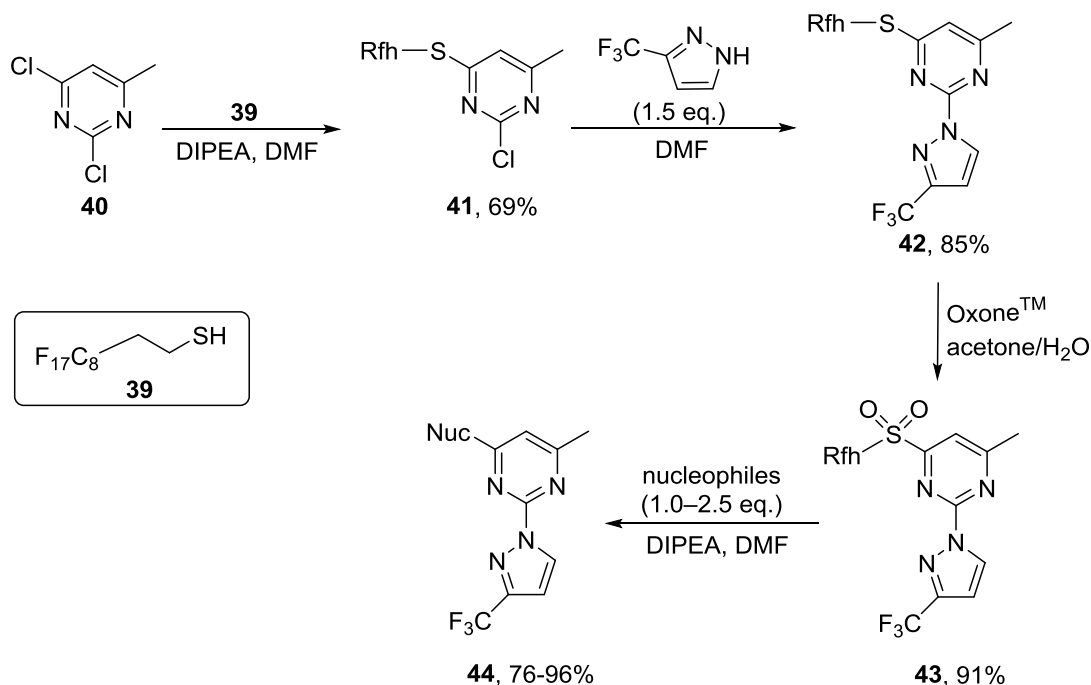


Figure 13. General structure of fluorous tags where X is 17-25, Y is 8-12 and Z is the functional group used to attach the tag to the molecule of interest.

2.1 Variations of Fluorous Tags

2.1.1 Thiol Tags

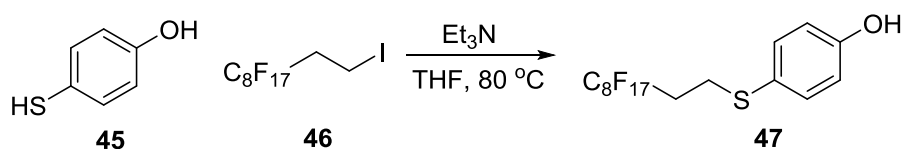
The fluorous thiol **39** (Scheme 15) was used by Zhang to displace a chlorine atom on the electron deficient 2,4-dichloro-6-methylpyrimidine in the presence of DIPEA by a nucleophilic substitution reaction.⁴⁸ The coupling of the thiol tag to the 2,4-dichloro-6-methylpyrimidine **40** provided the product **41** as the major regioisomer in a 3:1 ratio. The regioisomers can easily be separated by flash column chromatography and the major isomer then used for a second nucleophilic substitution reaction. Oxidation of the thioether moiety then permitted additional displacement of the resultant sulfone-linked tag, with 10 different nucleophiles used. The yields proved to be excellent, ranging from 76–96% with products being recovered in high purity after F-SPE.



Scheme 15. Use of thiol fluorous tags in displacement reactions.

2.1.2 FluoMarTM

FluoMarTM has been introduced as a fluorinated version of Marshall resin (Figure 14), a popular linker in solid phase organic synthesis. Marshall resin has shown advantages due to the ease of removal (oxidation of the sulfide to the sulfone) without the removal of any side chain protecting groups. The S-alkylation of 4-mercaptophenol **45** with 1-iodo-1*H*,1*H*,2*H*,2*H*-perfluorodecane **46** yields the product FluoMarTM **47** (Scheme 16).



Scheme 16. The synthesis of FluoMarTM.

The molecule can be analysed by conventional spectroscopic and chromatographic techniques as well as dissolving well in common organic solvents, meaning it has the general features of an organic compound and, therefore, can be used in “normal” organic reactions using standard techniques.

The same method of removal can be used for both the FluoMar™ protecting group as well as Marshall resin.

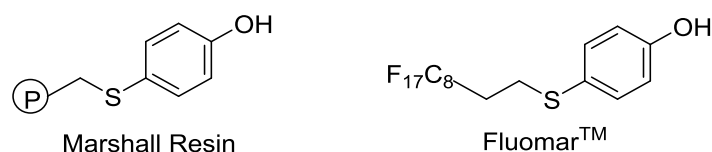


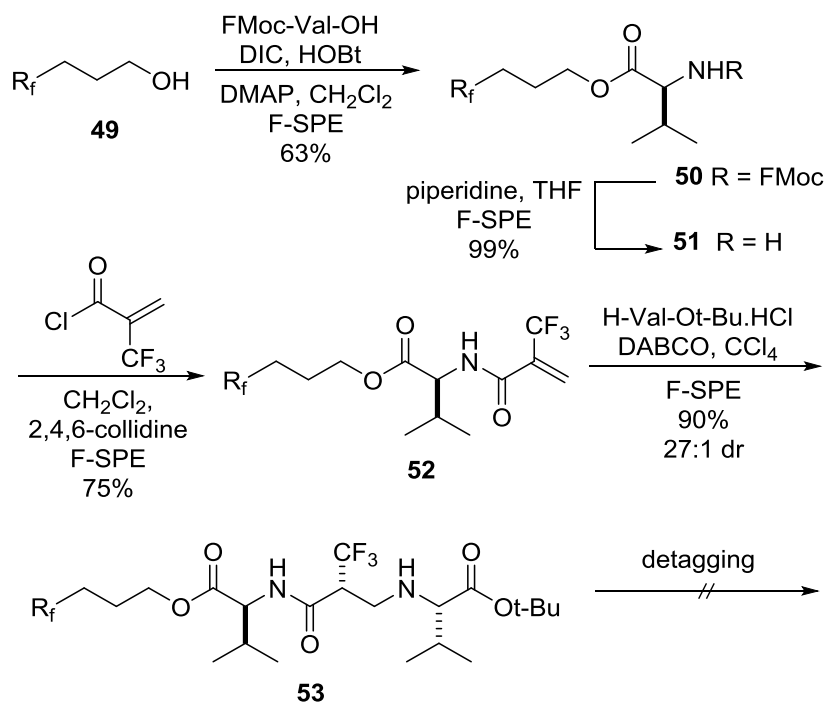
Figure 14. The fluoros analogue of Marshall Resin, FluoMar™.

The authors demonstrated the formation of an array of amides and diamides utilising FluoMar™ as a fluoros tag. These reactions mainly involved the attachment of the tag to various carboxylic acids and cleavage by amine displacement. The compounds were purified using F-SPE and the fluoros tag was recovered with yields of 65–70%. Interestingly, a follow-up was performed in which the reactivity difference between the Marshall resin and FluoMar™ was investigated. Equimolar amounts of the Marshall resin and FluoMar™ were reacted competitively with benzofuran-2-carboxylic acid under standard coupling conditions.⁴⁹ After washing, the filtrate was analysed by HPLC and the ratio of product to the unreacted FluoMar™ was 73:27. The assumption was made that the unreacted FluoMar™ was due to the competition with the Marshall resin and so the results suggest that the fluoros tag reacted at least 2.7 times faster than the Marshall resin. This is presumably due to the solubility of FluoMar™ in organic solvents as opposed to the polymer bound analogue.

2.1.3 Fluorous (Trimethylsilyl)ethanol (F^{TMSE}-OH)

Fustero *et al.* devised a silicon containing fluoros tag (Scheme 18, **48**) that could be used in peptide synthesis to protect the carboxylic acid group, due to the mild conditions in which the tag can be removed, ensuring that no epimerisation occurs.⁵⁰ The authors initially used the commercially available 3-(perfluorooctyl)propanol **49** as a tag and protecting group to afford a fluoros L-valine derivative **50** (Scheme 17). *N*-Fmoc-protected L-valine was used as the starting material to ensure the tag was placed on the carboxylic acid group. The fluoros amino acid product was then converted into Michael acceptor **52** and an

aza-Michael addition performed with L-valine *tert*-butyl ester hydrochloride to produce **53**.

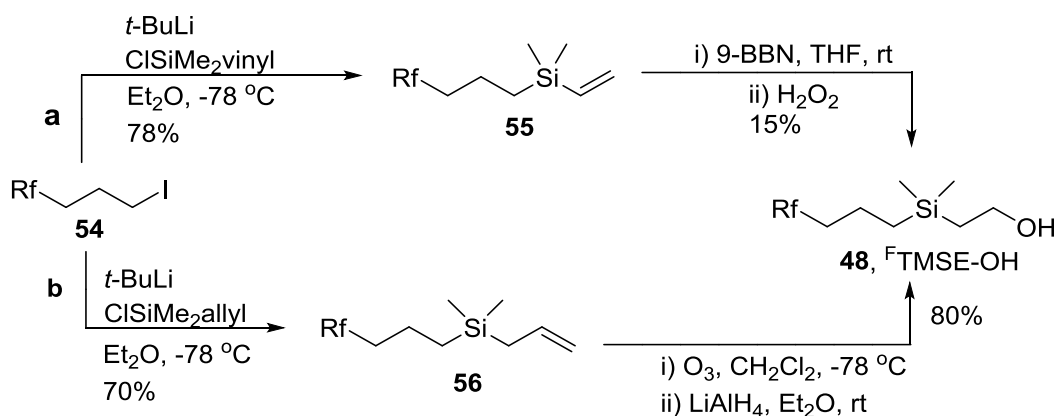


Scheme 17. A scheme to show the peptide coupling performed using 3-(perfluorooctyl)propanol **60** as the fluorous tag component.

The diastereoselectivity of the latter step (27:1 determined with the aid of ^{19}F NMR spectroscopy) was comparable to reported nonfluorous compounds (33:1)⁵¹ and is vastly improved compared to the equivalent reaction performed on solid phase (4.8:1),⁵² however, removal of the fluorous tag was found to be unworkable. Mild conditions are required to ensure that the peptide structure remains intact, but several transesterification reactions performed under compatible conditions all proved ineffective.

The authors decided to construct an alternative fluorous tag that would be easier to remove under mild conditions. The molecule $^{\text{F}}\text{TMSE-OH}$ **48** was formed as a fluorous analogue of 2-(trimethylsilyl)ethanol as it can be removed by transesterification in the presence of TBAF and 4 Å molecular sieves (MS). This tag was formed in two steps from the commercially available 3-(perfluorooctyl)propyl iodide **54**, which undergoes lithium-halogen exchange with *tert*-butyllithium and further reacts with either chloro(dimethyl)vinyl silane or allylchlorodimethylsilane (either route **a** or route **b** respectively; Scheme 18).

Hydroboration of the product from route **a** showed low yields of around 15%. However, ozonolysis of intermediate **56** followed by reduction gave a yield of 80%. Interestingly, the ozonide formed in the reaction with **56** was so stable that milder reducing agents failed to reduce this intermediate, so LiAlH₄ had to be used.



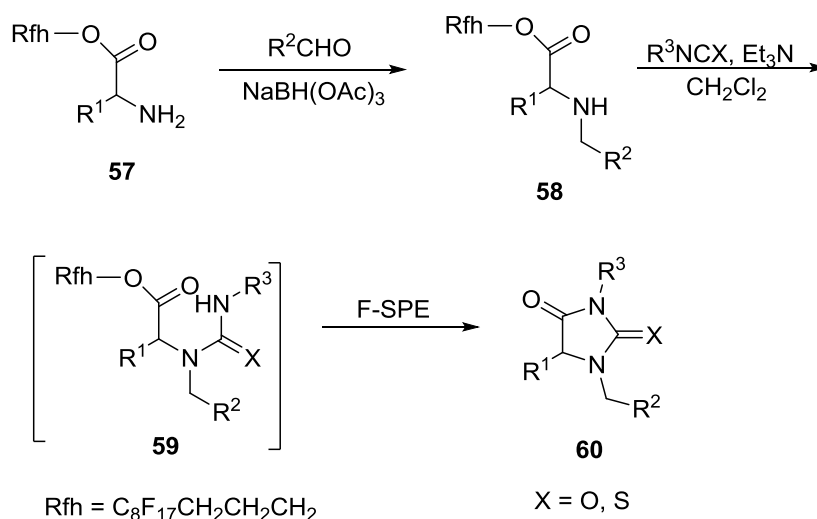
Scheme 18. Synthesis of fluoros (trimethylsilyl)ethanol.

Finally, the fluoros tag **48** was used to protect several different amino acid carboxylate groups which underwent coupling with different *N*-Boc-protected α - or β - amino acids to form dipeptides. It was shown that if tag removal with TBAF occurs in the presence of allyl bromide, the allyl ester is formed in place of the carboxylic acid. A Michael acceptor, a direct analogue of **52**, containing the ^FTMSE-OH tag was formed and then underwent the aza-Michael addition reaction with a variety of amino acids. After removal of the tag the diastereomeric ratios showed no variation compared to the retropeptide containing the fluoros tag.

2.1.4 Alcohol Tags

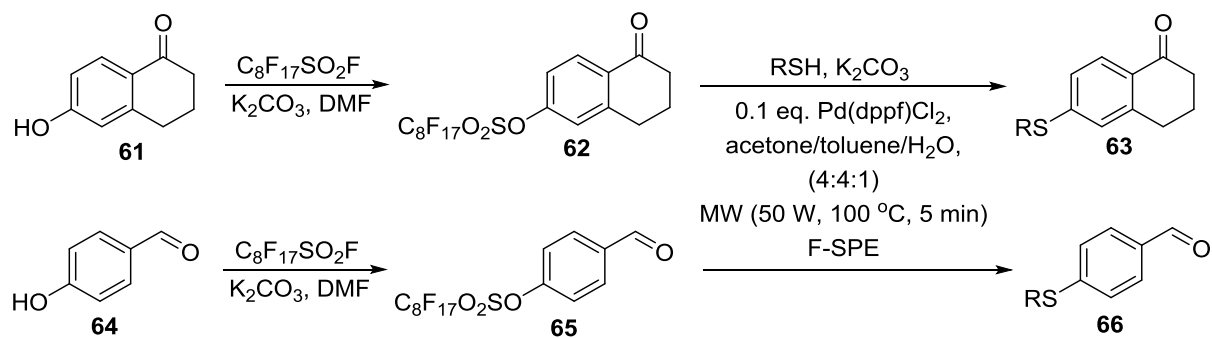
Zhang *et al.* compiled a library of hydantoin and thiohydantoin compounds with 120 members by parallel synthesis (Scheme 19).⁵³ A series of fluoros amino acid esters (structure **57**, Scheme 19) were employed in reductive amination with aldehydes under standard solution phase conditions, each intermediate was then purified by F-SPE and the fluoros fraction was reacted with isocyanates in the presence of triethylamine to promote cyclisation. The cyclisation displaces the

fluorous tag to form the hydantoin ring **60**, which was separated from the displaced tag using F-SPE. The yields of the final stage of the reaction showed a range of 46-98% (relative to the isocyanate) and the purities of the products were between 85–95%.



Scheme 19. Fluorous synthesis of hydantoins and thiohydantoins.

In the same year, the authors also showed that perfluoroalkylsulfonates could be coupled to aryl alcohols and the resulting fluorous products had a similar reactivity to aryl triflates.⁵⁴ Aryl triflates have long been known to be efficient and important substrates for a range of transformations, particularly aryl C-C bond forming reactions. The fluorous versions, having similar reactivity, are therefore, applicable in potentially improved versions of a wide range of processes. This was demonstrated by the palladium-catalyzed cross coupling of the aryl perfluoroalkylsulfonates with thiols (Scheme 20). The yields of fluorous intermediates **62** and **65** were very high, 85% and 90% respectively. The cross-coupling reactions were further optimised for microwave synthesis, and performed on a variety of thiol starting materials with yields ranging from 56–71%.



Scheme 20. Microwave assisted fluororous synthesis of aryl sulfides.

Since publication of the original paper describing fluororous tagged aldehyde **65**, there have been several more reports which have utilised this tag and the F-SPE technique. The majority of the papers which utilise this fluororous benzaldehyde derivative describe the Suzuki reaction as the preferred method of fluororous tag removal, as triflates, together with halides, are widely employed in these coupling reactions.^{55,56,57,58}

2.2 Fluorous Tag Synthesis

As described in the project aims section (Section 1.6), the initial aim of this project was to synthesise the fluorous tag **48** (Figure 15), which would then be used in the synthesis of a fluorous tagged isocynoacetate derivative for the synthesis of novel heterocycles. Several methods of synthesis have been attempted for its formation, including hydroboration of the vinyl precursor **55**, ozonolysis of the allyl precursor **56**, and cleavage of a diol formed from the allyl precursor **56**. These methods are described below.

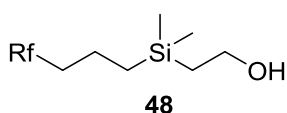
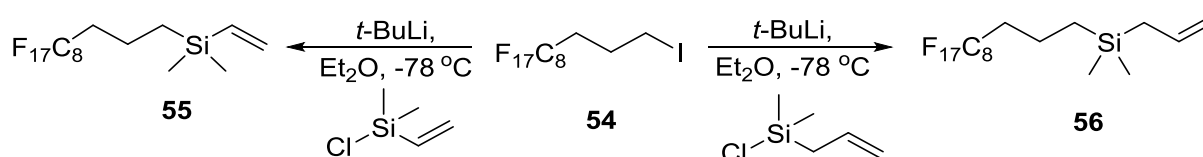


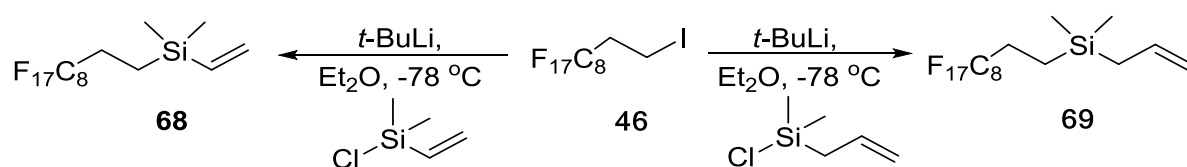
Figure 15. ^FTMSE-OH.

The first step of the synthesis (Scheme 21) was to form either vinyl precursor **55** or allyl precursor **56** according to the method laid out by Fustero *et al.*⁵⁰ The paper describes the method for synthesis of the allyl precursor **56** and the same procedure was applied for synthesis of the vinyl precursor **55**. These reactions involved halogen–lithium exchange of iodoalkyl starting material **54** using *tert*-butyllithium followed by reaction with either chloro(dimethyl)vinylsilane, to produce **55**, or allylchlorodimethylsilane to produce **56**. The reactions were generally reproducible with modest yields (typically 72% and 69%, respectively), however, analysis of the initial products showed further purification was required in addition to that reported. In both cases, distillation was found to provide pure product.



Scheme 21. The synthesis of vinyl(dimethyl)(3-(perfluorooctyl)ethyl)silane **55** and allyl(dimethyl)(3-(perfluorooctyl)ethyl)silane **56**.

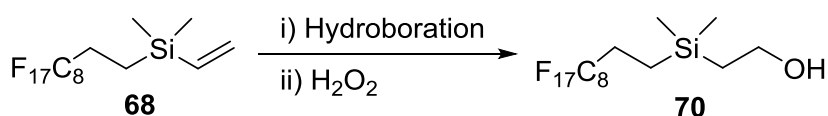
The starting material, 1*H*,1*H*,2*H*,2*H*,3*H*,3*H*-perfluoroundecyl iodide **54**, is expensive so an alternative was investigated to maximise the commercial potential and future development of the technology without altering reactivity. It was discovered that 1-iodo-1*H*,1*H*,2*H*,2*H*-perfluorodecane **46** was substantially cheaper than the original starting material with the only difference being the alkyl linker chain is one carbon shorter (ethyl as opposed to propyl). As stated above (start of section 2), the chemistry of fluorine tagged functional groups is not affected if at least a two-carbon linker is present, so the new starting material should be just as compatible with the planned chemistry. The revised reaction scheme is shown below (Scheme 22). Both products **68** and **79** were obtained in reasonable yields, 65% and 70% respectively. Detection of both products **68** and **69** was shown by a number of relevant characterisation methods (including NMR and IR spectroscopy) but no conclusive mass ion peak could be found by ES or EI mass spectrometry. LC-MS analysis of reaction mixtures showed no conclusive mass ion for the products could be detected.



Scheme 22. The reaction of 1-iodo-1*H*,1*H*,2*H*,2*H*-perfluorodecane with chloro(dimethyl)vinylsilane and allylchlorodimethylsilane to form the vinyl and allyl precursors.

The next step of the synthesis, hydroboration (Scheme 7), is where problems arose. The first attempt was made using 9-BBN followed by an oxidative work up with hydrogen peroxide, as suggested in the Fustero paper,⁵⁰ but using the method laid out by Soderquist *et al.*⁵⁹ using modified vinyl precursor **68**. ¹H NMR spectroscopy showed there was no product in the crude reaction material. Other hydroboration reagents and methods were used as shown in Table 3. When BH₃-THF solution was used, this provided a yield of 6% as determined by ¹H NMR spectroscopy; in contrast, dicyclohexylborane solution showed no product formation. The peaks considered when determining the yield by ¹H NMR spectroscopy were the single vinyl proton in the starting material, defined at 6.02-6.10 ppm as a multiplet, and the peak corresponding to the single hydroxyl proton

in the product, defined at ~1.59 ppm as a singlet. All crude mixtures were subjected to ES mass spectrometry to confirm whether or not the product was present in the sample. The hydroboration was also attempted under microwave conditions with both 9-BBN, which showed product formation of 2%, and the borane solution producing a purified yield of 26%. Given the increase of yield from batch to microwave conditions, the reaction was also attempted under continuous flow conditions using the borane solution in the hope that the yield could be further improved. However, after several attempts the maximum yield obtained under flow conditions was 12%. The low yields could be due to the instrumentation used which proved difficult to keep the reaction under anhydrous conditions.

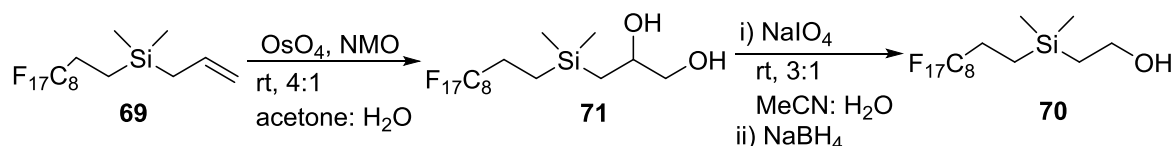


Scheme 23. The general reaction scheme for the hydroboration and oxidative workup of vinyl(dimethyl)(3-(perfluorooctyl)ethyl)silane.

Table 3. The reagents and conditions used for hydroboration optimisation.

Hydroboration reagent	Conditions	Yield (%)
9-BBN	Batch	-
BH_3 -THF	Batch	6
Dicyclohexylborane	Batch	-
9-BBN	Microwave	2
BH_3 -THF	Microwave	26
BH_3 -THF	Continuous Flow	12

Due to the low yields produced by the hydroboration step it was decided to attempt a different synthetic route (Scheme 24). The reaction of allyl precursor **69** with osmium tetroxide to form the diol **71**, followed by diol oxidation to form an aldehyde and finally the reduction of the resulting aldehyde with sodium borohydride to form the alcohol **70**.



Scheme 24. Diol formation and subsequent diol cleavage to form the fluorosilane alcohol.

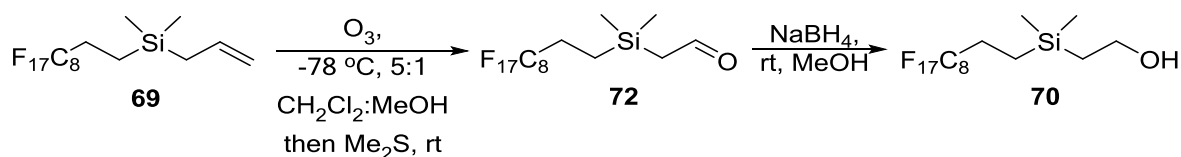
The treatment of the allyl precursor with osmium tetroxide and 4-methylmorpholine *N*-oxide in the first step showed an estimated 86% conversion to the diol by ^1H NMR spectroscopy and the mass ion was found by ES mass spectrometry. The diol oxidation was performed on the crude mixture using sodium periodate but after two attempts at this reaction there was no product detected based on crude ^1H NMR spectroscopy. TLC showed a range of new spots after work up implying side reactions were taking place. It has been postulated that the formation of **71** was not fully confirmed as the crude mixture was carried forward in the experiment and this could be the reason that the diol oxidation did not proceed as expected.

It was decided at this point to move on to the alternative approach based on ozonolysis of the allyl precursor **69**, due to the reduction in the number of steps and the literature precedent for this compound.⁵⁰ The first method of ozonolysis, as described by Fustero *et al.*,⁵⁰ involved bubbling ozone through a solution of **69** dissolved in dichloromethane until the solution became blue in colour, followed by reduction of the ozonide using LiAlH_4 , but no product was evident by ^1H NMR spectroscopy, concluded by the absence of a peak at ~ 1.59 ppm, which represents the hydroxyl proton in the product.

There were signs of the allyl starting material present in the ^1H NMR spectra showing either the reaction did not go to completion or the product was broken down into the starting material at some stage during the reaction. This method was attempted again with the addition of NaHCO_3 to reduce the acidity of the solution during the ozonolysis process. This method was successful in the formation of the fluorosilane tag (determined by ^1H NMR spectroscopy and ES mass spectrometry) with some starting material still present. The percentage conversion, based on ^1H NMR spectroscopy, was 68%. However, when an

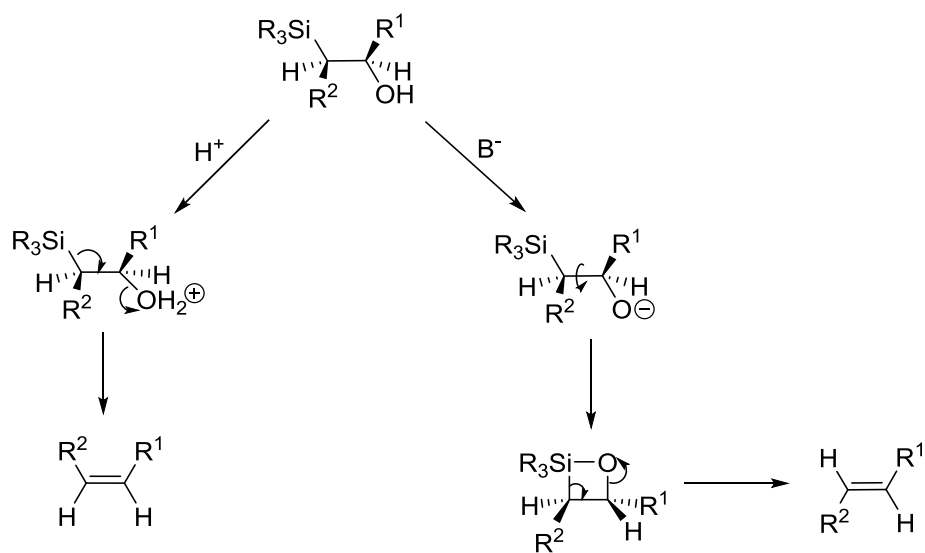
attempt to column the product on silica was made, it was not recovered and appeared to decompose on the column; this was confirmed by 2D TLC. The reaction was repeated and several different columns were run under different conditions in an attempt to determine a purification technique that does not decompose the product. The first column was eluted with a small amount of triethylamine mixed in with the solvent system to reduce the acidity of the column; the second column utilised basic alumina as the solid phase. Unfortunately, neither of these purification techniques yielded the pure product. Some starting material was recovered, however, the other fractions collected were not identifiable.

In order to avoid purification of the product by flash column chromatography the method of ozonolysis was altered. The second method involved the reduction of the ozonide using dimethyl sulfide to form aldehyde **72**, followed by reduction with sodium borohydride. The reaction was run in dichloromethane–methanol (5:1) with the addition of NaHCO₃ and was shown to provide the intermediate aldehyde by crude ¹H NMR spectroscopy. After the reduction with sodium borohydride (Scheme 25), the product was shown to be formed by a number of characterisation techniques (IR spectroscopy, ¹H, ¹³C and ¹⁹F NMR spectroscopy and mass spectrometry) with a yield of 42%.



Scheme 25. The ozonolysis and subsequent reduction to form the alcohol fluorous tag.

Due to the low yield of target compound **70** obtained in all of the methods attempted (the best being 23% over two steps) and the instability of the final product during purification process, potentially due to Peterson rearrangement (Scheme 26), it was decided that the investigation of other fluorous tags would be appropriate.



Scheme 26. Peterson rearrangement⁶⁰

1*H*,1*H*,2*H*,2*H*-perfluorodecan-1-ol **73** (Figure 16) is commercially available at relatively low cost and is analogous to the silicon based tag previously described.

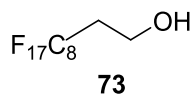
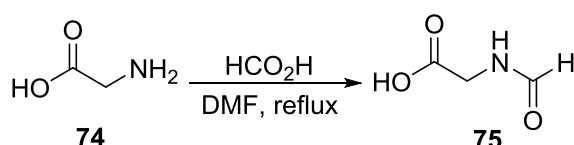


Figure 16. The commercially available 1*H*,1*H*,2*H*,2*H*-perfluorodecan-1-ol

2.3 Fluorous Tagged Isocynoacetate Synthesis

2.3.1 Coupling Reaction of Fluorous Alcohol and *N*-Formyl Glycine

The synthetic strategy utilising the commercially available fluorous alcohol **73** involves the coupling of **73** to *N*-formyl glycine **75** to form a fluorous ester group, followed by the dehydration of the formamide to the fluorous isocynoacetate derivative. The first stage of the synthesis was to formylate glycine **74** using formic acid, providing **75** (Scheme 27) in a high yield of 98%. The *N*-formylglycine was then esterified with the purchased fluorous alcohol to form 1*H*,1*H*,2*H*,2*H*-perfluorodecyl-*N*-formylglycine **76**. Firstly, the synthesis was attempted *via* a Mitsunobu reaction under standard conditions, however, after several hours there was no product formation evident by TLC and only starting materials present. Instead, a series of available peptide coupling reagents were used including CDI, PyBOP and DCC. These reactions were all run under standard conditions and after 20 hours were subjected to an acidic workup and then products isolated by F-SPE. As shown in Table 4 neither the reactions with CDI nor DCC showed any product formation and only the fluorous alcohol starting material was present in the recovered material. In contrast, the reaction using the coupling reagent PyBOP proved successful, showing product formation with a yield of 34%.



Scheme 27. Formylation of glycine.⁶¹

Table 4. The coupling reagents used for the coupling of fluorous alcohol to *N*-formyl glycine.

Coupling Reagent	Yield (%)
CDI	-
PyBOP	34
DCC	-

F17C8CH2CH2OH + NC(=O)C(=O)O >> F17C8CH2CH2OC(=O)C(=O)O
73 75 76

The fluoros alcohol appears to be quite unreactive and so several conditions for the reaction with PyBOP were tried to attempt to optimise the procedure. Various ratios of reagents were used to determine the best conditions (Table 5). The initial conditions were the stoichiometric quantities needed for the reaction (entry 1). Increasing the amount of *N*-formylglycine to a 50% molar excess had no effect, although adding the same excess of PyBOP as well led to a small improvement in yield, entry 3. Doubling the amount of DIPEA was shown to give the greatest improvement; a 5% increase in yield, entry 4. After several other variations in the molar ratio it was found that a ratio of 1:1.5:2:4 (fluorous alcohol: *N*-formylglycine: PyBOP: DIPEA) represented the optimal conditions that could be achieved by reagent variation, entry 6.

Table 5. The varying molar ratios of reagents used for optimisation of the coupling reaction.

Reaction scheme: $\text{F}_{17}\text{C}_8\text{CH}_2\text{CH}_2\text{OH}$ (73) + $\text{HOCH}_2\text{CH}_2\text{NHC(=O)H}$ (75) $\xrightarrow[\text{CHCl}_3]{\text{PyBOP, DIPEA}}$ $\text{F}_{17}\text{C}_8\text{CH}_2\text{CH}_2\text{OCH}_2\text{CH}_2\text{NHC(=O)H}$ (76)

Molar Ratio of Reagents					
Entry	Fluorous Alcohol 73	<i>N</i> - Formylglycine	PyBOP	DIPEA	Yield (%)
1	1	1	1	2	34
2	1	1.5	1	2	35
3	1	1.5	1.5	2	37
4	1	1.5	1.5	4	42
5	1	2	1.5	4	41
6	1	1.5	2	4	44
7	1	2	2	4	43

It was felt that there could still be improvement on a yield of 44% and so the effect of time and temperature were also investigated. The optimal molar ratio determined above (entry 6) was employed and the reaction carried out at room temperature or reflux for an extended period of 72 hours. During that time small aliquots of reaction solution were removed, subjected to an acidic work up and run through a F-SPE column. Yields were determined by the ratio of integrals of the starting material to the product by ^1H NMR spectroscopy. The peaks used to

determine the ratios were a triplet at ~3.90 ppm for the starting material and a doublet at ~4.13 ppm for the product, both peaks represent two protons.

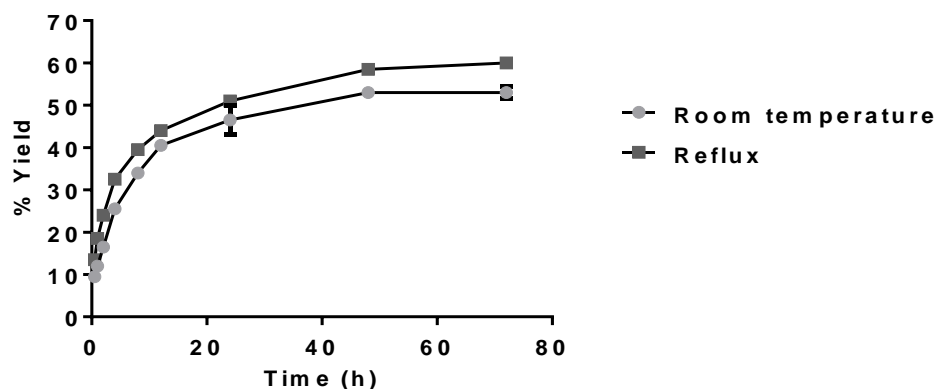
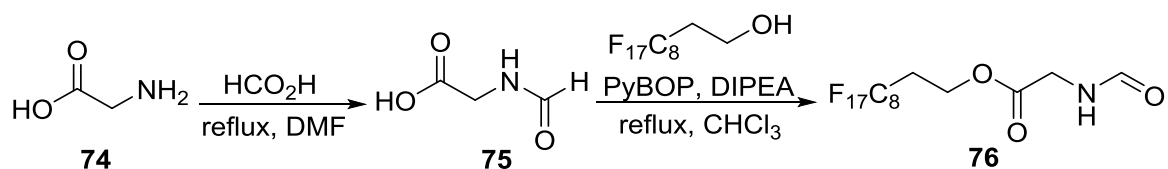


Figure 17. The effect of temperature and time on the coupling reaction.

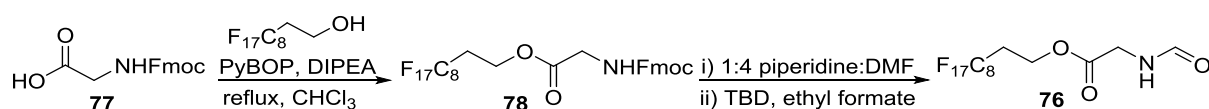
The graph above shows the difference in yield between the reactions occurring at room temperature and at reflux (Figure 17). When at reflux the reaction appeared to be somewhat higher yielding than the reaction at room temperature, as would be expected. It is evident that the original duration of 20 hours was sub-optimal, and that the yield appears to plateau between 48 hours and 72 hours for both cases. The difference in yield between these times was not significant and, therefore, judging from the data above it is clear that the optimal reaction conditions are reflux for 48 hours, to give a yield of 59%.



Scheme 28. The formylation of glycine followed by the coupling of *N*-formylglycine to the commercially available fluorinated alcohol.

It was considered that the coupling reaction using Fmoc-protected glycine may produce a higher yield of product as it was considered that the formamide group could be undergoing side reactions. The resulting intermediate could then be deprotected and formylated. Although there are more steps to this synthetic route the reactions are all known to produce high yields. The first step, the coupling

reaction between fluoros alcohol **73** and *N*-Fmoc-glycine, produced compound **78** in a yield of 72%. However, deprotection of the Fmoc group proved unexpectedly difficult. The standard deprotection protocol (1:4 piperidine: DMF) appeared to break down the ester to the fluoros alcohol starting material. This is in contrast to other alkyl esters such a methyl ester and *t*-butyl ester which generally survive these conditions. The deprotection step was then attempted using DBU, but no reaction was observed.



Scheme 29. The proposed reaction scheme for the synthesis of *N*-formylglycine fluoros ester **87** from Fmoc-protected glycine.

2.3.2 Coupling Reaction under Continuous Flow Conditions

It was considered that continuous flow conditions could be used to improve the yield of the peptide coupling with *N*-formylglycine. To determine the optimum conditions for the coupling reaction of *N*-formylglycine with the commercially available fluoros tag, calibrated HPLC analysis of reaction aliquots was proposed. As the Fmoc protected product **78** is visible at 254 nm, the preferred wavelength for HPLC detection, it was decided that Fmoc protected glycine **77**, which contains a chromophore, would be used instead in the reactions to determine the optimum conditions. The product of the latter reaction, **78**, can be detected by the UV detector and, therefore, a calibration curve can be formed to calculate the concentration of **78** in reaction aliquots and, therefore, assist in determining the optimum conditions for the reaction under continuous flow conditions. Duplicate samples of pure **78** were run through the HPLC column at a range of concentrations and a calibration curve (Figure 18) was determined using the value for the area under the peak (in mV.s).

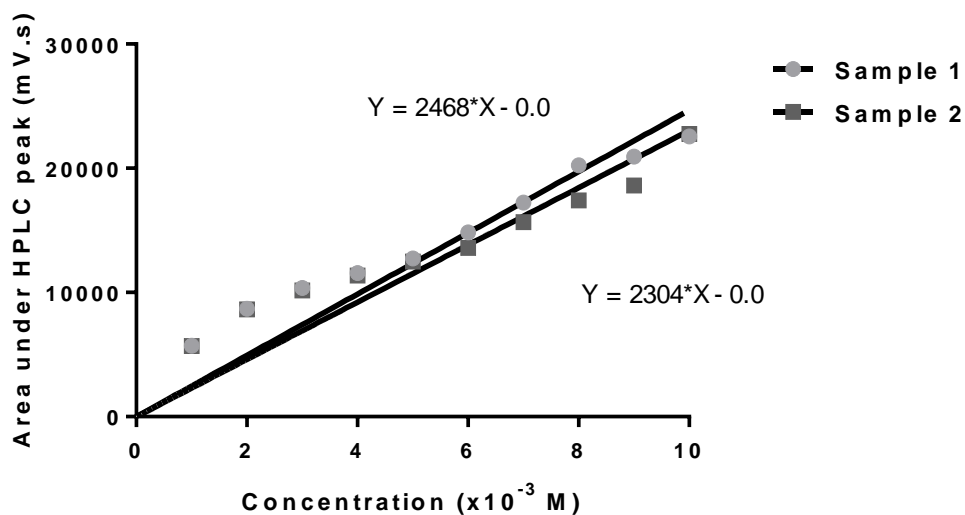
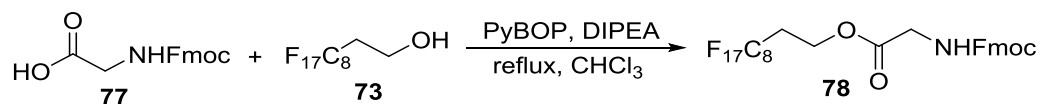


Figure 18. A graph to show the trend between the varying concentrations of fluoros Fmoc glycine ester samples and the area under the peak obtain by HPLC.

Using the fitted trend lines using GraphPad Prism 6 shown above (Figure 18), the calculated yields of the optimisation reactions are shown in Table 6 below. The optimum conditions for this reaction were shown to be a residence time of 40 mins at 60 °C which gave a yield of 59%, lower than the yield obtained in batch.



Scheme 30. Coupling reaction of Fmoc protected glycine to fluoros alcohol.

Table 6. The reaction residence times and temperatures used to determine the optimum conditions for the coupling reaction of Fmoc protected glycine and fluoros alcohol.

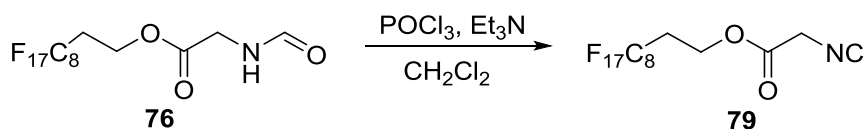
Time (mins)	Temperature (°C)	Calculated yield from HPLC (%)
10	30	17
10	40	23
10	50	29
20	30	33
20	40	39
20	50	44
40	60	59
40	70	41
40	80	39
50	60	38
50	70	46

The next stage was to attempt the reaction of **75** under the optimised continuous flow conditions. The starting material was not soluble in the original solvent (chloroform) so 3:1 dichloromethane:methanol was used instead, to circumvent this problem. Unfortunately, when it came to transferring the optimal continuous flow conditions to this *N*-formylglycine reaction no product was formed as shown by the crude NMR spectra as only the starting materials were present. This could be due to the large excess of methanol over the fluoros alcohol and so formation of the methyl ester is a possibility. No further optimisation attempts were performed.

2.3.3 Synthesis of the Isocyanide by Dehydration of the Fluorous Tagged *N*-formyl Ester

The final step in the reaction cascade towards the synthesis of fluoros tagged isocyanacetate was the dehydration of the fluoros tagged *N*-formyl ester **76**. Triphosgene and phosphorus oxychloride were both employed as dehydrating agents. It was found after several attempts that phosphorus oxychloride gave the

best yields (Scheme 31) but a number of problems with purification were encountered. The product was shown to be present in a crude IR spectrum by the presence of the isocyanide band ($\sim 2122\text{ cm}^{-1}$). The crude material was then run through the F-SPE cartridge, only to discover that the product was no longer present in the fluorinated fraction. The ^1H NMR spectra did show the presence of the fluorinated alcohol starting material **73**, suggesting the product was broken down on the F-SPE column. The reaction was repeated and a standard silica column was employed as the purification technique. Again no product was found after purification. Following this, purification was successfully realised by addition of 1% triethylamine when running the silica column to reduce the acidity. The product was obtained with a 38% yield, however, the ^1H NMR spectra and elemental analysis showed it had not been obtained in pure form. The estimated purity from ^1H NMR was 63%.

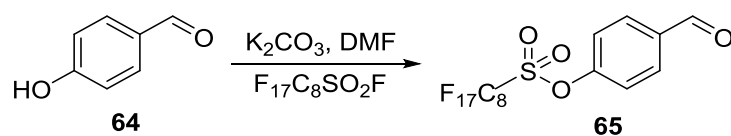


Scheme 31. The synthesis of fluorinated isocyanoacetate **79**.

With the difficulties presented by purification it was decided to use the isocyanide in subsequent steps without further purification. A heterocyclic formation reaction discussed in later chapters was performed to test the utility of this method. After two attempts at such reactions the majority component of the reaction mixture was determined by ^1H NMR as the fluorinated alcohol **73**. As the main benefit of using a fluorinated tag is the ease of separation due to the fluorinated chain, and the fluorinated chain should be straightforward to remove from the starting material or product in a controlled manner, all advantages of the fluorinated technology have been lost in the cases investigated here.

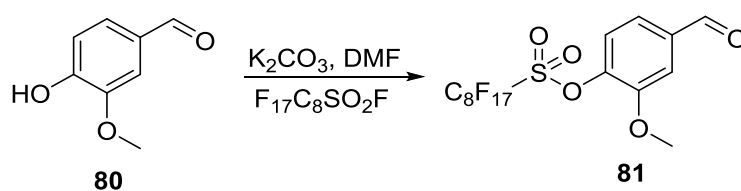
2.4 Synthesis of Fluorous Tagged Benzaldehyde

As isocyanide **79** proved to be unstable it was decided to carry on the proof-of-concept chemistry using an alternative fluorous-tagged compound. This would, therefore, allow the investigation of the use of fluorous technologies in the formation of heterocycles under continuous flow conditions, as originally planned. As described earlier in section 2.1.4 the fluorous tagged derivative of 4-hydroxybenzaldehyde has been utilised in a number of reactions since its introduction⁵⁴ and has the ability to be easily removed as the chemistry is similar to that of a triflate group. Since the multi-component reactions that were to be investigated in this project usually involve an aldehyde it was decided to tag the aldehyde instead.



Scheme 32. The synthesis of fluorous aldehyde.

The fluorous-tagged derivative of 4-hydroxybenzaldehyde was synthesised according to the method of Zhang *et al.*⁵⁴ in an excellent yield of 97% (Scheme 32). Due to the ease of synthesis combined with the high yield it was decided to continue with the heterocycle formation reactions under continuous flow conditions using benzaldehyde derivative **65**. The reaction was also carried out on vanillin **80** to form a fluorous vanillin derivative (Scheme 33) in a yield of 94%.



Scheme 33. The synthesis of fluorous vanillin derivative **81**.

2.5 Conclusions

As discussed in section 1.4 there are several advantages to the use of fluororous technologies in the separation of reaction mixtures. The separation of products using F-SPE has caused the number of 'light' fluororous chains used in synthesis to increase dramatically, several of which (including the varying types of fluororous tag) have been discussed in the introduction section (2.1.1-2.1.4). The methods of removal of these fluororous tags have also been developed, and these earlier studies should all help to determine the methods of formation and deprotection of other fluororous tagged compounds, such as the ones planned in this project.

Due to the mild conditions used to remove the fluororous tag in the work described by Fustero *et al.*⁵⁰ it was decided to use the same tag, **48** ^FTMSE-OH, in the heterocyclic formation reactions proposed to be performed under continuous flow chemistry, as described in section 1.6. Further purification techniques were required than reported and the expense of the starting material meant that another commercially available starting material was investigated.

Formation of the allyl **69** and vinyl **68** functionalised silyl intermediates was achieved in acceptable yields of 70% and 65% respectively according to the same method laid out by Fustero⁵⁰ with the extra purification step of distillation. Several attempts to convert these intermediates into alcohol **70**, the proposed fluororous protection reagent for *N*-formylglycine, by a variety of methods then followed: hydroboration; ozonolysis; diol formation, followed by oxidative cleavage. The only method that worked in synthesising alcohol **70** was ozonolysis, though the optimised conditions were varied from those laid out by Fustero *et al.*⁵⁰ The revised conditions involved changing the solvent from dichloromethane to a solvent system of 5:1 dichloromethane:methanol as well as the addition of sodium hydrogen carbonate. The ozonolysis was worked up using dimethyl sulfide and then the resulting aldehyde **72** was reduced with sodium borohydride. As the product was found to be unstable and proved difficult to purify, the use of a commercially available alternative **73** was adopted instead.

The Fustero group have reported the further use of the ^FTMSE-OH in peptide synthesis as described in the paper initially describing the fluororous tag⁵⁰ and also

in a follow-up publication describing the synthesis of β,β -difluorinated cyclic quaternary α -amino acid derivatives.⁶² There is no mention of instability when using or synthesising **48** in either paper and there have been no references from other groups of the fluoros tag to determine any problems in stability ascertained elsewhere. There is a possibility that switching to the cheaper starting material **46** may have been a retrograde step and caused further problems. The instability of the product is likely due to the Peterson rearrangement as described in section 2.2.

The coupling reactions of the commercially available fluoros alcohol with *N*-formylglycine were investigated and the optimum conditions were determined to be as follows, PyBOP as the coupling reagent, a ratio of reagents of 1:1.5:2:4 (fluoros alcohol: *N*-formylglycine: PyBOP: DIPEA) and 48 hours at reflux. These optimal conditions gave a yield of 58%.

The final step in the formation of the target intermediate, fluoros tagged isocyanoacetate derivative **79** was dehydration of the formamide to form the isocyanide group. Characterisation showed that the isocyanide was formed, however, there were issues with purification once again. After taking a crude mixture forward into the next stage of reaction, F-SPE provided mainly the recovered fluoros alcohol starting material, suggesting the fluoros ester is not as stable as expected. It was then decided that the advantages of F-SPE were lost given the instability of the product and the other difficulties encountered, so alternative fluoros tag strategies were investigated.

The synthesis of the fluoros tagged 4-hydroxybenzaldehyde **65** and fluoros vanillin **81** were performed as stated in the literature⁵⁴ and provided in excellent yields of 97% and 94% respectively. It was decided that these compounds would be the fluoros tagged reactants to be used in the heterocyclic formation reactions under continuous flow conditions.

3. Synthesis of Imidazo[1,2-a]pyrimidines

3.1 Introduction

Imidazo-heterocycles are versatile building blocks for use in lead compound discovery and have shown promise in a majority of therapeutic areas due to their pronounced biological activity.⁶³ Figure 19 shows the synthetic scaffold of fused imidazo-heterocycles that are commonly seen in biologically relevant compounds. A derivative of imidazo-pyrazines, **83**, have shown activity for cardiac stimulation, the treatment of depression and uterine relaxing.⁶⁴ Compounds containing the imidazo-[1,2-a]pyridazines structure **84** have been shown to be corticotrophin-releasing factor receptor 1 antagonists with efficacy in animal models of alcoholism.⁶⁵ Structure **85** is a chemotype representing the class of compounds loosely defined as imidazopyridines. The main use of these structures falls under the category of proton pump inhibitors.⁶⁶

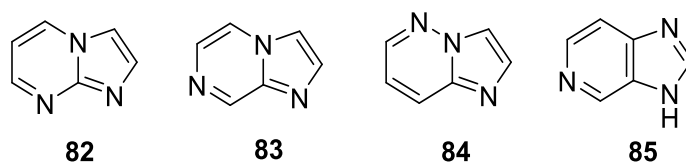


Figure 19. Commonly seen fused imidazo-systems in pharmacological relevant ligands.

This chapter focuses on the imidazo[1,2-a]pyrimidine substructure **82** which is central to several clinical candidates. Examples of these structures are shown in Figure 20 and include divaplone **86**, an antagonist of GABA_A receptors, investigated as anxiolytic and anticonvulsant agents.⁶⁷ The substructure can also be found in **87**, investigated as an androgen receptor antagonist and is currently under ongoing preclinical development.⁶⁸

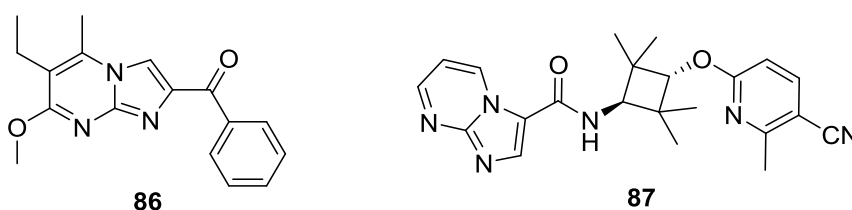
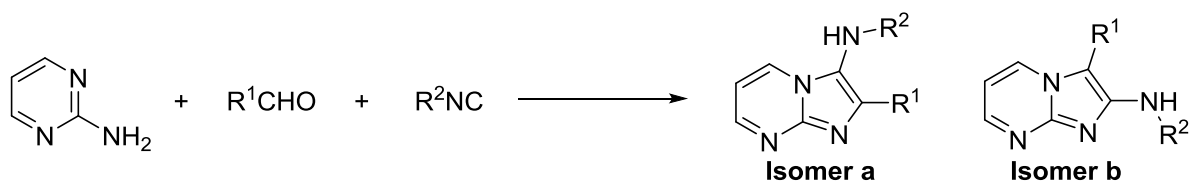


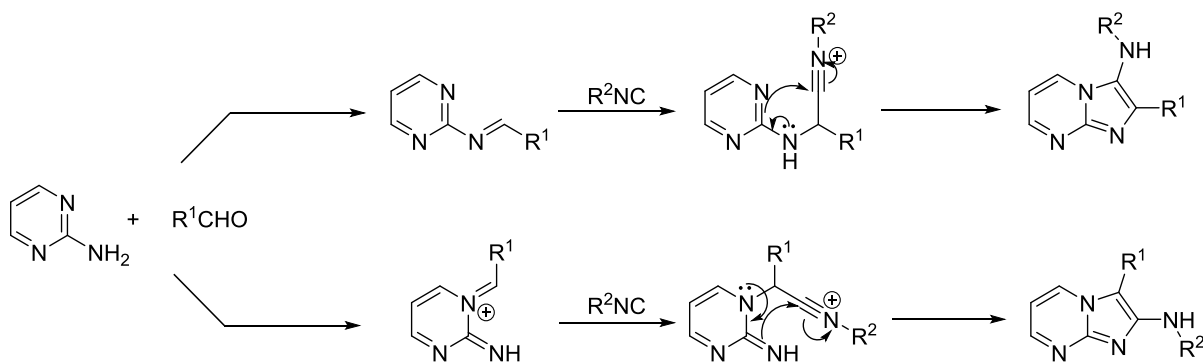
Figure 20. Examples of pharmaceutically viable candidates containing the imidazo[1,2-a]pyrimidine structure.

Several groups, Blackburn,⁶⁹ Bienaymé⁷⁰ and Groebke,⁷¹ independently reported the synthesis of imidazo[1,2-*a*]pyrimidines *via* an 'Ugi-type' MCR, which is commonly referred to as the Groebke-Blackburn reaction. The MCR involves the combination of an aldehyde, isocyanide and 2-aminopyrimidine (when in context of imidazo[1,2-*a*]pyrimidines), catalysed by either a Brønsted or Lewis acids (typically 2.5 mol% Sc(OTf)₃) in an organic solvent (Scheme 34).



Scheme 34. The Groebke-Blackburn three-component approach to imidazo[1,2-*a*]pyrimidines.

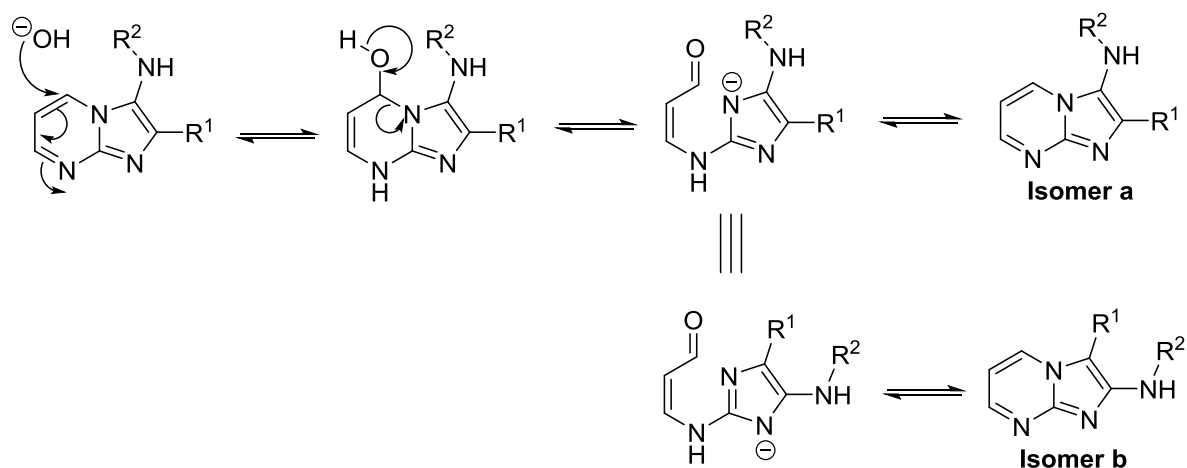
The reaction shown in Scheme 34 provides a mixture of regioisomers with a yield of approximately 50%. Scheme 35 shows the mechanistic rationale behind the production of the two isomers. The initial step of the mechanism is the formation of the iminium species, which can be generated by addition of the aldehyde to either the primary amine group or the ring nitrogen. This is followed by the attack of the isocyanide on the iminium group, intramolecular cyclisation, and finally aromatisation.



Scheme 35. Mechanistic rationale for the formation of a product mixture in the multicomponent reaction with 2-aminopyrimidine.

Although the MCR provides excellent atom efficiency, the mixture of regioisomers formed poses a problem in product efficiency. The Dimroth rearrangement allows the conversion of the 3-amino isomer **a** to the 2-amino isomer **b** with the addition

of a reaction step (Scheme 36).⁷² The rearrangement occurs *via* hydroxide attack at the 5-position to form a hemiaminal, which converts to the aldehyde intermediate. This structure can revert to the 3-amino isomer or convert to the 2-amino isomer. All the steps of the rearrangement are reversible. As the major product is the 2-amino isomer this is shown to be the thermodynamically favoured product.⁷³



Scheme 36. Dimroth rearrangement to the thermodynamically stable product.

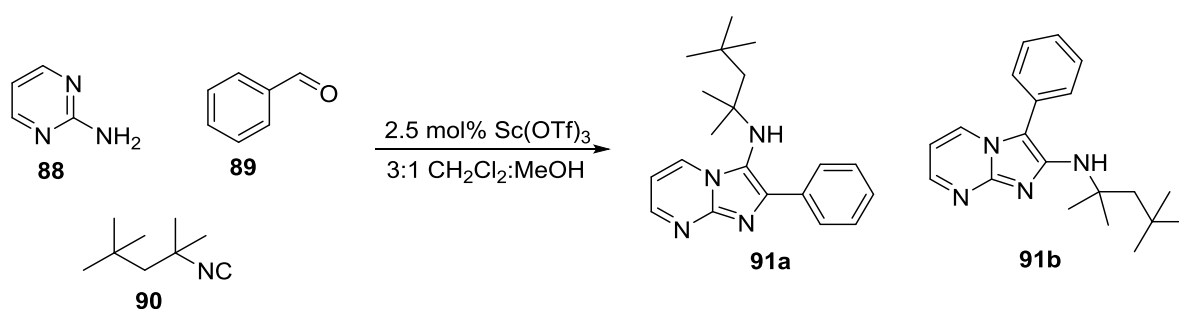
This group previously demonstrated, with the use of NOE experiments and X-ray crystallography, the faster eluting product on a column and, therefore, the less polar product, is the **b** isomer (2-amino).⁷⁴ The 3-amino isomer is the more polar product and eluted after the 2-amino isomer. It was also reported that a higher regioselectivity could be obtained using microwave conditions in the presence of hydrogen zeolite.¹⁰ These conditions were shown to be feasible for a variety of starting materials. However, scale-up has always been an issue when discussing microwave conditions for reactions. The main benefit of continuous flow chemistry is the ease of scale-up, and it was this reason why it was decided to investigate the synthesis of imidazo[1,2-*a*]pyrimidines using continuous flow conditions.

This work demonstrates the regioselective synthesis of 3-aminoimidazo[1,2-*a*]pyrimidines under continuous flow conditions and the synthesis of a small

library to show the scope of the reaction. The synthesis includes the use of 4-perfluorooctylsulfonyloxybenzaldehyde **65** to demonstrate the use of F-SPE in the formation of 3-aminoimidazo[1,2-a]pyrimidine and to compare the results of those synthesised without the use of a fluororous tag. Finally, the removal of the fluororous tag is demonstrated by a palladium cross coupling reaction.

3.2 Optimisation of Reaction Conditions

To produce the HPLC calibration curves required for optimisation of the reaction conditions it was first necessary to produce a significant quantity of both of the isomers so that concentration gradients could be made. This was done using batch conditions at 45 °C for 48 hours (Scheme 37) producing isomer **91a** in 23% yield and isomer **91b** in 25% yield. The calibration curves were produced using the area under the peak of analytical HPLC chromatographs at a variety of concentrations (method described in section 2.3.2).



Scheme 37. Reaction of 2-aminopyrimidine, benzaldehyde and Walborsky's reagent using 2.5 mol% of Sc(OTf)₃ to form a mixture of isomers used to form the calibration curves for reaction optimization.

To improve the yield and regioselectivities, a flow procedure was explored. Firstly the optimisation of residence time reactions were carried out. Reactions were performed with residence times of 2, 4, 6, 8, 10, 15, 20, and 50 mins and the results are shown in the graph below (Figure 21).

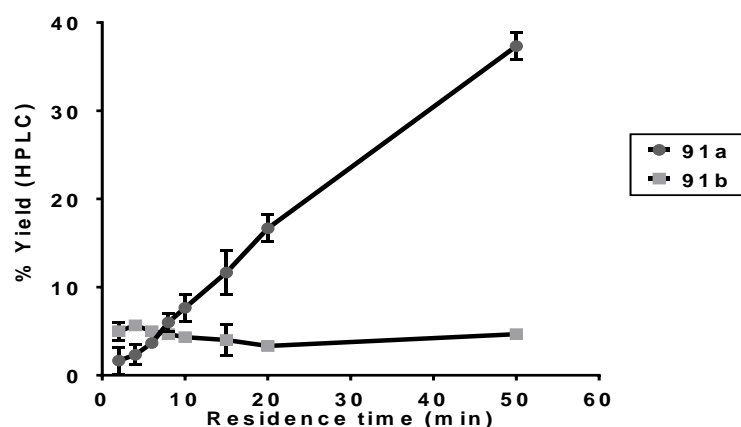
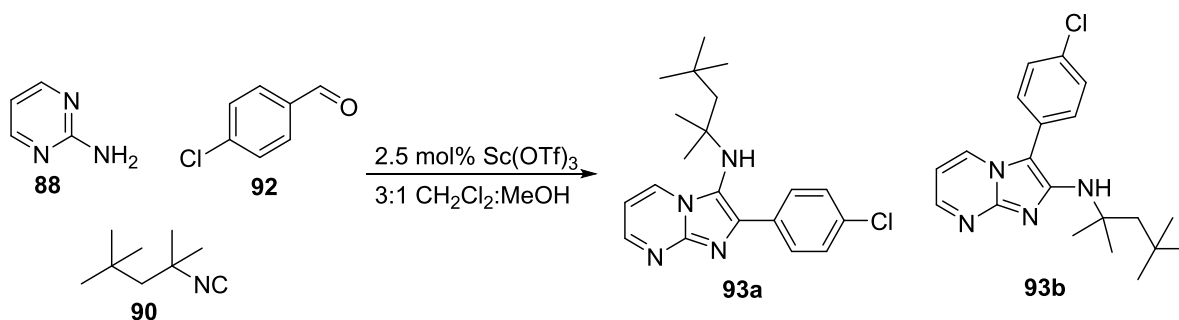


Figure 21. Yields of 2-phenyl-*N*-(2,4,4-trimethylpentan-2-yl)imidazo[1,2-*a*]pyrimidine-3-amine (**91b**) and 3-phenyl-*N*-(2,4,4-trimethylpentan-2-yl)imidazo[1,2-*a*]pyrimidin-2-amine (**91a**) with varying residence times at 70 °C using 10 mol% ZrCl₄.

The yield increases in a linear fashion as the residence time increases and this pattern continued up to 50 mins residence time maximum. It is likely that the yield of isomer **91a** would have continued to increase with residence times greater than 50 mins, however, the flow rates become too low to provide reproducible results at residence times longer than 50 mins.

It was noticed during the optimization of residence time reactions that in the earlier stages of the reaction the ratio of regioisomers is different to that after longer residence times. It would appear that the production of **91b** is greater at the start of the reaction and then decreases over time. It was decided to perform a timed experiment in batch conditions to determine if the pattern occurs under both conditions. The reaction of 2-aminopyrimidine, 4-chlorobenzaldehyde and Walborsky's reagent using 2.5 mol% loading of $\text{Sc}(\text{OTf})_3$ gave a mixture of **93a** and **93b** with yields of 19% and 24% respectively (Scheme 38). Calibration curves were constructed using varying concentrations of the products and analytical HPLC chromatographs as described above.



Scheme 38. The reaction of 2-aminopyrimidine, 4-chlorobenzaldehyde and Walborsky's reagent to form a mixture of isomers used to create calibration curves for the timed experiment.

Small aliquots of the reaction mixture were taken and diluted; analytical HPLC analysis was run on the samples over several periods of time. The aliquots were taken at 0.5, 1, 2, 4, 8, 12 and 24 hours (Figure 22). The results showed that shorter reaction times led to the formation of relatively more of isomer **b**. The ratio of isomer **b** to isomer **a** decreases with continued heating. The results imply that the system is held in dynamic equilibrium and, therefore, all the steps of the mechanism of the reaction (Scheme 35) are reversible. The results also imply

that isomer **b**, the 2-amino isomer, is the kinetic product and isomer **a**, the 3-amino isomer, is the thermodynamic product.

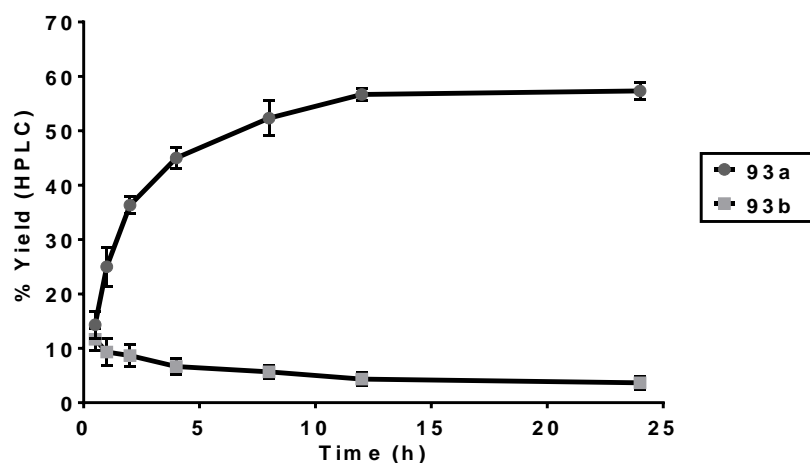


Figure 22. Yields of 2-(4-chlorophenyl)-*N*-(2,4,4-trimethylpentan-2-yl)imidazo[1,2-*a*]pyrimidine-3-amine (**93b**) and 3-(4-chlorophenyl)-*N*-(2,4,4-trimethylpentan-2-yl)imidazo[1,2-*a*]pyrimidine-2-amine (**93a**) over time using traditional batch conditions and 10 mol% ZrCl_4 .

The next stage of the optimization was to determine the requisite temperature of the reaction. The reaction was carried out under continuous flow conditions with the optimized residence time of 50 mins and a catalyst loading of 10 mol% ZrCl_4 . The crude reaction mixture was analysed by analytic HPLC to determine the yield. The results (Figure 23) show an increase in yield with the increase in temperature with the ratio of isomers remaining the same across the variations.

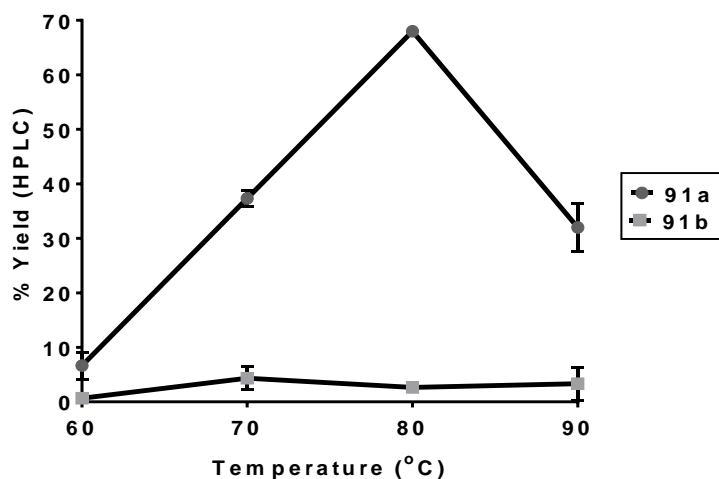


Figure 23. A graph to show the yield of 2-phenyl-*N*-(2,4,4-trimethylpentan-2-yl)imidazo[1,2-*a*]pyrimidine-3-amine (**91b**) and 3-phenyl-*N*-(2,4,4-trimethylpentan-2-yl)imidazo[1,2-*a*]pyrimidin-2-amine (**91a**) with varying temperature using 50 mins residence time and 10 mol% ZrCl_4 .

The yield decreases above 80 °C and the results are less reproducible. This is likely due to the temperature being significantly above that of the solvent boiling point and, therefore, there is partial evaporation of the solvent within the reactor coil causing an increase in system pressure. The results of the optimisation reactions show that the optimum conditions for the reaction occur at a residence time of 50 mins and at 80 °C.

The Groebke-Blackburn reaction has been published utilizing both $\text{Sc}(\text{OTf})_3$ ⁶⁹ and, more recently, ZrCl_4 ⁷⁵ as the Lewis acid catalysts. The next step was to evaluate the catalyst and the loadings under continuous flow conditions to determine which was the best catalyst to use. The results were also compared to the batch conditions to demonstrate the advantage of using the catalysts in the continuous flow reactions, and the reaction mixture was analyzed using analytic HPLC to determine the yield. The results and the comparison to the batch conditions⁷⁶ are depicted below (Figure 24). The results showed that while there is an increase in regioselectivity for the 3-amino isomer **91a** in batch conditions when the ZrCl_4 catalyst is employed, there is a greater improvement in regioselectivity for the 3-amino isomer **91a** across all catalysts when the reaction was conducted under continuous flow conditions.

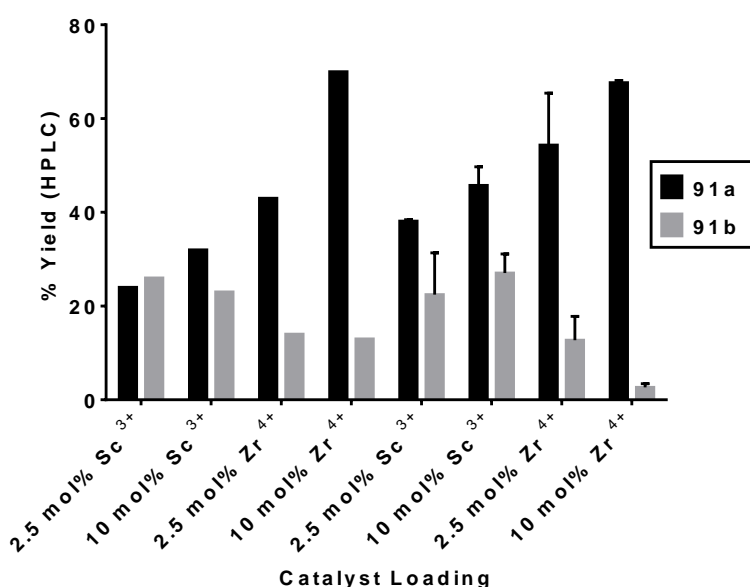


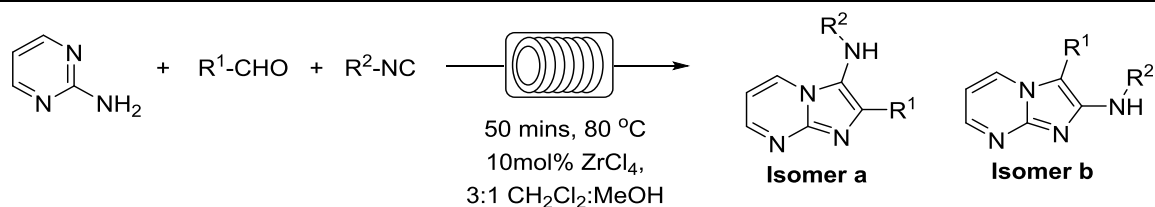
Figure 24. A graph to show the varying yield of 2-phenyl-*N*-(2,4,4-trimethylpentan-2-yl)imidazo[1,2-*a*]pyrimidine-3-amine (**91b**) and 3-phenyl-*N*-(2,4,4-trimethylpentan-2-yl)imidazo[1,2-*a*]pyrimidine-2-amine (**91a**) with varying Lewis acid catalyst and loadings under both batch and continuous flow conditions. Batch conditions; 45 °C for 24 hours. Continuous flow conditions; 80 °C for 50 mins.

The reaction run with 10 mol% of ZrCl_4 gave isomer **91a** in 68% yield, which is comparable to the result obtained under batch conditions (70%). However, the regioselectivity with this catalyst and loading has been vastly improved from 5:1 under batch conditions to over 20:1 using continuous flow conditions. It was, therefore, determined that the ideal conditions for the reaction are a residence time of 50 mins at 70 °C with 10 mol% ZrCl_4 catalyst.

3.3 Library Synthesis

To investigate the scope of the new reaction conditions a small library of compounds was synthesized (Table 7). The yields for the isolated products were shown to be consistent with the ratio of regioselectivity being consistently high.

Table 7. Library of compounds synthesised by the continuous flow adaption of the Groebke-Blackburn reaction with 2-aminopyrimidine.



Product	R ¹	R ²	% Yield Isomer a ^a	% Yield Isomer b ^a
91			61	3
93			52	2
94			45	2
95			60	<1
96			49	<1
97			55	<1
98			43	<1
99			46	-
100			55	<1
101			27	-
102			32	-

^a Isolated yields

All the regioisomer assignments in the table were determined by ^1H NMR spectroscopy as the chemical shifts and R_f values of the different regioisomers have been determined by previous work using NOE experiments and crystal structures.⁷⁷ It can be seen from the table that, in general, the flow synthesis gave high regioselectivity for the 3-amino isomer. In the case of **99b**, **101b**, and **102b** there was no product formed that could be identified by either ^1H NMR spectroscopy or by LC-MS.

The assignment of the isomers of **98a** and **98b** was not as straight forward as the peak for NH in the ^1H NMR spectra appears in the aromatic region and so the chemical shift was not significant enough to show a difference in the two isomers. Several NOE experiments were run to determine the regioselectivity of the major product from the reaction. The data was found to be inconclusive as the signal for the NH proton was close to another proton signal and therefore the signal could not be isolated. Other signals from the NOE experimental data were isolated but did not give any indication of the structure. The data is provided in the supplementary data section. After NOE experiments were not conclusive for the assignment it was decided that a crystal structure was required. The major product was recrystallised, the product had low crystallinity and so recrystallisation in DMF was the only way to form crystals. After crystals were formed, x-ray crystallography (Figure 25, CCDC 972695) helped to identify the structure of the major product of the reaction as the 3-amino isomer (**98a**) and so the regioselectivity of the reaction is maintained with the use of aromatic isocyanides.

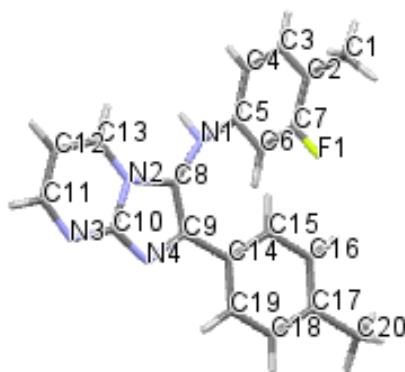
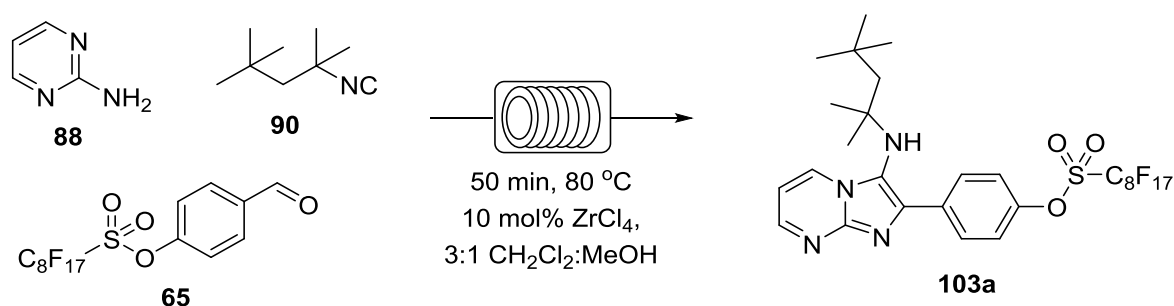


Figure 25. X-ray crystal structure of **98a** for regioisomer assignment.

Despite the products formed from the aliphatic aldehyde starting materials (**101** and **102**) being of a slightly lower yield than shown with the aromatic aldehydes in the library, it was very pleasing to see some product formation as only starting materials were recovered after 48 hours at reflux when the same reactions were run in batch conditions. The reaction mixture from the reaction performed in batch was analysed by ^1H NMR spectroscopy and by HPLC to show no formation of the desired product. As there was no isomer **b** formed in the reaction performed by continuous flow conditions it would not possible to compare the HPLC data, however, there was no desired product shown by ^1H NMR spectroscopy. It can therefore be stated that continuous flow conditions allow the reaction to occur when it does not occur in batch conditions.

3.4 Use of Fluorous Technologies in Imidazopyrimidine Synthesis

After the conditions for the continuous flow synthesis were optimised and shown to be effective for a range of starting materials, the MCR was carried out using the synthesised fluorous benzaldehyde derivative **65**. The reaction was performed with a residence time of 50 mins at 80 °C using Walborsky's reagent as the isocyanide component (Scheme 39). After the reaction was completed the crude mixture was purified by F-SPE. Firstly, the cartridge was washed with 4:1 MeOH: H₂O to remove the organic fraction followed by MeOH to remove the fluorous fraction containing the product. ¹H NMR spectroscopy showed that the mixture still contained some impurities and so a recrystallisation with CH₂Cl₂/petroleum ether was performed. After purification a product yield of 64% was obtained.



Scheme 39. The continuous flow synthesis of fluorous tagged 4-(3-(2,4,4-trimethylpentan-2-ylamino)imidazo[1,2-a]pyrimidin-2-yl)phenyl perfluorooctane-1-sulfonate **103a**.

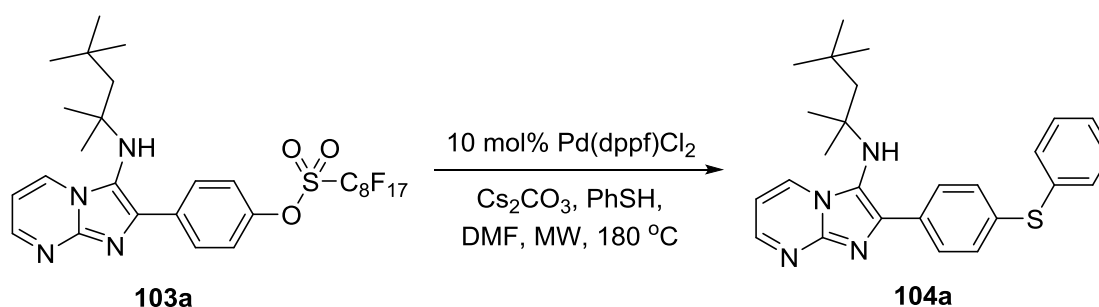
The yield of isolated product of the reaction is slightly higher than the yields of other compounds synthesised in the library. The highest yielding reaction in the library synthesis (section 3.3) was the reaction of Walborsky's reagent and benzaldehyde to give product **91a** to give a yield of isolated product of 61% (HPLC yield of 67%). The yield of **103a** being comparable to the synthesis of **91a** showed that the fluorous tag did not interfere with the reaction and the tag was stable under the reaction conditions. The increase in yield could be explained by considering the purification method. F-SPE is a short column that resembles more of a filtration rather than column chromatography and is also neutral as opposed to the slight acidity of silica. This could mean that the product is more

stable on the F-SPE column and so product recovery from purification is enhanced.

The crude ^1H NMR spectra of the reaction did not show peaks associated with isomer **104b**. However, this could have been due to a low concentration of product. After the F-SPE a second ^1H NMR spectrum was recorded that once again showed no peaks concurrent with isomer **104b** (a singlet peak that had an integral for one hydrogen ~ 4.30 ppm). After recrystallisation of the product from the F-SPE, the solvent system used was also separated, concentrated at reduced pressure and then analysed by ^1H NMR spectroscopy. Again there were no characteristic peaks for the isomer and so LCMS was run. The correct mass ion could not be found. It is, therefore, acceptable to conclude that the isomer **104b** was not synthesised by this method.

3.5 Removal of the Fluorous Tag

In 2004, Zhang and Lu⁷⁸ reported the formation of fluorous tagged imidazo[1,2-a]pyridines and the Pd catalysed cross-coupling reaction used to remove the fluorous tag. The reactions reported included a Suzuki reaction and a coupling with a thiol. Thus, it was decided to perform a Pd catalysed cross coupling reaction with thiophenol to demonstrate the ease of fluorous tag removal on these compounds (Scheme 40).



Scheme 40. The palladium cross coupling reaction of the fluorous tagged imidazopyrimidine and thiophenol.

The procedure was adapted slightly from that reported by Zhang and Lu,⁷⁸ a ramp time of 10 mins and a reaction time of 10 mins were employed. The reaction mixture was also subjected to an aqueous work up prior to purification by F-SPE as the Pd by-products can damage the F-SPE columns. The reaction was purified by F-SPE eluted with 4:1 MeOH:H₂O to give the non-fluorous fraction. The non-fluorous fraction was found to be impure and so the mixture was subjected to flash column chromatography to give the pure product in a 46% yield.

3.6 Conclusions

The Groebke-Blackburn reaction of 2-aminopyrimidine, an isocyanide and an aldehyde was optimised for formation under continuous flow conditions. The optimum reaction conditions were found to be a 50 mins residence time at 80 °C with 10 mol% ZrCl₄ catalyst. The results showed an improvement in regioselectivity from 5:1 under batch conditions to over 20:1 for the same reaction carried out under continuous flow conditions.

The scope of the reaction was investigated by the synthesis of a small library. The results of the library showed that the conditions worked for a range of starting materials and the regioselectivity was consistently high for all products. In some cases the regioselectivity was as high as 60:1 (in the case of **95**). The continuous flow conditions also allowed for the synthesis of products **101** and **102**, which were not found to be present when the reactions were carried out under batch conditions.

The reaction was then carried out utilising the fluororous tagged starting material **65** as the aldehyde component. The reaction provided the 3-amino isomer with a 64% yield and did not show any evidence of the formation of the 2-amino isomer. The fluororous tag removal was also demonstrated by a Pd catalysed cross coupling reaction with thiophenol to give the sulfide **104a** with a 46% yield.

4. Synthesis of Oxazolines

4.1 Introduction

The synthesis of oxazolines was first recorded in 1884 by Andreasch.⁷⁹ The author discovered that a new heterocyclic structure was present after the dehydrohalogenation of allylurea bromide, however, he did not correctly deduce the structure.⁸⁰ The structure was later determined by Gabriel who further studied the chemistry of the heterocycle.⁸¹ Oxazolines are 5-membered heterocyclic structures containing both oxygen and nitrogen heteroatoms and a double bond. There are three isomers of oxazolines (Figure 26); 2-oxazoline (**105**), 3-oxazoline (**106**), and 4-oxazoline (**107**). The only isomer that is commonly naturally occurring is the 2-oxazoline. The 3- and 4- oxazoline are rare but have been synthesised photochemically⁸² and as an intermediate in the synthesis of azomethine ylides⁸³ respectively.

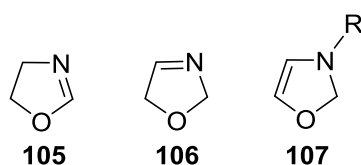


Figure 26. Isomers of the oxazoline heterocycle.

4.1.1 Uses of oxazolines

2-Oxazolines are important intermediates in the synthesis of β -hydroxyamino acids. These structures have been widely investigated due to their presence in several naturally occurring antibiotics (Figure 27). These include, Leucinostatins A and B (**108**) which are isolated from *Paecilomyces lilacinus* and have been shown to have antimicrobial activity against various strains of bacteria and fungi.⁸⁴ The antibiotic hypeptin (**109**) is predominately active against anaerobic bacteria and is isolated from *Pseudomonas*.⁸⁵ While the fermentations of *Lycobacter sp.* produce the antibiotic lysobactin (**110**) which is shown to be potent against Gram-positive aerobic and anaerobic bacteria.⁸⁶

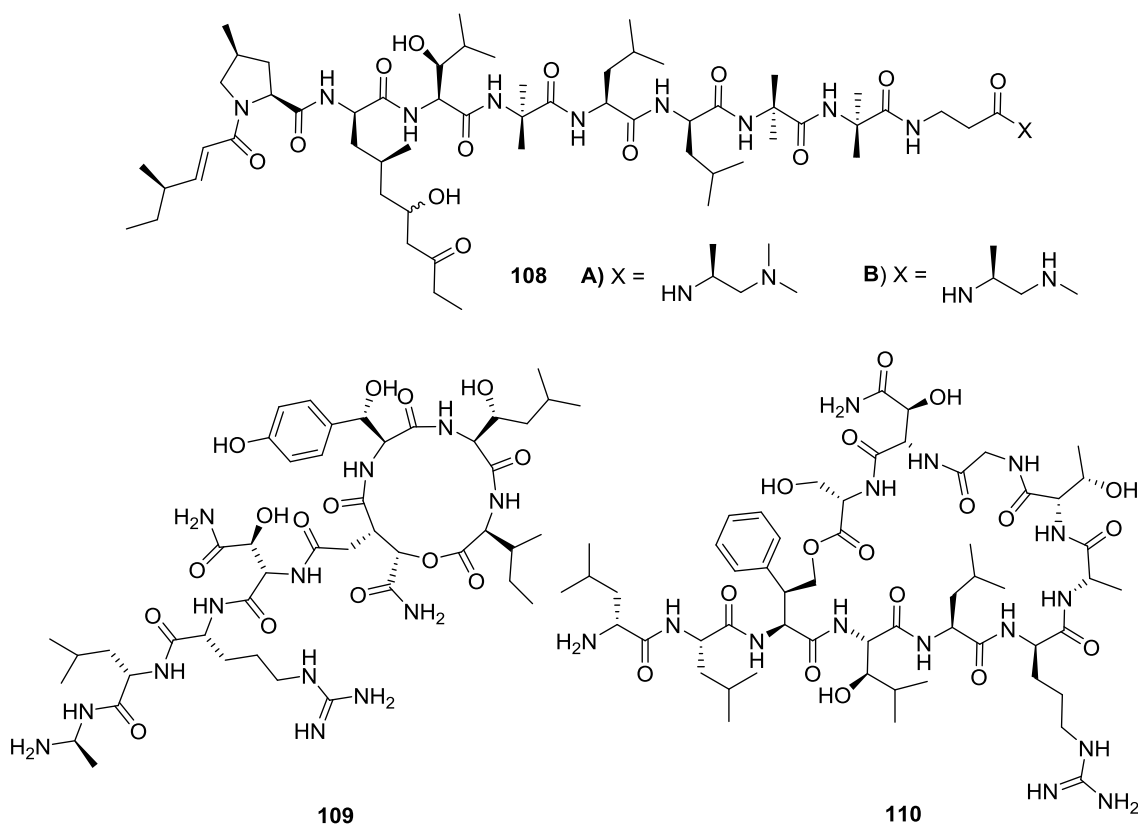
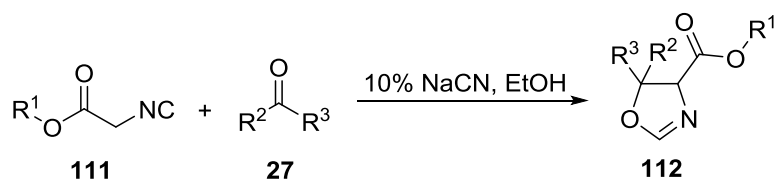


Figure 27. Antibiotics containing the β -hydroxyamino acid moiety.

Oxazolines have been widely reported to convert to the β -substituted serine derivative in the presence of concentrated acid, usually HCl.^{87,88,89} As this is such a widely documented transformation and the reaction is reported as generally high yielding (substrate dependant but usually >90%) it has been the synthesis of 2-oxazolines that have been extensively researched.

4.1.2 Base catalysed synthesis of oxazolines

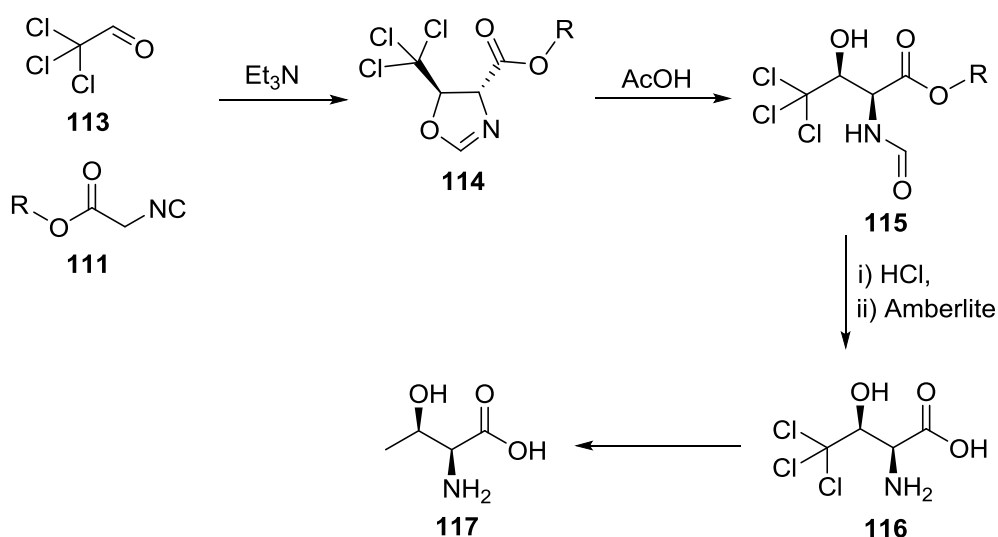
There have been a small number of references about the synthesis of oxazolines using bases. The base typically used is a catalytic amount of NaCN in ethanol which promotes the reaction of aldehydes and ketones with isocyanoacetate.⁹⁰



Scheme 41. Base catalysed synthesis of 2-oxazolines.

The reaction occurs fairly rapidly, in one hour and with high diastereoselectivity (>90% trans) when aldehydes were used compared to ketones. The authors further demonstrated the utility of the method by using an α -substituted isocyanoacetate starting material, ethyl α -isocyanopropionate, although the diastereoselectivity is reduced to <30% trans.

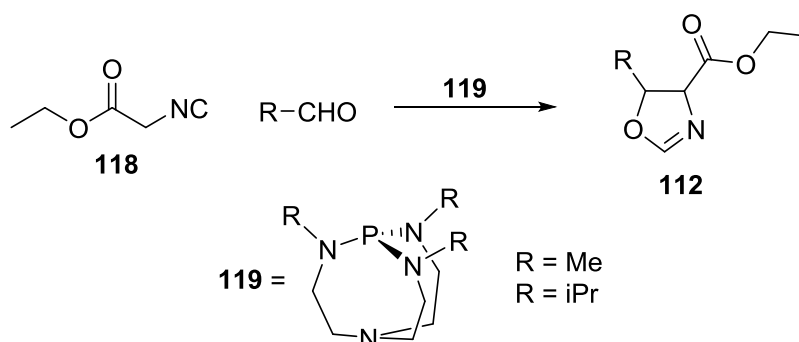
Matsumoto *et al.* reported the synthesis of oxazolines using stoichiometric amounts of Et_3N in the process of synthesising *threo*-4,4,4-trichlorothreonine (Scheme 42). The oxazoline is synthesised from chloral **113** and ethyl isocyanoacetate (**111** derivative). The electron withdrawing nature of the aldehyde allows for the reaction to occur without the need for a catalyst and the steric effect of the bulky trichloromethyl group means that the more thermodynamically favoured product, the trans isomer, is predominately formed giving a stereoselective route to the product **117**. The authors found no evidence of cis isomer formation by this method.



Scheme 42. The synthesis of *threo*-4,4,4-trichlorothreonine via oxazoline synthesis.

More recently, Verkade *et al.* demonstrated the use of a non-ionic catalytic proazaphosphatrane base **119**, previously synthesised by the same group,⁹¹ in the synthesis of several oxazolines (Scheme 43).⁹² The reaction was firstly carried out in THF; however, this afforded a mixture of uncharacterised products that were inseparable. The solvent was therefore changed to isobutyronitrile and this allowed for the synthesis of several oxazolines in high yields and purity. The yields ranged between 68-99% with the majority of the aldehydes used giving yields >90%. The conditions for the reaction, both time and temperature, were optimised for each of the products to obtain the reported yields with times ranging from 15 to 960 mins and the temperature from -63 to 25 °C (Scheme 43).

Even with optimisation for each individual reaction, there were some reactions that only produced small amounts of the product within a mixture of both uncharacterised products and the Knoevenagel product which were inseparable. The aldehyde starting materials that failed to yield any product, despite attempts at optimisation, included; p-nitrobenzaldehyde, isobutyraldehyde, n-heptaldehyde and n-butyraldehyde.



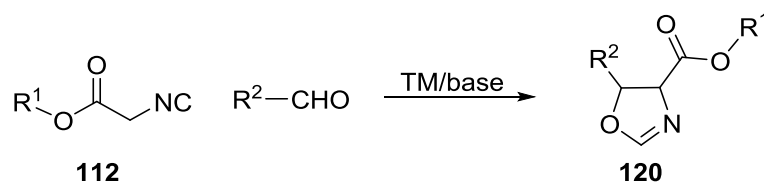
Scheme 43. The synthesis of oxazolines using catalytic bases **119**.

4.1.3 Transition metal catalysed synthesis of oxazolines

Transition metal catalysed formation of oxazolines is one of the most studied transformations in the chemistry of α -isocyanoacetate derivatives.⁴⁴ The complexation of the metal with the isocyano group increases the acidity of the α -H and therefore allows relatively weak bases to extract the proton. The first example of transition metal catalysis was reported by Saegusa *et al.* in 1971

utilising a Cu₂O catalyst.⁹³ The authors demonstrated the synthesis of oxazolines with moderate to good yields (41-85%) and with little to no stereoselectivity. The products were demonstrated using both benzyl isocyanide and ethyl isocyanoacetate as they both contain an acidic α -proton, as well as both aldehydes and ketones as the carbonyl component.

In 2006 Kirchner *et al.*⁹⁴ developed the highly selective and efficient catalytic system of CuCl/PPh₃ following the generalised scheme described below (Scheme 44). The reaction conditions were shown to be effective for a range of aromatic aldehyde starting materials and isobutyraldehyde with methyl isocyanoacetate in the presence of 5 mol% CuCl, 10 mol% PPh₃ and 10 mol% DIPEA. The resulting yields were all greater than 99%, including that of the aliphatic aldehyde example. The trans diastereoisomer is predominantly formed in all examples with high selectivity, >86%.



Scheme 44. Transition metal catalyzed reaction of isocyanoacetates and aldehydes to form oxazoline.

Enantioselective examples of oxazoline synthesis have not yet been reported with copper catalysts; however, there have been several examples of gold chiral complexes. The first was reported by Ito and Hayashi in 1986.⁸⁸ The paper discussed the *in situ* complexation of the previously reported bis(cyclohexyl isocyanide) gold (I) tetrafluoroborate⁹⁵ with the ferrocenylphosphine ligand (Figure 28, **121**) synthesised by the same method developed in an earlier report by Hayashi.⁹⁶ When benzaldehyde was used as the starting material the diastereoselectivity was shown to be 89% trans isomer. The enantioselectivity of the reaction was shown to be very high, 96% 4*R*,5*S*. Further reactions were carried out with several aliphatic aldehyde starting materials. The diastereoselectivity of the reaction improved with aliphatic aldehydes and improved again with increasing bulkiness. The enantioselectivity remained high for the 4*R*,5*S* configuration with the lowest value recorded at 84% ee.

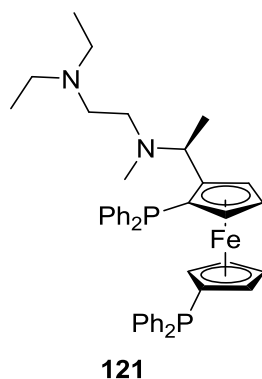


Figure 28. Ferrocenylphosphine ligand synthesised by Hayashi *et al.*

Several further reports have investigated the use of gold (I) catalysts in the formation of oxazoline, however, the majority of reports centre on the bis(cyclohexyl isocyanide) gold(I) tetrafluoroborate with a ferrocenyl phosphine ligand similar to **121** with the derivations around the amine group.^{97,98,99}

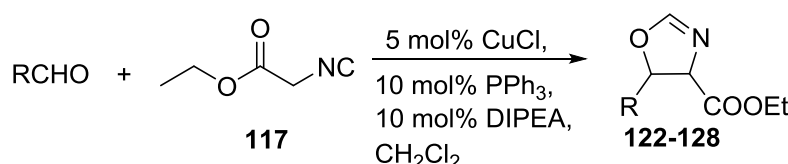
A report in 1997 by Hayashi *et al.*⁸⁹ compared the use of various transition metals as catalysts for this transformation, including Cu, Au, Ag, Pd and Rh. The majority of the transition metals gave high diastereoselectivity for certain substrates; however, the authors also presented results of the same catalyst and base system that showed no diastereoselectivity or even selectivity for the *cis* isomer over the *trans* isomer. The effect of the catalyst/base system as well as the electronic and steric effects of the starting material is profound when discussing diastereoselectivity with these catalysts.

As yet there have been no reports of enantioselectivity with catalysts other than the gold(I) and ferrocenyl catalysts similar to that described above (**121** derivatives) and diastereoselectivity has been shown to be unreliable with catalysts other than the CuCl/PPh₃ system and gold(I) catalysts.

The synthesis of oxazolines that has previously been reported requires the use of catalytic amounts of strong, often toxic bases or expensive heavy metal catalysts. This report aims to overcome these problems in the synthesis of oxazolines by using continuous flow conditions and with the use of fluoros technologies.

4.2 Oxazoline Synthesis under batch conditions

The reaction conditions optimised by Kirchner *et al.*⁹⁴ showed a consistently high diastereoselectivity and tolerance for a number of starting materials with a readily available catalyst system. These conditions were therefore selected to be investigated in this report (Scheme 45). The catalyst system consisted of 5 mol% CuCl, 10 mol% PPh₃ and 10 mol% N,N-diisopropylethylamine (DIPEA) in dichloromethane.



Scheme 45. Formation of oxazolines under Kirchner's conditions.⁹⁴

The reaction occurs readily in batch with a variety of aldehydes with varying yields as shown in Table 8. Of the oxazoline products shown in Table 8 only three were previously reported by Kirchner (Scheme 45; R= phenyl, 4-nitrophenyl and 2-chloro-6-fluorophenyl). Other aldehyde starting materials were selected to examine the scope of the reaction.

Table 8. Batch synthesis of oxazolines.

Product	R group	Yield (%)	Ratio of trans/cis ^a
122	phenyl	89	>99/<1
123	2-nitrophenyl	80	87/13
124	4-nitrophenyl	99	90/10
125	3-methoxyphenyl	82	91/9
126	4-acetylphenyl	95	90/10
127	2-chloro-6-fluorophenyl	87	93/7
128	<i>n</i> -propyl	55	>99/<1

^a Determined by ¹H NMR spectroscopy

The yields obtained in batch conditions were notably lower than those reported in the paper by Kirchner *et al.*⁹⁴ All yields for all starting materials were reported by Kirchner *et al.* as being >99% including that of the aliphatic aldehyde,

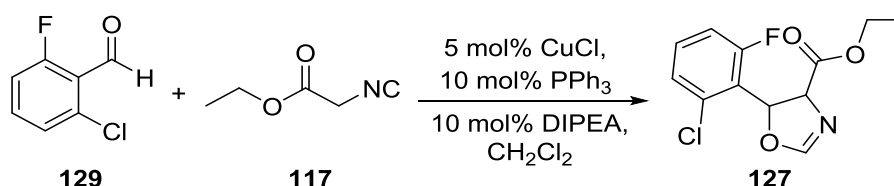
isobutyraldehyde. For comparison, the ratio of diastereoisomers reported by Kirchner for **122** is >99/<1, **124** 90/10 and **127** 93/7. As shown in Table 8 the results for the diastereoselectivity were comparable, if not same, when these conditions were performed under batch conditions.

When the reaction of the aliphatic aldehyde, propionaldehyde, was performed in batch a low yield of 55% was obtained, however, the ratio of diastereoisomers was very high at >99/<1 trans/cis determined by ¹H NMR spectroscopy. The yields of both para-substituted phenyl starting materials provided the highest yields as demonstrated by **124** and **126**. The yields of all aromatic starting materials were 80% or above after purification by flash column chromatography on silica. The products themselves were not very stable, signs of decomposition, through colour change, could be seen if the products were not stored in the freezer overnight. Analysis of the samples by 2D TLC suggested that the products were not particularly stable on silica. This could account for the decrease in yield obtained after purification by flash column chromatography.

After the results for the reaction in batch were obtained the next step was to transfer into continuous flow conditions.

4.3 Optimisation of continuous flow reaction conditions

To optimise the reaction using continuous flow conditions the reaction of ethyl isocyanoacetate **117** with 2-fluoro-6-chlorobenzaldehyde **129** was selected (Scheme 46) as the aldehyde component of the MCR as it is a sterically hindered aldehyde and the yield in batch was not as high as the other examples synthesised (Table 8), therefore optimisation of this reaction is advantageous.



Scheme 46. The reaction of 2-fluoro-6-chlorobenzaldehyde with ethyl Isocyanoacetate to form the corresponding oxazoline.

After the oxazoline product had been formed in batch and purified, several samples of varying concentration were analysed by HPLC. The calculated areas under the peaks obtained from the HPLC were plotted against the concentration to form a calibration curve (Figure 29).

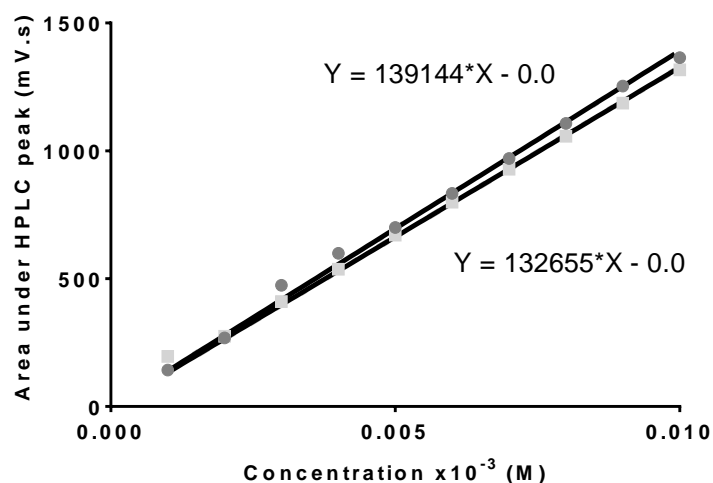


Figure 29. Calibration curve for oxazoline synthesis.

The added trend lines provide the graph equation and the gradient of the trend line were then used to calculate the unknown yield of a crude reaction product.

This allows for the accurate determination of the reaction yield without loss of product in the purification process.

The catalyst system (CuCl/PPh₃) proved to be the limitation for solubility, several solvents and solvent systems were therefore investigated. Solvents investigated included diethyl ether, ethyl acetate, THF and methanol. A reduced concentration (0.25 M) of reagents in a solvent system of 3:1 dichloromethane: methanol was found to be most effective. However, the reduction in the concentration for the reaction meant that the output of the reaction per hour would be drastically reduced and so it was decided to investigate the reaction under more soluble conditions. As there have been a limited number of reports of oxazoline synthesis utilising strong bases⁹⁰ it was decided to attempt the reaction under continuous flow conditions with a milder, more soluble base (DIPEA) in the absence of the Cu catalyst.

The reaction was carried out with a residence time of 10 mins at 60 °C and the crude reaction mixture was analysed by analytic HPLC. A 1 M solution of ethyl isocyanoacetate with a stoichiometric amount of DIPEA was mixed with a 1.14 M solution of 2-chloro-6-fluorobenzaldehyde. The chromatography showed a peak corresponding to the product **127** and ¹H NMR spectroscopy showed doublet peaks at ~4.80 ppm and ~6.10 ppm, each representing a single proton on the oxazoline heterocycle. These peaks appear to demonstrate the presence of the product in the crude reaction mixture and so it was decided that these reagents would be carried forward with optimisation reactions for oxazoline synthesis under continuous flow conditions.

During the construction of the calibration curve the highest concentration of pure oxazoline solution was 0.01 M. Therefore when the subsequent crude samples obtained from the continuous flow conditions were analysed it was assumed, while making the sample concentrations, that the sample contained pure product and so the area under the HPLC peaks could be compared to those of the calibration curve. The reaction was carried out under various conditions and the crude reaction mixture collected was subjected to an aqueous work-up. A 0.01 M

sample of the crude product is made, by weight, under the assumption that the sample was pure product. An analytical HPLC trace was then run on the sample and the value obtained for the area under the peak at the corresponding retention time is compared to the correlation curve. The reaction conditions (residence time and temperature) are then altered repeatedly and the results were analysed to determine the optimum conditions.

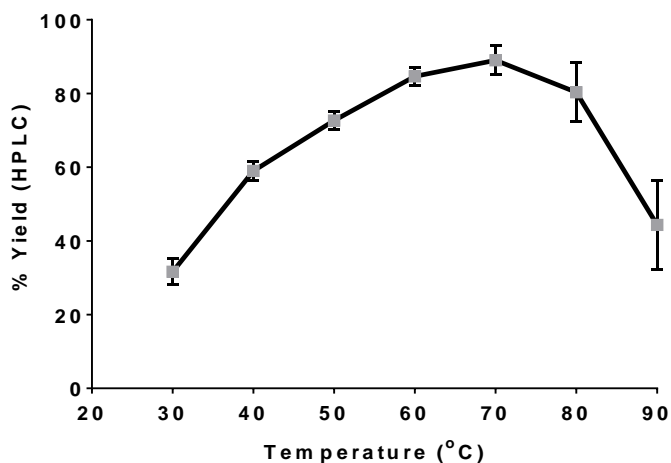


Figure 30. The optimisation of temperature under continuous flow conditions.

Firstly, the effect of temperature was explored. The reaction was run with a residence time of 10 mins and the results obtained from comparison with the HPLC calibration curve are plotted in a graph shown by Figure 30. The results show the temperature that produced the highest yield was 70 °C. Above this temperature the resulting yields drop and the results become less reproducible, possibly due to the temperature being well above that of the boiling point of the solvent and therefore there was likely to be slight evaporation within the tube reactor causing pressure spikes and drops.

The next step was to analyse the residence time. The temperature of the system was maintained at 70 °C and a range of residence times (5, 10, 15, 20, 25 and 30 mins) were explored. The results in comparison to the HPLC calibration curve are represented by Figure 31. At a residence time of 20 mins the maximum yield, an average of 100% yield, was obtained and the results level out to a plateau. It

was, therefore, decided to not continue any further with increasing residence time.

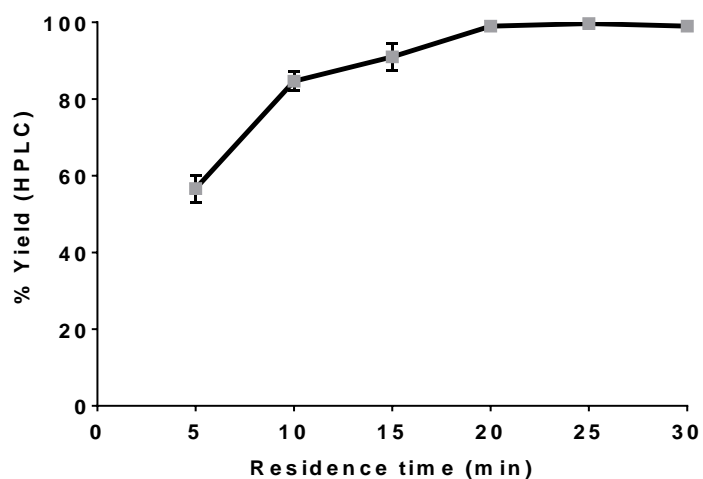


Figure 31. The optimisation of the residence time under continuous flow conditions.

The optimum conditions were therefore determined to be a residence time of 20 mins at a temperature of 70 °C with a stoichiometric amount of an organic base in the place of a catalyst.

4.4 Library Synthesis

Using the optimisation conditions determined several oxazolines were synthesised using a variety of aldehyde starting materials, the same aldehyde starting materials used in the batch conditions. The isolated product yields are shown in Table 8 below after purification with flash column chromatography.

The yield of isolated product **127** is notably less than that of the yield recorded by analytical HPLC, although the yield is comparable to that of the yield recorded for the batch conditions with the CuCl catalyst, and this could be due to the products instability during the purification process. The yield of **128** is markedly improved, by 12%, under continuous flow conditions compared to the batch conditions described above. The continuous flow method provided respectable yields for the other products although several yields were not as high as the batch method with the presence of a catalyst. The yields of the products with para-substitution are again shown to be higher yielding than ortho and meta-substituted products, again this is likely due to stability of the product.

The trans/cis ratio for the products formed under continuous flow conditions are comparable with those produced in batch, with the lowest value of 80/20 for oxazoline **126**. The highest trans/cis ratio across the products was for oxazoline **127** at 91/9 and this is equivalent to the results obtained in the presence of the CuCl catalyst. The trans/cis ratio for oxazoline **123** is improved under continuous flow conditions from 87/13 in batch to 93/7. Overall, the yields and trans/cis ratios are slightly reduced when in comparison to the batch conditions; however the reaction proceeds without the presence of a metal catalyst and within a reduced timeframe.

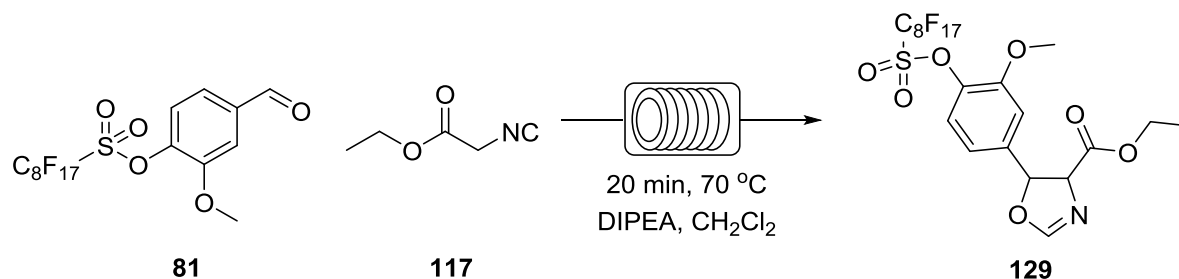
Table 9. The variation of products formed under the optimised continuous flow conditions and the yields obtained.

Product N°	Product	Yield	Ratio of trans/cis ^a
	<p style="text-align: center;">DIPEA, CH₂Cl₂ 20 min 70°C</p>		
122		72	85/15
123		65	93/7
124		74	88/12
125		62	82/18
126		77	80/20
127		86	91/9
128		67	86/14

^a As determined by ¹H NMR spectroscopy.

4.5 Fluorous tagged oxazoline synthesis

The next stage was to investigate the synthesis using fluororous technologies. 3-Methoxy-4-perfluorooctylsulfonyloxybenzaldehyde, **81**, starting material was utilised in this section.



Scheme 47. The reaction of fluororous tagged vanillin derivative and ethyl isocyanoacetate to form a fluororous tagged oxazoline product under continuous flow conditions.

The reaction was performed in slightly different conditions to those described in the library synthesis section above (section 4.4). As described in section 1.4.2, it was preferred that the fluororous starting material is the limiting reagent in the reaction to allow for more efficient purification by F-SPE where possible. The concentrations were altered to a 0.9 M solution of **81** instead of the 1.14 M solution of the previous aldehyde starting materials. After the reagents were subjected to a 20 mins residence time at 70 °C the product mixture was run through a F-SPE column using 4:1 MeOH: H₂O to remove the organic fraction, followed by MeOH to obtain the fluororous fraction.

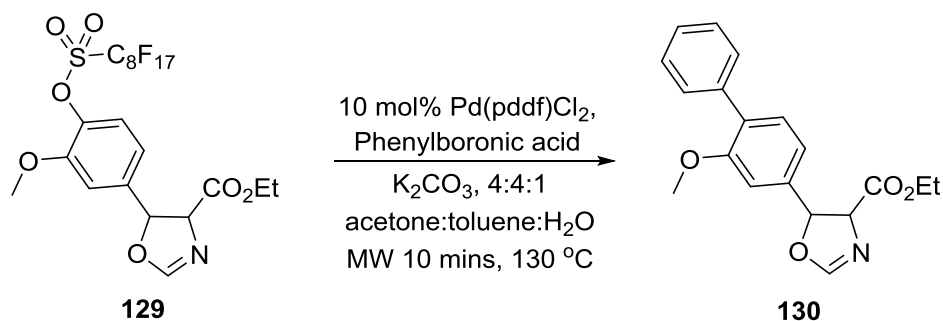
The fluororous fraction gave a white solid which was analysed by ¹H NMR spectroscopy and the spectra showed that the product was pure, with the exception of the mixture of isomers. The ratio of diastereoisomers, trans/cis, was found to be 91/9 (determined by ¹H NMR spectroscopy). Thus the diastereoselectivity of the reaction remained high with the addition of the fluororous tag and under continuous flow reactions.

The isomers were easily separated by running the isomeric mixture through a short column of silica eluted with 1:1 ethyl acetate: petroleum ether. The yield of the reaction was found to be 92% for the trans isomer. The yield was greatly

improved over previous examples under continuous flow conditions. This could be due to the added stability of the product; the previous examples showed signs of degradation overnight, whilst the fluorinated tagged product showed no such signs. The purification method of F-SPE is a mild condition for purification and only a short silica column is required to separate the isomers, compared to the slow running silica column required to purify non-fluorinated tagged products which can cause degradation of the products as shown by 2D TLC analysis.

4.6 Removal of the fluorous tag

Initially the Suzuki reaction was considered for the removal of the fluorous tag due to the extensive literature for this method, with this particular fluorous tag. The reaction was carried out under the microwave conditions laid out by Zhang *et al.* (Scheme 48).¹⁰⁰



Scheme 48. Suzuki reaction of fluorous oxazoline under microwave conditions.

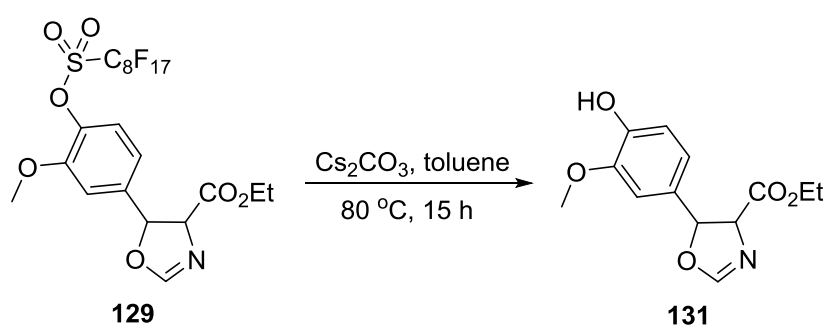
The reaction mixture was purified by F-SPE and the organic fraction was collected. The collected fraction did not show any of the characteristic oxazoline peaks by ¹H NMR spectroscopy (~4.5 dd, ~5.5 d, and ~7.0 d all representing one proton). The spectra showed the presence of an uncharacterised product(s). The fluorous fraction was also collected and the ¹H NMR spectra showed the presence of starting material, however, this was only a small amount in relation to the uncharacterised side product(s). The results described above, the lack of product in the organic fraction and the presence of starting material in the fluorous fraction, were both confirmed by LCMS.

The reaction was also carried out under batch conditions over 72 h at reflux. There was no starting material remaining in the fluorous fraction collected by F-SPE. There was also no product present in the organic fraction, again determined by ¹H NMR spectroscopy and LCMS.

There are a number of studies into the removal of aryl triflate and sulfonic esters including the reduction by lithium aluminium hydride,¹⁰¹ deprotection of the alcohol using TiCl₃ and Li,¹⁰² and countless bases, notably NaOH.¹⁰³ These reagents are either strong reducing agents and therefore unsuitable for the

presence of 2-oxazoline or require an acidic work up which, again, was unsuitable in the presence of a 2-oxazoline.

A recent paper by Agouridas *et al.*¹⁰⁴ demonstrated the cleavage of an aryl trifluoromethanesulfonate group using cesium carbonate. As neither a hard nucleophile nor strong reducing agent was required the protocol was considered a mild approach. These conditions were applied to the deprotection of **129** to form the phenol product **131** (Scheme 49).



Scheme 49. Deprotection of the aryl sulfonate.

The reaction mixture was purified by F-SPE and the organic fraction was collected and analysed by ¹H NMR spectroscopy. The spectra did not show the presence of the characteristic oxazoline peaks described above. The LC-MS of the organic fraction confirmed the reaction did not form the required product. The fluoruous fraction contained a small quantity of starting material, along with unidentified side products (analysis by ¹H NMR spectroscopy).

4.7 Conclusions

The reaction of an isocyanoacetate and an aldehyde to form an oxazoline was optimised for formation under continuous flow conditions. The optimisation reaction was carried out with ethyl isocyanoacetate and 2-chloro-6-fluorobenzaldehyde and the conditions were found to be 20 mins residence time and 70 °C reactor temperature. The reaction was shown to occur under continuous flow conditions in the presence of an organic base, DIPEA, without the need for further catalysis and with high diastereoselectivity.

The scope of the reaction was investigated by the formation of a small library of oxazolines. The synthesis of the library showed that the conditions were adaptable to a range of starting materials. The yields ranged from 62-86% with the stability of the product being accountable for the reduction in yield compared to previously reported yields.⁹⁴ The diastereoselectivity of the reaction was also shown to be high across all the products.

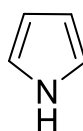
The reaction was also performed utilising the previously synthesised fluoruous vanillin **81** under the optimised continuous flow conditions. The product isomers were purified by F-SPE followed by a short silica column to provide the fluoruous tagged product with a yield of 92% which is markedly higher than the products purified using standard flash column chromatography. The diastereoselectivity of the reaction was unaffected by the presence of the fluoruous tag.

After the deprotection reaction and attempts at palladium-catalysed cross-coupling reactions failed to form the desired products it was decided that the oxazoline structure was not stable enough for the removal of this fluoruous tag. In this case fluoruous technologies are not useful for the synthesis of oxazolines alone. However, the method shows an improvement in yield and purification that could be considered in reactions where the synthesis of the oxazoline is used as an intermediate as the final product could be more stable to the removal process.

5. Synthesis of Pyrroles under continuous flow conditions

5.1 Introduction

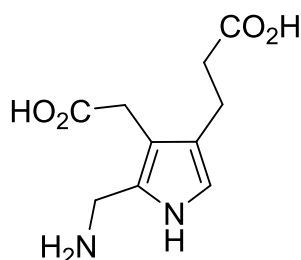
Pyrroles are 5-membered aromatic, nitrogen containing heterocycles with the basic structure shown in Figure 32. The simplest of the compounds, pyrrole (Figure 32) was first isolated in 1834 from coal tar and then in 1857 from the pyrolysate of bone.¹⁰⁵



132

Figure 32. Basic structure of pyrroles.

Pyrroles occur repeatedly in nature, notably in essential macrocycles such as chlorophyll and the porphyrins of haem. Both of these structures are synthesised in cells from glycine and succinyl CoA *via* the trialkyl-substituted pyrrole porphobilinogen **133**.¹⁰⁶



133

Figure 33. Porphobilinogen.

The pyrrole structure can also be found in several naturally occurring antibiotics, including; pyrrolnitrin **134**, pyoluteorin **135**, and pyrrolomycin A and B (**136** and **137**, Figure 34). Pyrrolnitrin is produced by *Pseudomonas pyrrocinia* and has been shown to have antifungal activity and be highly active against dermatophytes.¹⁰⁷ Pyoluteorin is isolated from *Pseudomonas aeruginosa* and has been shown to have a broad spectrum of applications, demonstrating antifungal,

antibiotic and herbicidal activity.¹⁰⁸ Pyrrolomycins A and B are broad spectrum antimicrobial substances isolated from actinomycetes SF-2080.¹⁰⁹

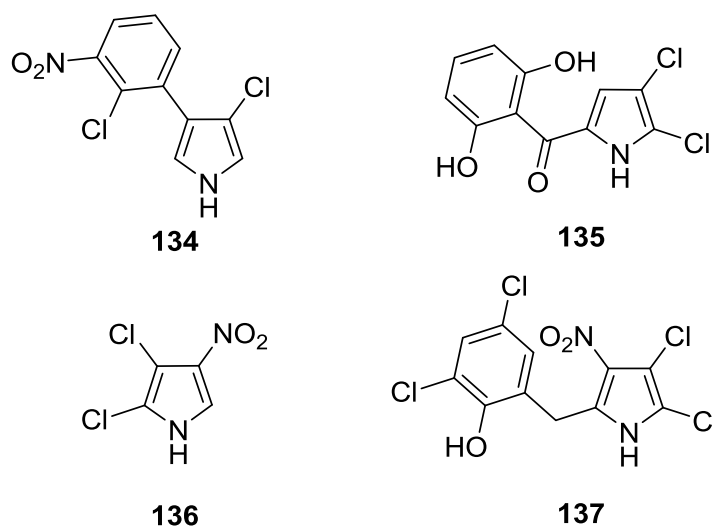
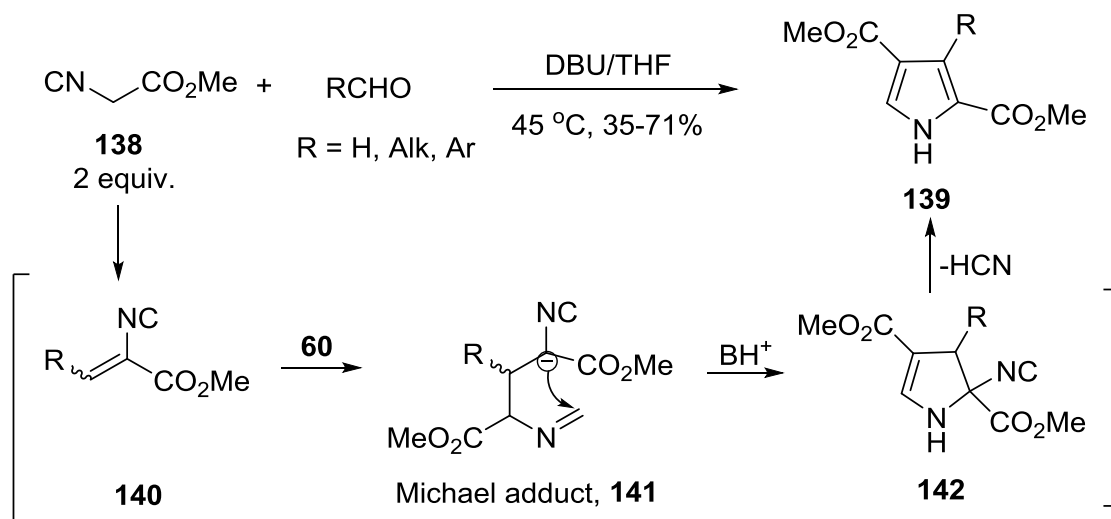


Figure 34. Naturally occurring antibiotics containing the pyrrole moiety.

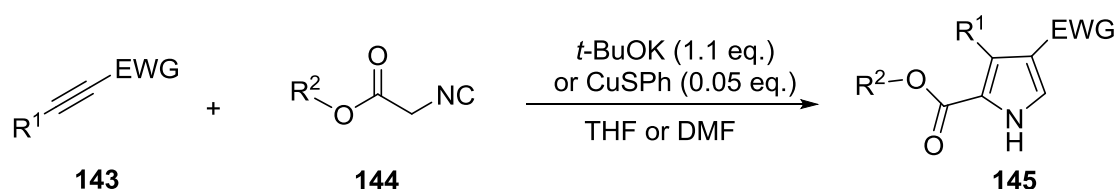
5.1.1 Synthesis of pyrroles from isocyanoacetate derivatives

Pyrroles can be readily formed from the reaction of 2 equivalents of α -isocyanoacetate and 1 equivalent of aldehyde in the presence of DBU.¹¹⁰ The reaction has been performed on a variety of aliphatic and aromatic aldehydes which all showed moderate to good yields without the need for excessive heat, anhydrous conditions or long reaction times. The reaction is thought to proceed *via* Michael addition of a second isocyanoacetate molecule followed by cyclisation to give the intermediate **142**. The pyrrole **139** is then formed by elimination of HCN (Scheme 50).



Scheme 50. Formation of pyrroles *via* the Michael adduct

The formation of pyrroles can also be achieved by the reaction of isocyanoacetates with activated alkynes. In 2005, de Meijere *et al.* found that in the presence of a copper(I) benzenethiolate catalyst or 1.1 equivalents of a strong base, pyrroles could be obtained from isocyanoacetates and alkynes (Scheme 51).¹¹¹ Firstly, the reaction was tried using DBU but a poor yield was obtained, the authors increased the basicity using potassium *tert*-butoxide and obtained a yield of 96%. The reaction was also attempted using copper powder which, gave a moderate yield of 51% and so the authors decided to optimise the reaction. After the use of several copper catalysts it was found that copper(I) benzenethiolate provided the best yields (up to 97%).



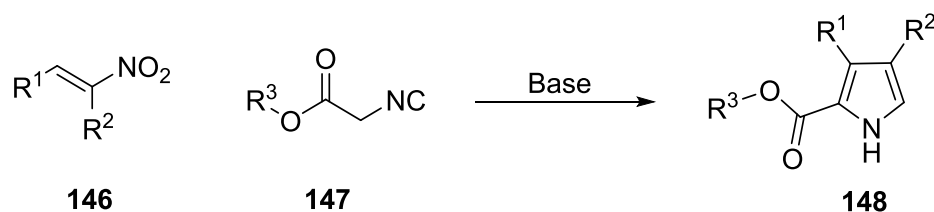
EWG = CO_2Alk , $\text{PO}(\text{OEt})_2$

R^1 = Alk, Ar R^2 = Me, *t*-Bu

Scheme 51. Reaction of isocyanoacetates with activated alkynes.

A more recent study by de Meijere *et al.* provided a route using terminal alkynes, as opposed to activated alkynes.¹¹² The reaction requires the use of 1 equivalent of CuI and base. This is believed to occur *via* the carbocupration of the copper

acetylenide (formed between CuI and the alkyne) by the deprotonated isocyanoacetate. Subsequent cyclisation and aromatisation form the pyrrole product.



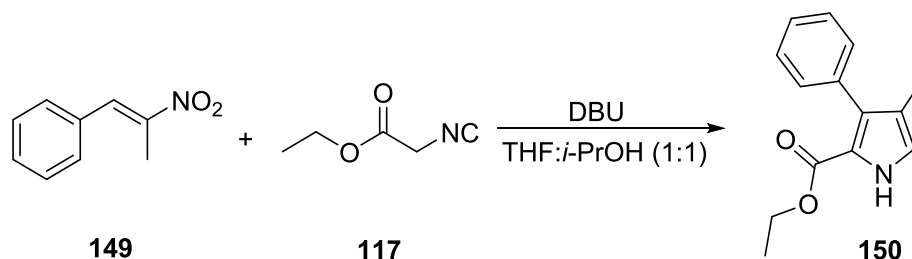
Scheme 52. Barton-Zard synthesis of pyrroles.

The most commonly used method for the synthesis of tri-substituted pyrroles synthesis from isocyanoacetate derivatives utilises DBU and a nitroalkene. This method has been described as the Barton-Zard synthesis since its publication in 1985.¹¹³ The authors reported the synthesis of several pyrroles using DBU, DMAP and guanidine as the base component (Scheme 52). Yields ranged from 55-97%, however, when using DBU as the base the yields were slightly lower (a drop of 10% in yield was described) and the reaction times were longer.

This chapter focuses on the synthesis of pyrroles by the Barton-Zard synthesis under continuous flow conditions. These reaction conditions were chosen as they use readily soluble reagents and only require one equivalent of the isocyanoacetate starting material. The conditions were optimised over a series of reactions and then a small library of pyrroles was synthesised after the nitroalkene starting materials had been synthesised. Attempts at the fluororous tagged synthesis of pyrroles are subsequently described.

5.2 Pyrrole synthesis under continuous flow conditions

As described in previous chapters, the reaction selected was initially performed under batch conditions to ensure the reaction occurred as stated and to obtain the product for HPLC analysis.



Scheme 53. Pyrrole formation from *trans*- β -methyl- β -nitrostyrene with ethyl isocyanoacetate.

The selected reaction utilised the commercially available *trans*- β -methyl- β -nitrostyrene via the method laid out by Barton and Zard to form tri-substituted pyrroles (Scheme 53).¹¹³ The batch process was complete after 5 hours and provided a yield of 79%. The purified product was used to produce a HPLC calibration curve as previously described in section 2.3.2 (Figure 35).

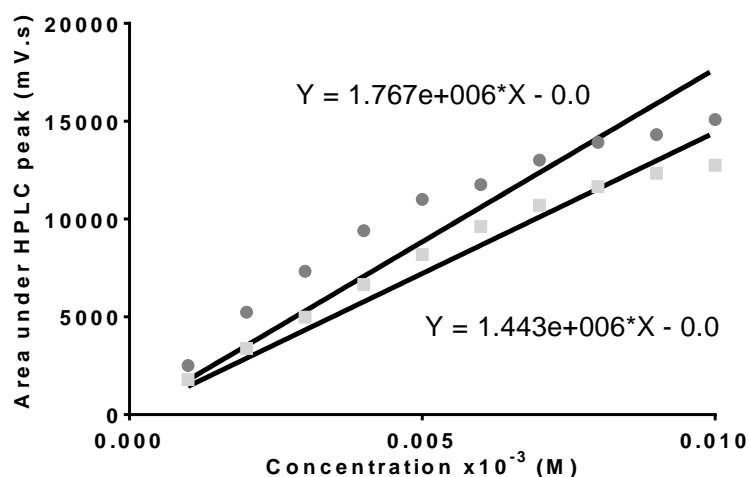


Figure 35. Calibration curve for pyrrole synthesis.

5.2.1 Continuous Flow Conditions

Reactions were run at 5 mins residence time over a variation of temperatures from 40-90 °C and a HPLC trace was obtained for the resulting samples. The

HPLC peaks were compared to those created for the calibration curve to give the calculated yield and the results are shown in the graph below (Figure 36).

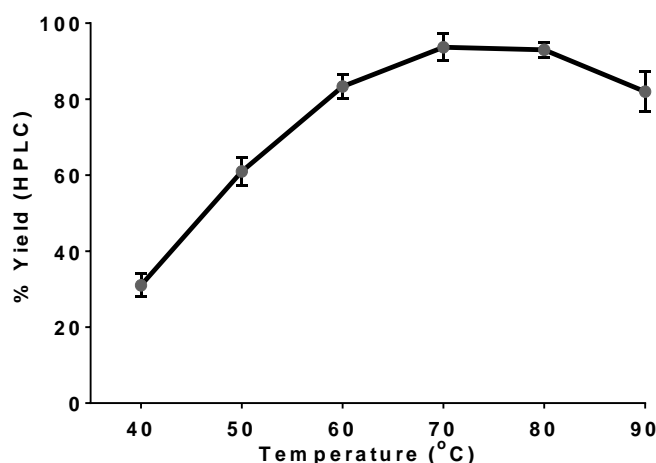


Figure 36. The yield of pyrrole formation over a variety of temperature at 5 mins residence time.

The yield of the reaction increased until reaching a maximum of 94% at 70 °C. At over 80 °C the yield of the reaction dipped to lower than the maximum, this is believed to be due to the formation of side products at higher temperatures. It was, therefore, decided that the optimum reaction temperature was 70 °C.

The next stage of the optimisation process was to determine residence time. As the yield was already high after 5 mins residence time shown by the temperature optimisation reactions, it was expected that only short residence times would be needed. The graph shown in Figure 37 shows the results of the residence time optimisation reactions. At a residence time of 10 mins and above the reaction reaches the calculated maximum of 100%. The yield of pyrrole production does drop after 20 mins, again this is likely due to the formation of side products formed due to slower flow rates.

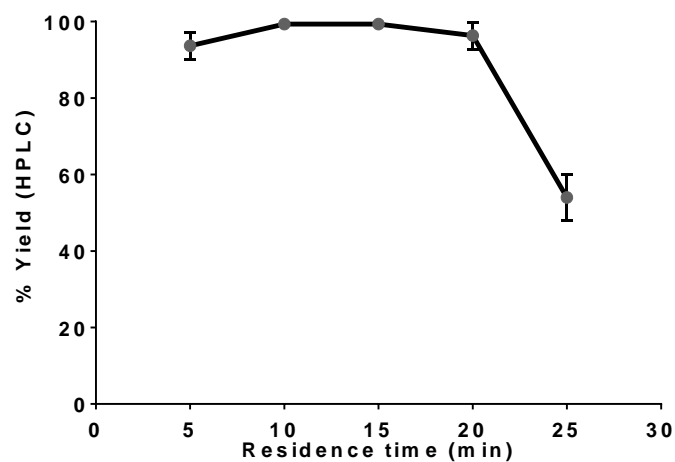


Figure 37. The yield of pyrrole formation with variation of residence time at 70 °C.

After the series of optimisation reactions the optimum conditions were determined to be 70 °C over a 10 mins residence time. The calculated yield was 100% according to the calibration curve. The reaction was run again under continuous flow conditions and the product was purified by flash column chromatography to provide **150** in a yield of 96%.

5.2.2 Nitrostyrene synthesis

There are a limited number of commercially available nitrostyrenes; however, they can be made from more readily available aldehydes. The general method of synthesis for nitrostyrenes involves the base catalysed Henry reaction, which, if under acidic conditions, will eliminate water to form the required nitrostyrene (Figure 38).

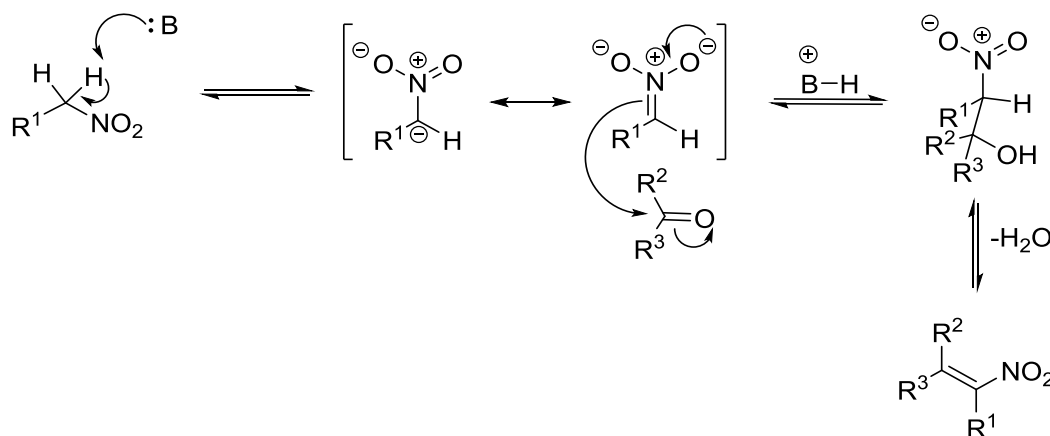
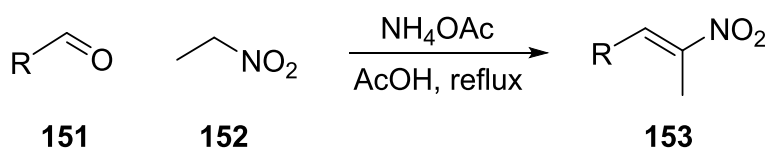


Figure 38. Mechanism of nitrostyrene synthesis *via* Henry reaction.

Several nitrostyrene and nitropropene derivatives were synthesised according to the method laid out in the patent by Kumar *et al.* as shown in Scheme 54.¹¹⁴ The experimental procedure for the synthesis of the nitrostyrene was reported in the patent.¹¹⁴

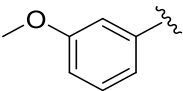
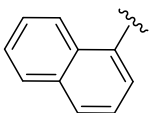
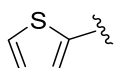
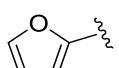
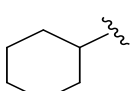


Scheme 54. Synthesis of nitrostyrenes.

All nitrostyrenes were synthesised with high yields (67-88%) including the product from the aliphatic aldehyde **158** (Table 10). The thiophene and furyl nitropropenes showed a reduction in yield of around 10%, potentially due to the instability of the final product. They were shown by TLC to degrade at room temperature overnight, potentially due to polymerisation. The cyclohexyl

nitropropene **158** also showed a drop in yield, again potentially due to the reactivity of the product and the increased reactivity of the starting material leading to further side product formation.

Table 10. The yields and products obtained in the synthesis of nitrostyrenes.

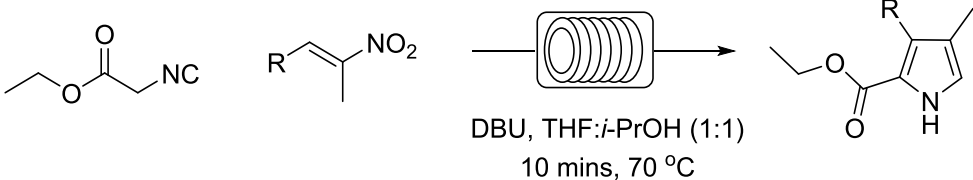
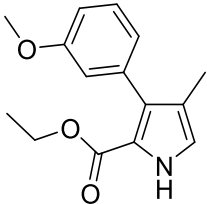
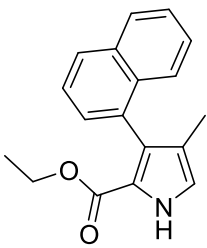
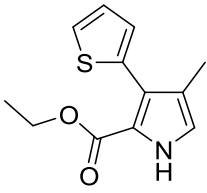
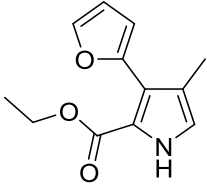
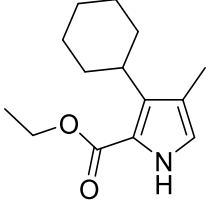
Product N ^o	R	% Yield
154		82
155		88
156		72
157		73
158		67

No conclusive mass ion peak was found by ES or EI mass spectrometry for products **155**, **156** and **157**. The products were characterised by other methods including IR, ¹H NMR, and ¹³C NMR spectroscopy.

5.2.3 Library synthesis

The nitropropene derivatives described above were used in the synthesis of a small library of pyrroles under the continuous flow conditions laid out in section 5.2.1. The results of the reaction, after purification with flash column chromatography (Table 11).

Table 11. The yields of pyrroles synthesised under continuous flow conditions.

Product N ^o	Product	% Yield
		
159		86
160		83
161		75
162		78
163		-

The products formed were of consistently high yield when using the aromatic nitropropene derivatives to give products **159-162**. The products **159** and **160**, formed from nitrostyrene derivatives, showed yields of 86% and 83% respectively. This value is above those stated in the literature, which described yields of 70-80%.¹¹⁵ The products **161** and **162** showed slightly lower yields of 75% and 78% respectively, potentially due to the instability of the starting material. No literature value for the yield of these products could be found for comparison.

The reaction of the aliphatic nitropropene **163** with ethyl isocyanoacetate under continuous flow conditions showed no product. The crude ¹H NMR spectrum showed no product formation (characteristic peak for *NH* proton at ~9.0 ppm was not present in the spectra) and no product was detected by mass spectrometry. There was no literature precedent for this compound found.

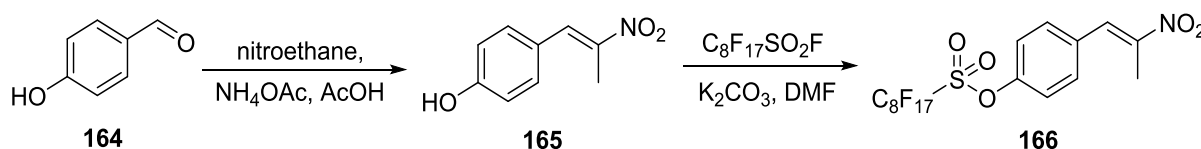
The synthesis of this small library showed the high yielding synthesis of pyrroles under continuous flow conditions with the use of an aromatic nitropropene starting material with a range of aromatic substituents. The reactions conditions were not viable for aliphatic counterparts.

5.3 Fluorous tagged pyrrole synthesis

After the synthesis of a library under continuous flow conditions showed the competency of the method it was decided to continue with the synthesis using a fluororous tag to aid with purification. The first stage was to synthesise the fluororous tagged nitrostyrene starting material using the method laid out in section 5.2.2. This was followed by the synthesis of the corresponding pyrroles using the optimised continuous flow conditions laid out in section 5.2.1.

5.3.1 Fluorous nitrostyrene synthesis

The first proposed synthesis route for the fluororous tagged nitrostyrenes involved the formation of the 4-hydroxynitrostyrene **165** followed by the fluororous protection of the hydroxyl group to form **166**.

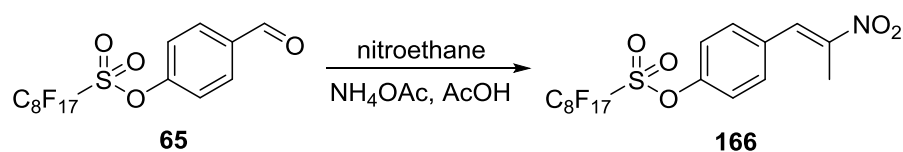


Scheme 55. The reaction cascade for the synthesis of (*E*)-1-(2-nitroprop-1-enyl)-3-methoxy-4-perfluorooctylsulfonyloxybenzene **166**.

The synthesis of the 4-hydroxynitrostyrene **165** was performed using the method outlined by Kumar *et al.* as with the nitrostyrenes and derivatives shown above.¹¹⁴ The reaction proceeded with no complications in a yield of 76%. The second step of the synthesis was altered slightly from the method used to synthesise the fluororous tagged aldehydes according to the method developed by Zhang *et al.* due to the reactive nature of the nitrostyrene group.⁵⁴ The alteration involved the use of 3 molar equivalents of potassium carbonate to react with any fluorine ions that could be present. Both ^1H NMR spectroscopy and LC-MS did not reveal the formation of the product.

As the reaction series outlined in the scheme above (Scheme 55) did not provide the product it was decided to use the fluororous tagged benzaldehyde derivative,

65. The reaction conditions described by Kumar *et al.* were used with **65** as the starting material.¹¹⁴



Scheme 56. The attempted synthesis of (*E*)-1-(2-nitroprop-1-enyl)-3-methoxy-4-perfluorooctylsulfonyloxybenzene.

The ¹H NMR spectrum of the crude reaction mixture showed the presence of the product (a singlet peak at 8.05 ppm). After purification by F-SPE and flash column chromatography eluted with 1:9 ethyl acetate:petroleum ether the product was still not obtained in pure form. As the ¹H NMR spectrum still showed the presence of a peak at 8.05 ppm after purification, the mixture was analysed by mass spectrometry. There was no mass ion found for the product. However, as described in section 5.2.2, no conclusive mass ion peak was determined for a number of the nitropropene derivatives. The synthesis of several other fluoruous nitrostyrene derivatives were attempted to determine the viability of the reaction (Table 12).

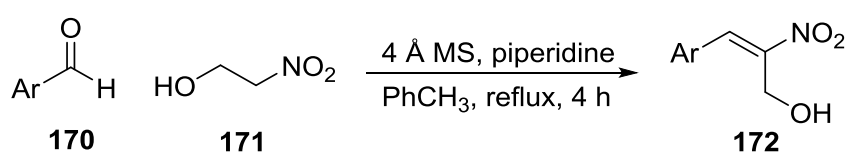
Table 12. Reagents used in nitrostyrene synthesis reaction.

$\text{R}^1\text{-CHO} \xrightarrow[\text{NH}_4\text{OAc, AcOH}]{\text{R}^2\text{-NO}_2} \text{R}^1\text{-CH}=\text{CHNO}_2$		
Product N ^o	Aldehyde	Nitroalkane
166	65	
167	65	
168	81	
169	81	

All the products described in Table 12 showed similar results with peaks at 8.00-8.25 ppm *via* ¹H NMR spectroscopy but were not pure after flash column

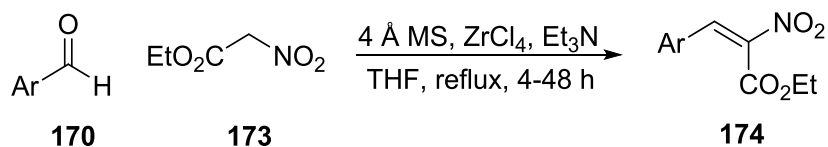
chromatography, showing the presence of uncharacterised side products. No mass ion peaks were found by LC-MS for any of the products.

The work of Fioravanti *et al.* described the one-pot synthesis of α -substituted nitroalkenes by two separate methods.¹¹⁶ The first method used piperidine to synthesise (*E*)-2-nitro allylic alcohol (Scheme 57). As several *para*-substituted benzaldehyde derivatives were used by the group it was decided to try this method with **65** as the aldehyde and 2-nitroethanol **171**. The ¹H NMR spectrum did not show the formation of the product and this result was confirmed by LC-MS. The reaction was also tried under the same conditions for nitroethane **152** but once again no product was found by ¹H NMR spectroscopy or LC-MS.



Scheme 57. Synthesis of (*E*)-2-nitroallylic alcohol.

The second method described by the same group involved the use of ZrCl₄ and Et₃N to form α -nitro acrylates and cinnamates (Scheme 58).¹¹⁶ As shown previously in section 3.4, the fluoros tagged benzaldehyde derivatives are stable in the presence of ZrCl₄ and so the product **65** was reacted with ethyl nitroacetate **173** under the conditions described by Fioravanti *et al.*



Scheme 58. Synthesis of α -nitro acrylates and cinnamates.

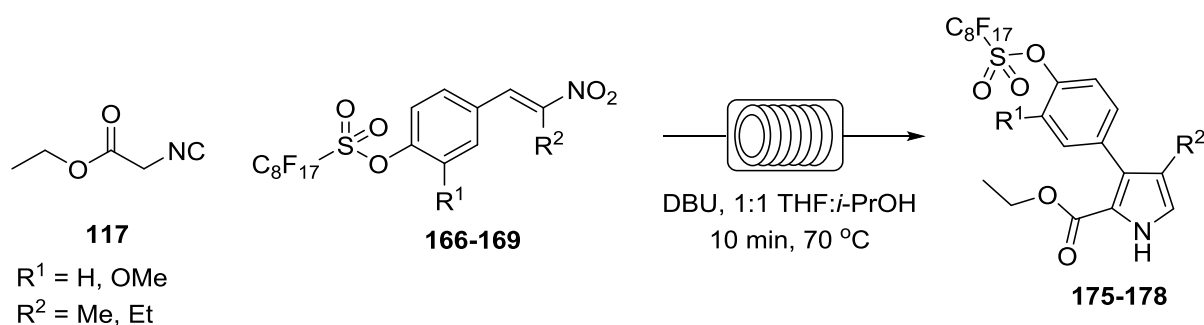
The crude mixture could not be sufficiently analysed for the presence of the product by ¹H NMR spectroscopy and so the mixture was subjected to F-SPE. After the purification the ¹H NMR spectra did not show the presence of the product and the result was confirmed by LC-MS. Again, no product formation was

observed by ^1H NMR spectroscopy and LC-MS when the reaction was conducted with nitroethane.

After further methods did not show any product synthesis it was decided to revisit the nitrostyrene synthesis that provided products using the method laid out by Kumar *et al.*¹¹⁴ As products **166-169** were not fully characterised, its presence could not be confirmed but the reaction conditions for pyrrole synthesis have been shown to be viable for a number of aromatic starting materials (section 5.2.3). It was hoped that the reaction would occur if the nitrostyrene product was present in the mixture and the side products would be easily separable from the final pyrrole product.

5.3.2 Fluorous pyrrole synthesis

The fluorous nitrostyrene derivatives were used in pyrrole synthesis reactions under the continuous flow conditions optimised in section 5.2.1.



Scheme 59. The synthesis of fluorous tagged pyrroles under continuous flow conditions.

The crude reaction mixture was analysed by ^1H NMR spectroscopy. The characteristic peak for the *NH* proton in a pyrrole is a broad singlet peak at ~9.00 ppm. None of the spectra obtained for the reactions with the four different starting materials showed a peak corresponding to this characteristic *NH*. The LC-MS of the crude reaction mixture found no mass ion peak for the pyrrole products. As there had been no previous problems obtaining mass ion peaks for pyrrole products it was determined that the impure nitrostyrene mixture may not have

contained the fluorous nitrostyrene product and, therefore, the pyrrole products could not be formed.

5.4 Conclusion

The reaction of ethyl isocyanoacetate and a nitrostyrene in the presence of DBU to form a tetra-substituted pyrrole was optimised under continuous flow conditions. The optimised reaction occurred with ethyl isocyanoacetate **117** and *trans*- β -methyl- β -nitrostyrene **149**. The conditions were found to be 10 mins residence time and 70 °C reactor temperature.

The next stage was to show the utility of this method by the synthesis of a small library. In order to synthesise the library it was first necessary to generate the nitroalkene starting materials. The method used was described in the patent by Kumar *et al.* and several nitro alkenes were synthesised, including an aliphatic example.¹¹⁴ The nitroalkenes were then used to synthesise the pyrroles under the optimised continuous flow conditions. The conditions improved the yields of the pyrroles that had been reported and several unreported products were also formed in high yields. The reaction using the aliphatic nitro alkene starting material **158** showed no product formation.

Initially, the fluorous protection of the synthesised 4-hydroxynitrostyrene **165** was attempted. This provided no product and so the reaction of the fluorous aldehydes and nitroalkanes were performed using the method laid out by Barton and Zard, however, and there was no conclusive evidence that the products were formed.¹¹³ After several other methods were attempted it was decided to determine the presence of the nitrostyrene derivatives formed by utilising the mixture in the pyrrole synthesis reactions using the method devised in section 5.2. Both ¹H NMR spectroscopy and LC-MS did not show the presence of the pyrrole product in the crude reaction mixture. Therefore, this method of pyrrole synthesis is not viable with the fluorous tag technology.

6. Conclusions and future work

The work in this thesis presents a fluorine tagged route to the synthesis of several heterocycles under continuous flow conditions. The introduction of continuous flow reactors has reduced reaction times and in many cases improved the yield of reactions. The development of F-SPE and 'light' fluorine tags has allowed for an ease of separation of products similar to that of solid-phase synthesis with all the advantages of solution-phase chemistry.

6.1 Chapter 2 conclusions

The originally proposed fluorine tag, ¹⁹F-TMSE-OH **70**, was selected due to the mild conditions for the removal of the tag. However, after many different attempts at the synthesis of this product (using a slightly different starting material to that used by Fustero *et al.*⁵⁰), the expense and overall yield of the product, 23% over the two steps, and the instability of the final product, lead to the investigation of a different fluorine tag. The alkyl analogue of ¹⁹F-TMSE-OH, 1*H*,1*H*,2*H*,2*H*-perfluorodecan-1-ol was taken forward in the synthetic route.

The conditions of the coupling reaction of the fluorine alcohol to *N*-formyl glycine were evaluated. The optimum coupling reagent was found to be PyBOP. The reaction with Fmoc protected glycine was also investigated as an attempt to further improve the yield of the reaction. The removal of the Fmoc protecting group proved problematic as no amine product was observed. The dehydration of the *N*-formyl fluorine product, to give the isocyanoacetate derivative, was investigated. Characterisation suggested the synthesis of the isocyanoacetate derivative was successful, however, after purification the product appeared to break down into the fluorine alcohol starting material.

It was, therefore, decided to continue the work described in this thesis using a known fluorine tagged benzaldehyde derivative to demonstrate the utility of the method. The reactions to couple both 4-hydroxybenzaldehyde and vanillin to

perfluoro-1-octanesulfonyl fluoride were successful in the formation of fluorous benzaldehyde derivatives.

Further work could be performed to investigate the reasons behind the failure of the fluorous isocyanoacetate derivative synthesis. The synthesis of the alkyl isocyanoacetate analogue has been described in a single paper¹¹⁷ and the synthesis of slightly different alkyl chains have been described.¹¹⁸ As there has been little research into these compounds, future work could involve the evaluation of the stability of these compounds.

6.2 Chapter 3 conclusions

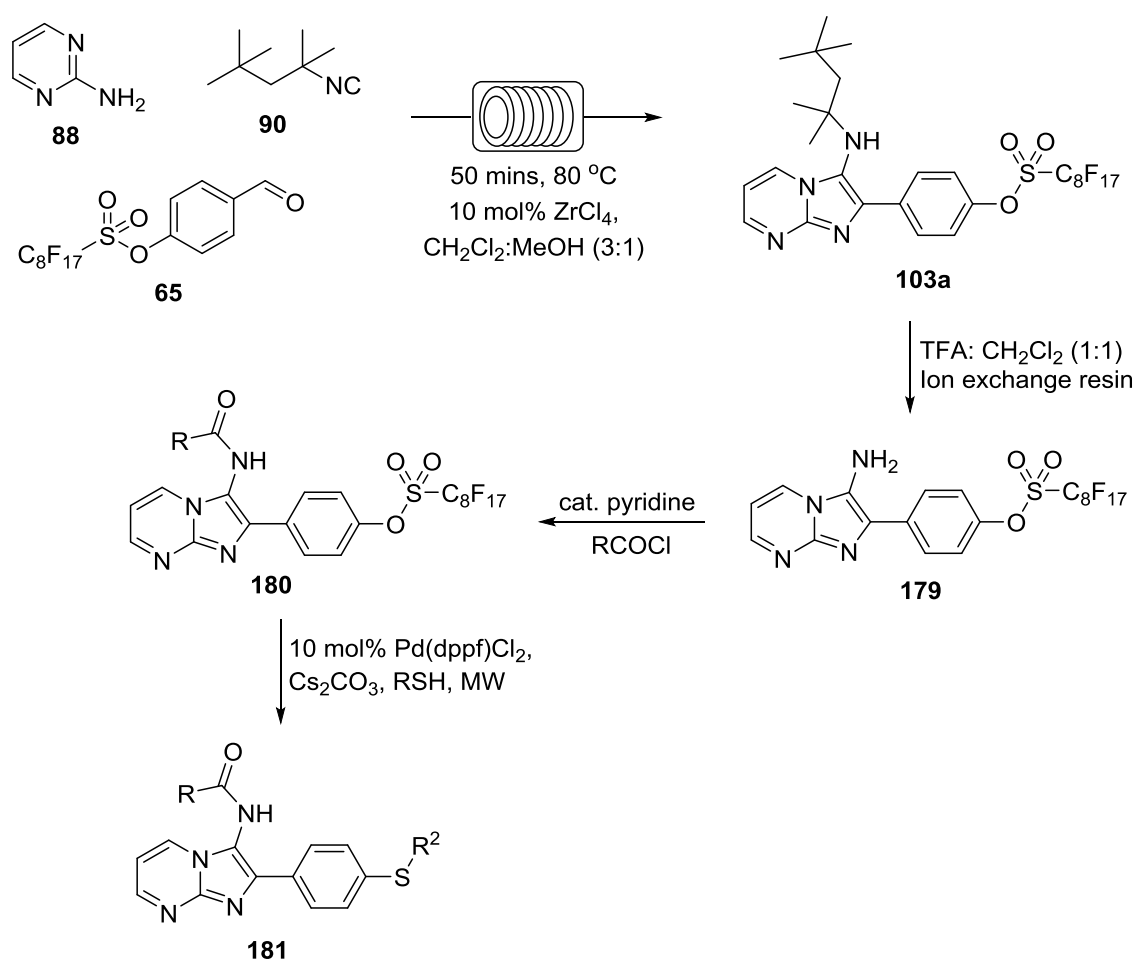
The synthesis of imidazo[1,2-*a*]pyrimidines was optimised under continuous flow conditions and a reactor temperature of 80 °C over a residence time of 50 mins were found to be the optimum conditions. The catalyst and loading was also investigated and the highest yield and regioselectivity for the 3-isomer was found when using 10 mol% ZrCl₄. The isolated yield of product was 61%. The regioselectivity was vastly improved under continuous flow conditions, going from 5:1 for the 3-amino isomer in batch conditions, to 20:1 under continuous flow conditions.

A small library of imidazo[1,2-*a*]pyrimidines were formed to demonstrate the utility of this method. All products were formed in good yields, ranging from 27-61%, with excellent regioselectivity for the 3-amino isomer, with some examples having no evidence of the 2-amino isomer being formed at all. The method also allowed for the synthesis of products formed from aliphatic aldehydes, which showed no product formation under batch conditions.

The reaction was performed using the fluorous benzaldehyde derivative, previously described, Walborsky's reagent, and 2-aminopyrimidine. The product was purified by F-SPE and subsequent recrystallisation provided the pure product with a yield of 64% of the 3-amino isomer product with no evidence of the 2-amino isomer being formed. The removal of the fluorous tag was achieved by

the palladium catalysed cross-coupling reaction with thiophenol to give a yield of 46%.

The fluoros imidazo[1,2-a]pyrimidine was synthesised with Walborsky's reagent, which is commonly known to be a convertible isocyanide. The 1,1,3,3-tetramethylbutyl amino group can be converted into the primary amine in the presence of an acid. Previous work by the Chen group investigated the use of ion exchange resins and found that the dealkylation with TFA provided the better yields.⁷⁶ This could lead to the functionalisation of the amine to form an extended library of products (Scheme 60).



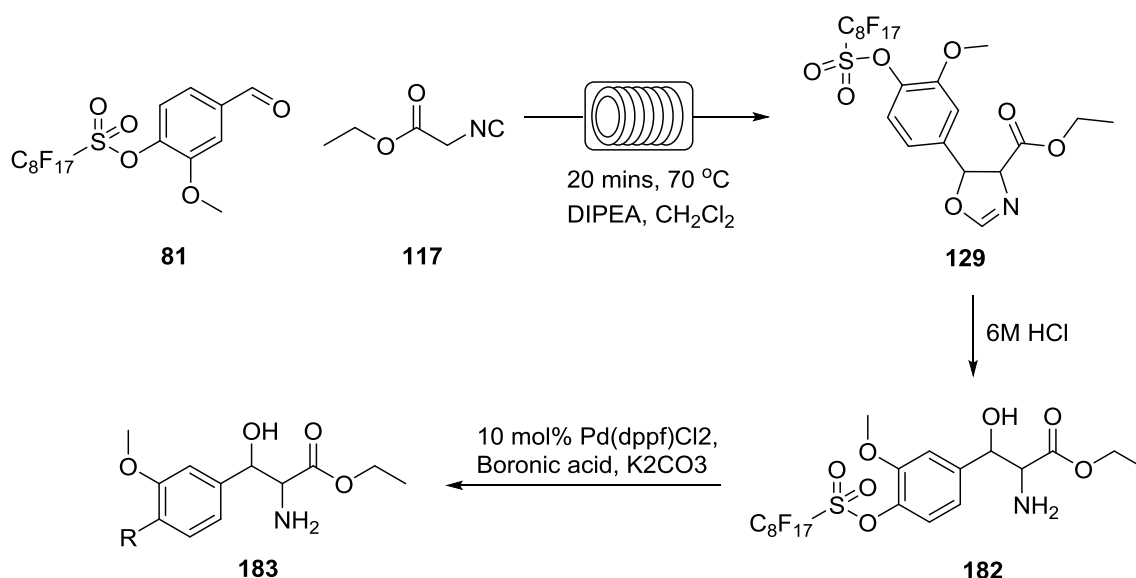
Scheme 60. Functionalisation of the amino group to synthesise an extensive library using fluoros technologies and continuous flow conditions.

6.3 Chapter 4 conclusions

The synthesis of 2-oxazolines from an aldehyde and ethyl isocyanoacetate was optimised under continuous flow conditions. The optimum conditions were found to be a reactor temperature of 70 °C over a residence time of 20 mins. A small library of 2-oxazolines was synthesised to show the versatility of the method. Yields ranged from 62-86%. The diastereoselectivity of the reaction was also high, with the ratios of *trans/cis* being comparable to those found under batch conditions.

The continuous flow method was used to synthesise the fluororous tagged 2-oxazoline derivative. The yield of the isolated product was found to be 92% which is higher than those yields found by traditional purification methods. The diastereoselectivity of the reaction calculated to be 91/9 in favour of the *trans* isomer. Several methods were attempted for the removal of the fluororous tag. The methods attempted for the tag removal showed no product formation.

Future work in this field would involve further attempts to remove the fluororous tag. 2-Oxazolines are known intermediates for the synthesis of β -hydroxyamino acids. Due to the instability of the oxazoline product and the problems occurring with the removal of the fluororous tag, it is postulated that the synthesis of the β -hydroxyamino acid should be performed before the removal of the fluororous tag.



Scheme 61. Synthesis of β -hydroxyamino acid followed by the removal of the fluororous tag.

There are also several papers describing the use of NaOH followed by a work up with HCl.¹⁰³ Therefore, the reaction can be performed using HCl a reaction can be designed so the fluororous tag removal and the β -hydroxyamino acid synthesis can be performed simultaneously.

6.4 Chapter 5 conclusions

The Barton-Zard synthesis of pyrroles from nitrostyrenes and isocyanoacetate derivatives was optimised under continuous flow conditions. A residence time of 10 mins at 70 °C reactor temperature was found to provide the product in a quantitative yield when calculated from a HPLC calibration curve.

A small library of nitroalkenes was synthesised as starting materials for the reaction under continuous flow conditions. The library yields ranged from 67-88% with the inclusion of an aliphatic example. The synthesised nitroalkenes were used in the optimised continuous flow reaction and the aromatic starting materials provided products with yields of 75-96%. The aliphatic starting material did not provide a pyrrole product.

Several methods of nitrostyrene synthesis were attempted for the synthesis of a fluororous tagged nitrostyrene. The only reaction that appeared to be successful by ¹H NMR spectroscopy was the nitroalkene synthesis used for the small library described above as proposed by Kumar *et al.*¹¹⁴ on the fluororous tagged benzaldehyde derivatives synthesised in section 2.4. The product mixture was not able to be purified and so the crude mixture was taken forward into the pyrrole synthesis reaction. No pyrrole product was found and so it was decided that the fluororous nitrostyrene derivative was not synthesised.

There has been an extensive amount of research into the synthesis of nitrostyrenes including the work by Kantam *et al.* that utilised a diamino-functionalised mesoporous material as a catalyst, giving yields ranging from 62-100%.¹¹⁹ More recently, a 'green' method of nitrostyrene synthesis has been developed using ionic liquids by Alizadeh *et al.* which provided yields of 60-97%.¹²⁰ There has also been the solid-phase synthesis of nitrostyrenes using

polymer bound triphenylphosphine with iodine and imidazole, to yield products in 55-93%.¹²¹

With the large amount of research in this field a number of further reactions could be performed in an attempt to synthesise the fluorine tagged nitrostyrene derivatives. After a method has been determined for the synthesis of fluorine nitrostyrene, the method developed for pyrrole synthesis under continuous flow conditions could be employed. As described in section 5.1, pyrroles can be used in the synthesis of many naturally occurring structures and drug-like compounds.

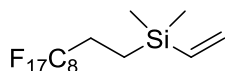
It has also been considered that the fluorine nitrostyrene derivatives are not stable and, therefore, this could be the reason that no conclusive characterisation was obtained. This would mean that this method of pyrrole synthesis is not viable with fluorine technologies, hence other methods of pyrrole synthesis (some described in section 5.1.1) could be investigated.

7. Experimental Data

General Procedures:

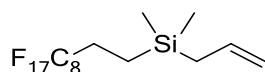
All reagents were purchased from commercial sources and used as supplied without further purification. Dry solvents were collected from an internal Grubbs solvent facility and used without further purification. All reactions were conducted with equipment and apparatus stored at ambient conditions, unless otherwise stated. Thin-layer chromatography was performed using aluminium backed silica gel 60 plates and visualised using either ultra-violet light or staining with a solution of alkaline potassium permanganate. Flash column chromatography was carried out using silica gel (43-60 mesh). All flow reactions were performed using a vapourtec R4 reactor using apparatus supplied by Vapourtec. All flow reactions were programmed using Flow Commander™ software supplied by vapourtec. Microwave reactions were performed on a CEM discovery microwave reactor. Melting points were determined with a Gallenkamp machine. $^1\text{H}/^{13}\text{C}/^{19}\text{F}$ NMR spectra were recorded at 250 or 400 MHz on a Bruker AV-1400 model or a Bruker AV-1250 model. NMR chemical shifts were reported in ppm with the solvent resonance as an integral standard. ^{13}C NMR spectra were recorded with complete proton decoupling. The signals in ^{13}C NMR for the fluororous tag chains (C_8F_{17}) are obscured due to their low intensity. Accurate masses were obtained using a Water-Micromass LCT electrospray mass spectrometer. Infrared spectra were recorded on FTIR machines as thin films on sodium chloride plates. HPLC was performed on Water Separation Module with a ZORBAX® Bonus-RP analytical column (4.6 mm x 150 mm, 5-Micron, 5-95 % MeCN in water over 20 mins at 1 mL/min, 15 μL injection, UV detection at 254 nm).

7.1 Experimental Data for Chapter 2



Vinyl(dimethyl)(3-(perfluorooctyl)ethyl)silane 68

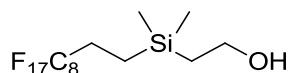
To a stirred solution of 1-iodo-1*H*,1*H*,2*H*,2*H*-perfluorodecane (2.00 g, 3.8 mmol) in Et₂O (70 mL) was added *t*-BuLi (1.7 M in pentane, 5.0 mL, 8.5 mmol) at –78 °C. The mixture was warmed to –10 °C and stirred for 30 mins. The reaction was again cooled to –78 °C and chloro(dimethyl)vinyl silane (0.86 mL, 5.7 mmol) was added. The temperature was increased to rt and the mixture was stirred for 3 h and then quenched with water. The organic layer was washed with brine, dried over Na₂SO₄ and concentrated at reduced pressure. The crude product was purified by flash column chromatography with petroleum ether to give the title compound as colourless oil (1.2 g, 65% yield). R_f 0.9 (petroleum ether). ν_{\max} (ATR)/cm⁻¹ 3081, 2960, 2875, 1646, 1368, 1243. ¹H NMR (CDCl₃, 400 MHz): δ 0.19 (6H, s), 0.96-1.03 (2H, m), 2.02-2.08 (2H, m), 5.64-5.73 (2H, m), 6.02-6.10 (1H, m). ¹³C NMR (CDCl₃, 100 MHz): δ -4.1, 4.1, 22.7, 25.7, 113.4, 134.2. ¹⁹F NMR (CDCl₃, 250 MHz): δ -80.7 (t, *J* 10.0), -114.4 (p, *J* 18.0, 16.0, 16.0, 18.0), -121.9, -122.7, -123.6, -126.1 (q, *J* 17.0, 10.0, 17.0).



Allyl(dimethyl)(3-(perfluorooctyl)ethyl)silane 69

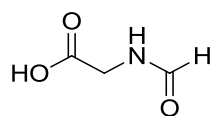
To a stirred solution of 1-iodo-1*H*,1*H*,2*H*,2*H*-perfluorodecane (2.00 g, 3.8 mmol) in Et₂O (70 mL) was added *t*-BuLi (1.7 M in pentane, 5.0 mL, 8.5 mmol) at -78°C. The mixture was warmed to -10 °C and stirred for 30 mins. The reaction was again cooled to -78 °C and allylchlorodimethylsilane (0.86 mL, 5.7 mmol) was added. The temperature was increased to rt and the solution was stirred for 3 h, the reaction was quenched with water and the phases were separated. The organic layer was washed with brine, dried over Na₂SO₄ and concentrated at reduced pressure. The crude product was purified by flash column chromatography with petroleum ether followed by distillation to give the title

product as colourless oil (1.34 g, 70 % yield). R_f 0.9 (petroleum ether). ν_{\max} (ATR)/ cm^{-1} 3082, 2959, 2909, 1633, 1207, 1153. ^1H NMR (CDCl_3 , 400 MHz): δ 0.08 (6H, s), 0.77-0.82 (2H, m), 1.59 (2H, d, J 8.0), 1.96-2.13 (2H, m), 4.85-4.94 (2H, m), 5.72-5.85 (2H, m). ^{13}C NMR (CDCl_3 , 100 MHz): δ -4.1, 4.1, 22.7, 25.7, 113.5, 134.2. ^{19}F NMR (CDCl_3 , 250 MHz): δ -80.7 (t, J 10.0), -114.5 (p, J 17.5, 16.5), -121.9, -122.7, -123.7, -126.1 (q, J 17.5, 10.0, 17.5).



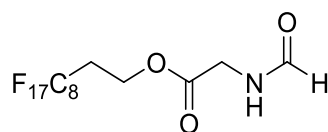
2-(Dimethyl-(3-(perfluorooctyl)ethyl)silyl)-ethanol **70**

Ozone was bubbled through a solution of allyl(dimethyl)(3-(perfluorooctyl)ethyl)silane (1.03 g, 1.88 mmol) and sodium hydrogen carbonate (1.00 g) in 5:1 CH_2Cl_2 : CH_3OH (60 mL) at $-78\text{ }^\circ\text{C}$ until the solution turned blue. Dimethyl sulphide was added to the solution and it was stirred at $-78\text{ }^\circ\text{C}$ for 1 h. The temperature was then increased at hourly intervals to $-10\text{ }^\circ\text{C}$, $0\text{ }^\circ\text{C}$ and finally stirred at rt for 1 h. The suspension is filtered and concentrated at reduced pressure. A solution of the resulting oil and NaBH_4 (0.07 g, 1.9 mmol) in methanol was stirred at rt for 18 h. Water was added (0.5 mL) and the solution was dried over Na_2SO_4 then concentrated at reduced pressure. The product was extracted with diethyl ether and solvent was evaporated under a reduced pressure. The crude material was purified by F-SPE to give the title compound as a colourless solid (0.44 g, 42% yield). R_f 0.4 (1:4 ethyl acetate: petroleum ether). ν_{\max} (solid)/ cm^{-1} , 3337, 2959, 2908, 1242, 1063. ^1H NMR (CDCl_3 , 400 MHz): δ 0.10 (6H, s), 0.75-0.82 (2H, m), 1.03 (2H, t, J 8.0), 1.59 (1H, s), 1.98-2.12 (2H, m), 3.79 (2H, t, J 8.0). ^{13}C NMR (CDCl_3 , 100 MHz): δ -3.5, 4.8, 20.0, 25.7, 29.7, 59.6. ^{19}F NMR (CDCl_3 400 MHz): δ -80.7 (t, J 10.0), -116.1 (p, J 17.0, 10.5, 10.5, 17.0), -121.4, -122.2 (m), -122.7, -123.2, -126.1 (q, J 18.0, 10.0 18.0). HRMS (ES-TOF) m/z : $[\text{M}+\text{H}]^+$ Calcd. for $\text{C}_{14}\text{H}_{15}\text{F}_{17}\text{OSi}$ 550.0621, found 550.0647.



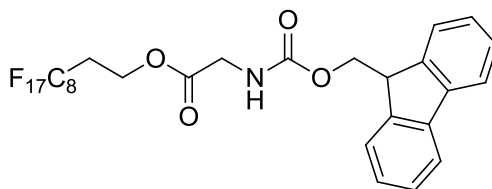
N-formyl glycine **75**⁶¹

A mixture of formic acid (1.92 mL, 51 mmol), glycine (2.25 g, 30 mmol) and *N,N*-dimethylformamide (15 mL) were heated to reflux until reaction completion, monitored by TLC (30 mins). The solvent was removed at reduced pressure and the crude product was recrystallised from toluene to give the title compound as a brown solid (1.34 g, 98% yield). MP: 115 °C. ¹H NMR (D₂O, 400 MHz): δ 3.90 (2H, s), 8.00 (1H, s). ¹³C NMR (D₂O, 100 MHz): δ 43.4, 164.6, 173.2. HRMS (ES-TOF) *m/z*. [M+H]⁺ Calcd. for C₃H₆NO₃ 103.0269, found 103.0269.



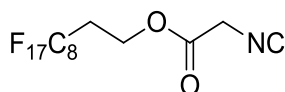
1H,1H,2H,2H-perfluorodecyl-*N*-formyl glycine **76**

1H,1H,2H,2H-perfluorodecan-1-ol (0.50 g, 1.07 mmol) was added to DIPEA (0.745 mL, 4.28 mmol) in CHCl₃ and was stirred for 10 mins at room temperature. Then PyBOP (1.11 g, 2.14 mmol) and *N*-formyl glycine (0.14 g, 1.61 mmol) were added. The mixture was stirred at 50 °C for 42 h. When the reaction was complete the solution was concentrated at reduced pressure and F-SPE afforded the title compound as a white solid (0.34 g, 58% yield). R_f 0.4 (1:1 petroleum ether: ethyl acetate). *v*_{max} (solid)/cm⁻¹, 3323, 1752, 1668, 1203, 1148. ¹H NMR (CDCl₃, 400 MHz): δ 2.52 (2H, m), 4.13 (2H, d, *J* 5.5), 4.49 (2H, t, *J* 6.5), 6.35 (1H, s), 8.28 (1H, s). ¹³C NMR (CDCl₃, 100 MHz): δ 30.4 (t, *J* 22.0), 39.8, 57.4, 161.2, 169.1. HRMS (ES-TOF) *m/z*. [M+H]⁺ Calcd. for C₁₃H₉F₁₇NO₃ 550.0311, found 550.0296. Elemental analysis found: C, 28.5; H, 1.5; N, 2.6. C₁₃H₈F₁₇NO₃ requires C, 28.4; H, 1.5; N, 2.6.



1H,1H,2H,2H-perfluorodecyl-Fmoc-glycine ester 78

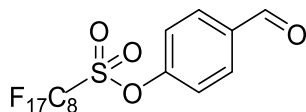
1H,1H,2H,2H-perfluorodecan-1-ol (0.50 g, 1.07 mmol) was added to DIPEA (0.745 mL, 4.28 mmol) in CHCl₃ and was stirred for 10 mins at room temperature. Then PyBOP (0.56 g, 1.07 mmol) and Fmoc protected glycine (0.37 g, 1.23 mmol) were added. The mixture was stirred at room temperature for 20 h. When complete the solution was concentrated at reduced pressure and F-SPE afforded the title compound as a white solid (0.57 g, 72% yield). R_f 0.8 (1:4 ethyl acetate/petroleum ether). MP: 95 °C. ν_{\max} (solid)/cm⁻¹ 3054, 2987, 1726, 1443, 1422, 1412, 1264, 1242. ¹H NMR (CDCl₃, 400 MHz): δ 2.53 (2H, m), 3.80 (2H, s), 4.05 (2H, t, *J* 5.5), 4.26 (1H, t, *J* 7.0), 4.40-4.53 (2H, m), 5.25-5.34 (1H, m), 7.30-7.81 (8H, m). ¹³C NMR (CDCl₃, 100 MHz): δ 33.8 (t, *J* 71.0), 42.6, 52.4, 55.2, 67.2, 119.9, 121.0, 125.1, 127.1, 127.7, 128.7, 143.8, 156.3. HRMS (ES-TOF) *m/z*: [M+H]⁺ Calcd. for C₂₇H₁₉F₁₇NO₄ 744.1043, found 744.1025. Elemental analysis found: C, 43.7; H, 2.4; N, 1.8. C₂₇H₁₈F₁₇NO₄ requires C, 43.6; H, 2.4; N, 1.9%.



1H,1H,2H,2H-perfluorodecyl Isocyanoacetate 79

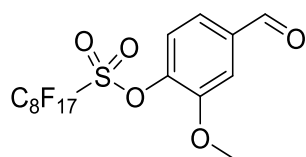
1H,1H,2H,2H-perfluorodecyl-N-formyl glycine (0.20 g, 0.36 mmol) was dissolved in 25 mL dichloromethane and triethylamine (0.126 mL, 0.9 mmol) was added to the stirring mixture. Then POCl₃ (0.05 mL, 0.54 mmol) was added to the mixture drop wise. After stirring for 2 h a saturated solution of NaHCO₃ (10 mL) was added drop wise to the reaction. The layers were then separated and the organic layer was washed with brine (3 x 10 mL) and then dried over MgSO₄. The solution was concentrated at reduced pressure and the product was purified by flash column chromatography (1:1 ethyl acetate: petroleum ether) to yield the title compound as a pale yellow solid (0.12 g, 64% yield). R_f 0.9. ν_{\max} (solid)/cm⁻¹

2958, 2931, 2235, 1747, 1689, 1387, 1367. ¹H NMR (CDCl₃, 400 MHz): δ 2.52 (2H, m), 4.27 (2H, m), 4.55 (2H, t, *J* 6.5). HRMS (ES-TOF) *m/z*: [M+H]⁺ Calcd. for C₁₃H₅F₁₇NO₂ 530.0049, found 530.0058.



4-Perfluorooctylsulfonyloxybenzaldehyde 65⁵⁴

To a stirred solution of hydroxy benzaldehyde (13.40 g, 110 mmol) in DMF (30 mL) was added K₂CO₃ powder (18.70 g, 135 mmol) at rt. The mixture was stirred for about 10 mins before the perfluorooctanesulfonyl fluoride (45.70 g, 91 mmol) was added. The mixture was heated at 70 °C for 8 h. The cooled solution was filtered and the solid was rinsed with EtOAc. The filtrate was washed with water, dried over MgSO₄ and concentrated at reduced pressure. The residue was purified by flash column chromatography (1:9 ethyl acetate: petroleum ether) to afford the title compound as a tacky white solid (53.30 g, 97% yield). R_f 0.6. ¹H NMR (CDCl₃, 400 MHz): δ 7.48 (2H, d, *J* 9.0), 8.01 (2H, d, *J* 9.0), 10.06 (1H, s). ¹³C NMR (CDCl₃, 100 MHz): δ 122.2, 131.7, 135.9, 153.5, 190.1. HRMS (ES-TOF) *m/z*: [M+H]⁺ Calcd. for C₁₅H₆F₁₇O₄S 604.9709, found 604.9709.



3-Methoxy-4-perfluorooctylsulfonyloxybenzaldehyde 81⁵⁴

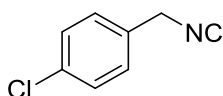
To a stirred solution of 3-methoxy-4-hydroxybenzaldehyde (16.70 g, 110 mmol) in DMF (30 mL) was added K₂CO₃ powder (18.70 g, 135 mmol) at room temperature. The mixture was stirred for about 10 mins before the perfluorooctanesulfonyl fluoride (45.70 g, 91 mmol) was added. The mixture was heated at 70 °C for 8 h. The cooled solution was filtered and the solid was rinsed with EtOAc. The filtrate was washed with water, dried over MgSO₄ and concentrated at reduced pressure. The residue was purified by flash column chromatography (1:9 ethyl acetate: petroleum ether) to afford the title compound

as a tacky white solid (65.60 g, 94% yield). Rf 0.6. ^1H NMR (CDCl_3 , 400 MHz): δ 4.02 (3H, s), 7.43 (1H, d, J 8.0), 7.53 (1H, dd, J 2.0, 8.0), 7.59 (1H, d, J 2.0), 10.00 (1H, s). ^{13}C NMR (CDCl_3 , 100 MHz): 56.5, 11.8, 123.0, 124.0, 136.8, 143.0, 152.3, 190.3. HRMS (ES-TOF) m/z : $[\text{M}+\text{H}]^+$ Calcd. for $\text{C}_{16}\text{H}_7\text{F}_{17}\text{O}_5\text{S}$ 633.9743, found 633.9762.

7.2 Experimental Data for Chapter 3

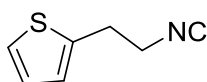
General synthesis of Isocyanides

The appropriate primary amine (10 mmol) was stirred for 24 h with 1,5,7-triazabicyclo[4.4.0]dec-5-ene (0.14 g, 1 mmol) in ethyl formate. Where the formamide intermediate was a liquid, the reaction mixture was dried under high vacuum for several hours. Where the formamide was a solid, it was collected by filtration and washed several times with petroleum ether 40/60. The formamide intermediate was then dissolved in anhydrous CH_2Cl_2 (50 mL) under N_2 and triethylamine (2.5 equiv) was added. The solution was cooled to 0 °C and POCl_3 (1.5 equiv) was added dropwise over 10 mins. After 1 h, sat. NaHCO_3 solution (20 mL) was added and the reaction continued for a further 1.5 h. After this time the organic layer was separated and dried over MgSO_4 . The solution was then concentrated at reduced pressure and purified by flash column chromatography on silica, as detailed below for each sample.



*4-Chlorobenzyl isocyanide*¹²²

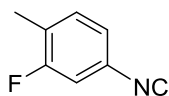
4-Chlorobenzyl amine afforded the title compound as a colourless oil, purified by flash column chromatography eluted 1:4 ethyl acetate: petroleum ether (1.4 g, 93% yield). R_f 0.9. ^1H NMR (CDCl_3 , 400 MHz): δ 4.61 (2H, s), 7.28 (2H, d, J 9.0), 7.37 (2H, d, J 9.0). ^{13}C NMR (CDCl_3 , 100 MHz): δ 45.0 (t, J 8.0), 128.1, 129.2, 130.9, 134.4, 157.1 (t, J 8.0). HRMS (ES-TOF) m/z : $[\text{M}+\text{H}]^+$ Calcd. for $\text{C}_8\text{H}_6^{35}\text{ClN}$ 151.0189, found 151.0182.



*2-(Thiophene)ethyl isocyanide*⁷⁴

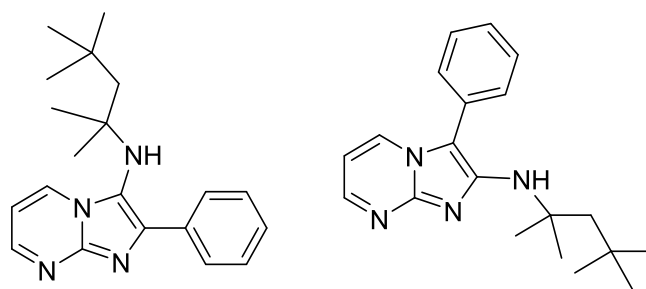
2-(Thiophene)ethyl amine afforded the title compound as a colourless oil, purified by flash column chromatography eluted 1:4 ethyl acetate: petroleum ether (1.043

g, 76% yield). Rf 0.9. ^1H NMR (CDCl_3 , 400 MHz): δ 3.25 (2H, t, J 2.0), 3.68 (2H, t, J 2.0), 6.97 (1H, d, J 1.0), 7.01 (1H, dd, J 1.0, 2.0), 7.23 (1H, d, J 2.0). ^{13}C NMR (CDCl_3 , 100 MHz): δ 30.0, 43.2 (t, J 7.0), 124.7, 126.3, 127.2, 138.5, 157.2 (t, J 5.0). HRMS (ES-TOF) m/z . $[\text{M}+\text{H}]^+$ Calcd. for $\text{C}_7\text{H}_7\text{NS}$ 137.030, found 137.029.



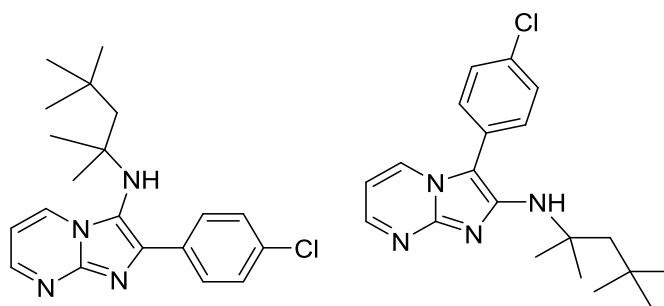
*2-Fluoro-4-isocyano-1-methylbenzene*⁷⁴

3-Fluoro-4-methylaniline (1.25 g, 10 mmol) and 4-tolylsulfonic acid (0.17 g, 1 mmol) were dissolved in methyl formate. The reaction mixture was heated to reflux for 3 days. Ethyl acetate was added and the mixture was extracted with HCl (1 M). The organic layer was separated, washed with aqueous NaHCO_3 and dried over MgSO_4 . The solution was then concentrated at reduced pressure and recrystallised from diethyl ether. The solution was cooled to 0 °C and POCl_3 (1.5 equiv) was added dropwise over 10 mins. After 1 h, sat. NaHCO_3 solution (20 mL) was added and the reaction continued for a further 1.5 h. After this time the organic layer was separated and dried over MgSO_4 . The solution was then concentrated at reduced pressure and purified by flash column chromatography on silica eluted with CH_2Cl_2 with 1% triethylamine to give the title compound as a yellow oil (0.72 g, 53% yield). ^1H NMR (CDCl_3 , 400 MHz): δ 2.30 (3H, s), 7.09 (2H, m), 7.21 (1H, t, J 2.0). ^{13}C NMR (CDCl_3 , 100 MHz): δ 14.5 (d, J 3.0), 113.5 (d, J 26.0), 122.0 (d, J 4.0), 127.2 (d, J 18.0), 132.0 (d, J 6.0), 160.6 (d, J 248.0), 164.7. HRMS (ES-TOF) m/z . $[\text{M}+\text{H}]^+$ Calcd. for $\text{C}_8\text{H}_7\text{FN}$ 136.0563, found 136.0569.



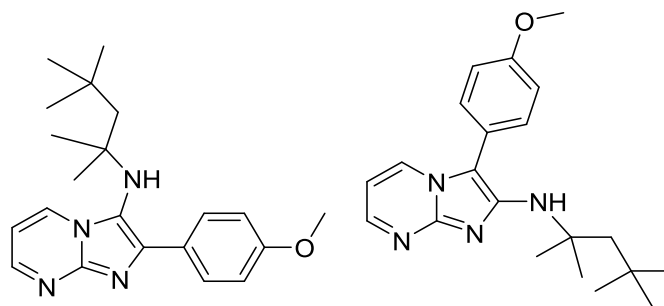
2-phenyl-N-(2,4,4-trimethylpentan-2-yl)imidazo[1,2-a]pyrimidine-3-amine **91b** and 3-phenyl-N-(2,4,4-trimethylpentan-2-yl)imidazo[1,2-a]pyrimidin-2-amine **91a**.⁷⁴

2-Aminopyrimidine (0.95 g, 10 mmol), benzaldehyde (1.02 mL, 10 mmol) and Sc(OTf)₃ (0.12 g, 0.25 mmol) were stirred in 1:3 MeOH:CH₂Cl₂ (100 mL) for 30 mins at rt. Walborsky's reagent (1.75 mL, 10 mmol) was then added, and the mixture heated at 45 °C for 48 h. The solvent was removed under reduced pressure and the product was purified by flash column chromatography on basic alumina, eluted with 20→30→50% ethyl acetate: petroleum ether then CH₂Cl₂, followed by 1% MeOH: CH₂Cl₂ to provide (**91b**) (0.71 g, 22% yield) as a yellow solid. R_f 0.9 (1:4 ethyl acetate: petroleum ether). MP: 215-225 °C. ¹H NMR (CDCl₃, 400 MHz): δ 1.01 (9H, s), 1.60 (6H, s), 1.93 (2H, s), 4.37 (1H, s), 6.71 (1H, dd, *J* 4.5, 6.5), 7.38 (1H, t, *J* 7.5), 7.47-7.58 (3H, m), 8.24 (1H, dd, *J* 2.0, 4.5), 8.36 (1H, dd, *J* 2.0, 6.5). ¹³C NMR (CDCl₃, 100 MHz): δ 30.2, 31.7, 31.8, 53.0, 56.1, 102.1, 107.5, 126.7, 127.5, 127.8, 129.0, 129.8, 144.6, 145.5, 151.3. HRMS (ES-TOF) *m/z*. [M+H]⁺ Calcd. for C₂₀H₂₇N₄ 323.2236, found 323.2250. **91a** was obtained as a pale yellow solid (0.812 g, 25% yield). R_f 0.6 (1:1 ethyl acetate: petroleum ether). MP: 88-94 °C. ¹H NMR (CDCl₃, 400 MHz): δ 0.96 (6 H, s), 1.03 (9H, s), 1.57 (2H, s), 3.33 (1H, s), 6.84 (1H, dd, *J* 4.0, 7.0), 7.35 (1 H, t, *J* 7.5), 7.45 (2H, t, *J* 7.5), 7.92 (2H, t, *J* 7.5), 8.49 (1H, dd, *J* 2.0, 4.0), 8.56 (1H, dd, *J* 2.0, 7.0). ¹³C NMR (CDCl₃, 100 MHz): δ 29.0, 31.7, 31.8, 56.9, 60.9, 107.8, 121.8, 127.9, 128.3, 128.6, 131.2, 134.8, 141.5, 144.2, 149.3. HRMS (ES-TOF) *m/z*. [M+H]⁺ Calcd. for C₂₀H₂₇N₄ 323.2236, found 323.2235.



2-(4-chlorophenyl)-N-(2,4,4-trimethylpentan-2-yl)imidazo[1,2-a]pyrimidine-3-amine (**93b**) and 3-(4-chlorophenyl)-N-(2,4,4-trimethylpentan-2-yl)imidazo[1,2-a]pyrimidine-2-amine (**93a**).⁷⁴

2-Aminopyrimidine (0.38 g, 4 mmol), *p*-chlorobenzaldehyde (0.56 g, 4 mmol) and Sc(OTf)₃ (0.20 g, 0.4 mmol) were stirred in 1:3 MeOH:CH₂Cl₂ (50 mL) for 30 mins at rt. After this time, Walborsky's reagent (0.702 mL, 4 mmol) was introduced to the reaction flask and the mixture heated to 45 °C for 1 h. The solution was concentrated at reduced pressure and the crude material purified by flash column chromatography on basic alumina, eluted with 10→30→50 ethyl acetate: toluene affording **93b** (0.41 g, 29% yield) as a yellow solid. R_f 0.8 (1:9 ethyl acetate: toluene). MP: 205–212 °C. ¹H NMR (CDCl₃, 400 MHz): δ 1.00 (9H, s), 1.59 (6H, s), 1.91 (2H, s), 4.30 (1H, s), 6.72 (1H, dd, *J* 4.5, 6.5), 7.42 (2H, d, *J* 8.5), 7.51 (2H, d, *J* 8.5), 8.24 (1H, dd, *J* 2.0, 4.5), 8.29 (1H, dd, *J* 2.0, 6.5). ¹³C NMR (CDCl₃, 100 MHz): δ 29.0, 31.6, 31.8, 56.8, 60.8, 107.9, 121.9, 128.2, 129.7, 131.4, 133.2, 133.4, 139.9, 145.0, 149.4. HRMS (ES-TOF) *m/z*: [M+H]⁺ Calcd. for C₂₀H₂₆³⁵ClN₄ 357.1846, found 357.1831. **93a** was also obtained as a bright yellow solid (0.16 g, 11% yield). R_f 0.7 (1:1 ethyl acetate: toluene). MP: 62–72 °C. ν_{max} (solid)/cm⁻¹ 3244, 2950, 2890, 1567, 1496, 1478, 1188. ¹H NMR (CDCl₃, 400 MHz): δ 0.98 (6H, s), 1.05 (9H, s), 1.59 (2H, s), 3.29 (1H, s), 6.88 (1H, dd, *J* 4.0, 7.0), 7.42 (2H, d, *J* 8.5), 7.93 (2H, d, *J* 8.5), 8.52 (2H, dd, *J* 2.0, 4.0), 8.55 (2H, dd, *J* 2.0, 7.0). ¹³C NMR (CDCl₃, 100 MHz): δ 30.1, 31.7, 31.8, 52.9, 56.2, 101.9, 107.7, 126.7, 127.5, 129.1, 130.1, 133.0, 145.0, 146.6, 151.4; HRMS (ES-TOF) *m/z*: [M+H]⁺ Calcd. for C₂₀H₂₆³⁵ClN₄ 357.1846, found 357.1868.

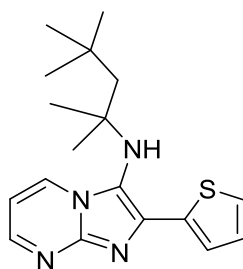


2-(4-methoxyphenyl)-N-(2,4,4-trimethylpentan-2-yl)imidazo[1,2-a]pyrimidine-3-amine **94b** and 3-(4-methoxyphenyl)-N-(2,4,4-trimethylpentan-2-yl)imidazo[1,2-a]pyrimidine-2-amine **94a**.⁷⁴

2-Aminopyrimidine (0.38 g, 4 mmol), *p*-chlorobenzaldehyde (0.56 g, 4 mmol) and Sc(OTf)₃ (0.20 g, 0.4 mmol) were stirred in 1:3 MeOH:CH₂Cl₂ (50 mL) for 30 mins at rt. After this time, Walborsky's reagent (0.702 mL, 4 mmol) was introduced to the reaction flask and the mixture heated to 45 °C for 1 h. The solution was concentrated at reduced pressure and the product purified by flash column chromatography on basic alumina, eluted with 33→50 % ethyl acetate: toluene which yielded **94b** as a yellow solid (0.34 g, 23% yield). R_f 0.8 (1:3 ethyl acetate: toluene). MP: 195-202 °C. ¹H NMR (CDCl₃, 400 MHz): δ 0.98 (9H, s), 1.56 (6H, s), 1.89 (2H, s), 3.86 (2H, s), 4.16 (1H, s), 6.64 (1H, dd, *J* 4.0, 7.0), 7.03 (2H, d, *J* 9.0), 7.35 (2H, d, *J* 9.0), 8.13 (1H, dd, *J* 2.0, 4.0), 8.19 (1H, dd, *J* 2.0, 7.0). ¹³C NMR (CDCl₃, 100 MHz): δ 30.2, 31.7, 31.8, 53.0, 55.4, 56.0, 102.3, 107.3, 115.3, 120.8, 126.5, 129.8, 144.0, 146.1, 151.1, 159.1. HRMS (ES-TOF) *m/z*. [M+H]⁺ Calcd. for C₂₁H₂₉N₄O 353.2341, found 353.2324. **94a** was obtained as a yellow solid (0.07 g, 5% yield). R_f 0.6 (1:1 ethyl acetate: toluene). MP: 90–92 °C. ¹H NMR (CDCl₃, 400 MHz): δ 0.93 (6H, s), 1.02 (9H, s), 1.55 (2H, s), 3.27 (1H, s), 3.81 (3H, s), 6.79 (1H, dd, *J* 4.0, 7.0), 6.96 (2H, d, *J* 9.0), 7.87 (2H, d, *J* 9.0), 8.42 (1H, dd, *J* 2.0, 4.0), 8.49 (1H, dd, *J* 2.0, 7.0). ¹³C NMR (CDCl₃, 100 MHz): δ 29.0, 31.7, 31.8, 52.3, 56.9, 60.8, 107.6, 113.7, 121.1, 127.3, 129.8, 131.0, 141.3, 145.0, 158.3, 159.3. HRMS (ES-TOF) *m/z*. Calcd. for C₂₁H₂₉N₄O 353.2341, found 353.2350.

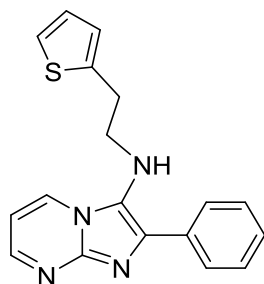
Continuous Flow Synthesis of Imidazo[1,2-a]pyrimidines. General Procedure.

Intake line A was charged with a solution of 0.2 M 2-aminopyrimidine, 0.2 M starting aldehyde, and 0.02 M $ZrCl_4$ in $MeOH:CH_2Cl_2$ (1:3), which had been premixed for at least 30 mins prior to use. Line B was charged with a solution of 0.2 M isocyanide in the same solvent system. The solutions were combined and passed through the reactor at 80 °C with a residence time of 50 mins. The crude product solution was concentrated under reduced pressure then the residue purified as indicated for each individual case.



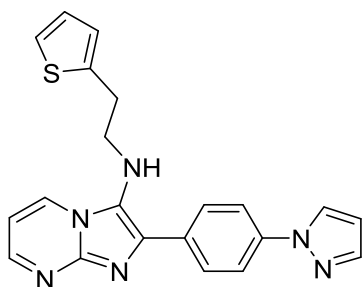
2-(thiophen-2-yl)-N-(2,2,4-trimethylpentan-2-yl)imidazo[1,2-a]pyrimidin-3-amine **95a**.⁷⁴

General procedure followed using 2-thiophenecarboxaldehyde and Walborsky's reagent. Flash column chromatography on basic alumina, eluted with 20→30→50 % ethyl acetate: petroleum ether yielded the product as a yellow amorphous solid (0.08 g, 60% yield). R_f 0.6 (1:1 ethyl acetate: petroleum ether). 1H NMR ($CDCl_3$, 400 MHz): δ 1.10 (9H, s), 1.14 (6H, s), 1.71 (2H, s), 3.28 (1H, s), 6.83 (1H, dd, J 4.0, 7.0), 7.13 (1H, dd, J 4.0, 5.0), 7.37 (1H, dd, J 1.0, 5.0), 7.66 (1H, dd, J 1.0, 4.0), 8.49 (1H, dd, J 2.0, 7.0), 8.50 (1H, dd, J 2.0, 4.0). ^{13}C NMR ($CDCl_3$, 100 MHz): δ 29.3, 31.8, 31.9, 57.1, 61.2, 107.8, 121.0, 125.7, 126.1, 127.3, 131.2, 136.5, 136.7, 149.5, 158.3. HRMS (ES-TOF) m/z : $[M+H]^+$ Calcd. for $C_{18}H_{25}N_4S$ 329.1800, found 329.1793.



2-Phenyl-N-(2-(thiophen-2-yl)ethyl)imidazo[1,2-a]pyrimidin-3-amine **96a**.⁷⁴

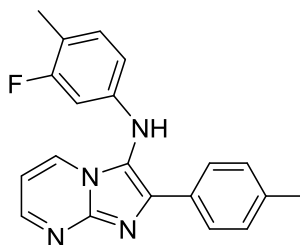
General procedure was followed using benzaldehyde and 2-(thiophene)ethyl isocyanide. Flash column chromatography on basic alumina, eluted with 33→50→80 % ethyl acetate: petroleum ether yielded the product as a yellow amorphous solid (0.063 g, 49% yield). R_f 0.8 (4:1 ethyl acetate: petroleum ether). ¹H NMR (DMSO-d₆, 400 MHz): δ 3.02 (2H, t, *J* 7.0), 3.23 (2H, q, *J* 6.0), 5.11 (1H, t, *J* 6.0), 6.82 (1H, dd, *J* 7.0 and 4.0), 6.89 (1H, dd, *J* 1.0, 3.5), 7.01 (1H, dd, *J* 3.5, 5.0), 7.25 (1H, dd, *J* 1.0, 5.0), 7.38–7.32 (1H, m), 7.52–7.40 (2H, m), 7.94–8.02 (2H, m), 8.17 (1H, dd, *J* 2.0, 7.0), 8.50 (1H, dd, *J* 2.0, 4.0). ¹³C NMR (DMSO-d₆, 100 MHz): δ 31.0, 49.3, 108.1, 123.9, 124.1, 125.8, 127.1, 127.3, 127.9, 128.7, 130.1, 133.4, 137.3, 141.4, 144.5, 149.2. HRMS (ES-TOF) *m/z*: [M+H]⁺ Calcd. for C₁₈H₁₇N₄S 321.1170, found 321.1170.



2-(4-(1H-pyrazol-1-yl)phenyl)-N-(2-(thiophen-2-yl)ethyl)imidazo[1,2-a]pyrimidin-3-amine **97a**.⁷⁶

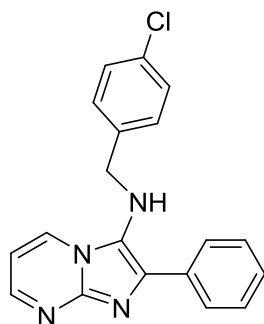
General procedure followed using 4-(1H-pyrazol-1-yl)benzaldehyde and 2-(thiophene)ethyl isocyanide. The product was purified by flash column chromatography on silica with 20→50→80% ethyl acetate: petroleum ether to give a yellow amorphous solid (0.09 g, 55% yield). R_f 0.8 (4:1 ethyl acetate: petroleum ether). ¹H NMR (DMSO-d₆, 400 MHz): δ 3.05 (2H, t, *J* 7.0), 3.27 (2H, q, *J* 7.0), 5.15 (1H, t, *J* 6.0), 6.58 (1H, t, *J* 2.0), 6.87 (1H, d, *J* 3.5), 6.94 (1H, dd, *J*

3.5, 5.0), 7.02 (1H, dd, *J* 4.0, 7.0), 7.33 (1H, dd, *J* 1.0, 5.0), 7.79 (1H, d, *J* 1.0), 7.92 (2H, d, *J* 9.0), 8.25 (2H, d, *J* 9.0), 8.48 (1H, dd, *J* 2.0, 4.0), 8.37 (1H, d, *J* 2.5), 8.63 (1H, dd, *J* 2.0, 7.0). ¹³C NMR (DMSO-d₆, 100 MHz): δ 31.1, 49.7, 108.5 (d, *J* 16.5), 118.8, 119.5, 124.4, 125.5, 125.8, 127.4, 128.1 (d, *J* 8.2), 129.1, 131.8, 132.3, 134.7, 139.1, 141.5, 142.2, 144.2, 149.9. HRMS (ES-TOF) *m/z*: [M+H]⁺ Calcd. for C₂₁H₁₉N₄S 387.1392, found 387.1404.



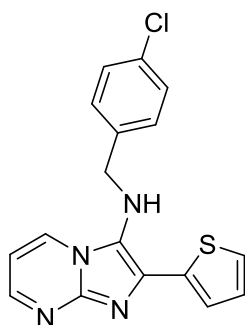
2-p-tolyl-N-(3-fluoro-4-methylphenyl)imidazo[1,2-a]pyrimidin-3-amine 98a.⁷⁶

General procedure followed using p-tolualdehyde and 2-fluoro-4-isocyano-1-methylbenzene. The crude material was subjected to column chromatography on silica, eluted with 0→1→2→4% MeOH:CH₂Cl₂, providing the title compound as a yellow solid (0.06 g, 43% yield) after further recrystallisation from CH₂Cl₂/hexane. (0.05 g, 37% yield). MP: 89-97 °C. ¹H NMR (DMSO-d₆, 500 MHz): δ 2.06 (3H, s), 2.30 (3H, s), 6.22 (1H, d, *J* 8.5), 6.28 (1H, d, *J* 12.0), 6.99 (1H, t, *J* 8.5), 7.03 (1H, dd, *J* 4.5, 6.5), 7.22 (2H, d, *J* 8.0), 7.93 (2H, d, *J* 8.0), 8.32 (1H, s), 8.39 (1H, d, *J* 7.0), 8.55–8.57 (1H, m). ¹³C NMR (DMSO-d₆, 125 MHz): δ 13.3 (d, *J* 2.5), 20.8, 100.0 (d, *J* 26.5), 108.8, 113.5 (d, *J* 17.5), 116.7, 126.6, 129.2, 130.2, 131.26, 132.3 (d, *J* 7.0), 137.4, 138.7, 144.9, 145.2 (d, *J* 10.0), 150.4, 161.4 (d, *J* 239.5). HRMS (ES-TOF) *m/z*: [M+H]⁺ Calcd. for C₂₀H₁₈FN₄ 333.1510, found 333.1518.



*2-Phenyl-N-(4-Chlorobenzyl)imidazo[1,2-a]pyrimidin-3-amine 99a.*⁷⁶

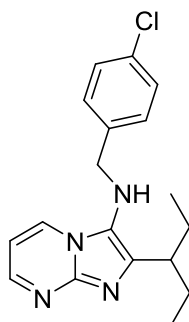
General procedure followed using benzaldehyde and Chloro-4-(isocyanomethyl) benzene. Flash column chromatography on basic alumina, eluted with 0→5→10→10→50 % ethyl acetate: petroleum ether yielded the product as a yellow amorphous solid (0.06 g, 46% yield). R_f 0.6 (1:1 ethyl acetate: petroleum ether). ¹H NMR (DMSO-d₆, 400 MHz): δ 4.02 (1H, s), 4.17 (2H, s), 6.80 (1H, dd, *J* 4.0, 7.0), 7.17–7.26 (4H, m), 7.34–7.40 (1H, m), 7.43–7.49 (2H, m), 8.03 (2H, d, *J* 7.5), 8.32 (1H, dd, *J* 2.0, 7.0), 8.40 (1H, dd, *J* 2.0, 4.0). ¹³C NMR (DMSO-d₆, 100 MHz): δ 51.7, 108.3, 123.8, 127.4, 128.1, 128.7, 128.8, 129.6, 130.2, 133.1, 133.6, 137.3, 137.4, 144.3, 149.6. HRMS (ES-TOF) *m/z*: [M+H]⁺ Calcd. for C₁₉H₁₆³⁵ClN₄ 335.1063, found 335.1079.



*2-(thiophen-2-yl)-N-(4-chlorobenzyl)imidazo[1,2-a]pyrimidin-3-amine 100a.*⁷⁶

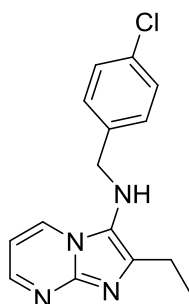
General procedure followed using thiophene-2-carboxaldehyde and 4-chlorobenzyl isocyanide. Successive recrystallisations from EtOAc/hexane, then CH₂Cl₂/hexane, provided the title compound as a dark yellow amorphous solid (0.08 g, 55% yield). ¹H NMR (DMSO-d₆, 400 MHz): δ 4.15 (2H, d, *J* 6.5), 5.46 (1H, t, *J* 6.5), 6.96 (1H, dd, *J* 4.0, 7.0), 7.17 (1H, dd, *J* 3.5, 5.0), 7.32–7.39 (4H, m), 7.58 (1H, dd, *J* 1.0, 5.0), 7.68 (1H, dd, *J* 1.0, 3.5), 8.43 (1H, dd, *J* 2.0, 4.0),

8.52 (1H, dd, J 2.0, 7.0). ^{13}C NMR (DMSO- d_6 , 100 MHz): δ 50.0, 108.0, 123.3, 124.5, 126.1, 127.8, 128.2, 130.1, 131.3, 131.7, 132.3, 136.7, 138.7, 143.6, 149.5; HRMS (ES-TOF) m/z : $[\text{M}+\text{Na}]^+$ Calcd. for $\text{C}_{17}\text{H}_{13}^{35}\text{ClN}_4\text{NaS}$ 363.0447, found 363.0446.



N-(4-Chlorobenzyl)-2-(2-ethylbutyl)imidazo[1,2-*a*]pyrimidin-3-amine **101a**.

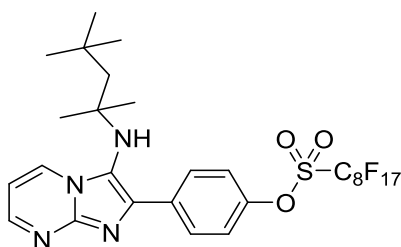
Prepared by the general procedure with 2-ethylbutyraldehyde and 4-chlorobenzyl isocyanide. Flash column chromatography on silica, eluted with 20→33→50→80% ethyl acetate: petroleum ether provided the title compound as a yellow amorphous solid (0.04 g, 27% yield). R_f 0.9 (1:1 ethyl acetate: petroleum ether). Purity (HPLC): 92%. ν_{max} (solid)/ cm^{-1} 3228, 3069, 2960, 2929, 2871, 1615, 1492, 1408, 1374, 1318. ^1H NMR (CDCl_3 , 400 MHz): δ 0.81 (6H, t, J 7.5), 1.72–1.90 (4H, m), 2.55–2.63 (1H, m), 3.45 (1H, s), 4.13 (2H, s), 6.75 (1H, dd, J 4.0, 7.0), 7.27–7.32 (4H, m), 8.17 (1H, dd, J 2.0, 7.0), 8.41 (1H, dd, J 2.0, 4.0). ^{13}C NMR (CDCl_3 , 100 MHz): δ 12.6, 27.9, 41.4, 53.0, 107.7, 124.7, 128.8, 129.6, 129.6, 133.5, 137.6, 143.9, 144.6, 148.4. HRMS (ES-TOF) m/z : $[\text{M}+\text{H}]^+$ Calcd. for $\text{C}_{18}\text{H}_{22}^{35}\text{ClN}_4$ 329.1533, found 329.1519.



N-(4-Chlorobenzyl)-2-propylimidazo[1,2-*a*]pyrimidin-3-amine **102a**.

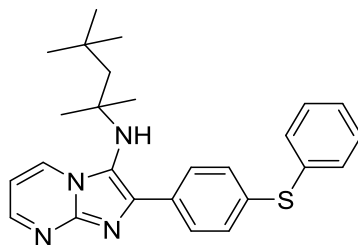
Prepared by the general procedure with propionaldehyde and 4-chlorobenzyl

isocyanide. Flash column chromatography on silica, eluted with 20→50→80% ethyl acetate: petroleum ether provided the title compound as a yellow amorphous solid (0.04 g, 32% yield). R_f 0.9 (4:1 ethyl acetate: petroleum ether). Purity (HPLC): 93%. ν_{\max} (solid)/ cm^{-1} 3228, 2932, 2875, 1654, 1614, 1596, 1519, 1491, 1462, 1408, 1340. ^1H NMR (CDCl_3 , 400 MHz): δ 1.33 (3H, t, J 7.5), 2.73 (2H, q, J 7.5), 3.54 (1H, s), 4.14 (2H, s), 6.80 (1H, dd, J 4.0, 7.0), 7.21–7.31 (4H, m), 8.26 (1H, dd, J 2.0, 7.0), 8.44 (1H, dd, J 2.0, 4.0). ^{13}C NMR (CDCl_3 , 100 MHz): δ 13.8, 20.4, 52.7, 108.0, 128.8, 129.2, 129.7, 129.8, 133.6, 137.6, 142.5, 148.7. HRMS (ES-TOF) m/z : $[\text{M}+\text{H}]^+$ Calcd. for $\text{C}_{15}\text{H}_{16}^{35}\text{ClN}_4$ 287.1063, found 287.1058.



4-(3-(2,4,4-Trimethylpentan-2-ylamino)imidazo[1,2-a]pyrimidin-2-yl)phenyl perfluorooctane-1-sulfonate **103a**.

Prepared by the general procedure with 4-Perfluorooctylsulfonyloxybenzaldehyde **65** and Walborsky's reagent. The crude material was purified by F-SPE followed by a further recrystallisation with CH_2Cl_2 /petroleum ether to provide the title compound as a yellow solid (0.21 g, 64% yield). MP: 147-152 °C. Purity (HPLC): 96%. ν_{\max} (solid)/ cm^{-1} 3256, 3088, 2955, 2923, 1609, 1592, 1556, 1525, 1504, 1494, 1420, 1411, 1370. ^1H NMR (CDCl_3 , 400 MHz): δ 1.01 (6H, s), 1.04 (9H, s), 1.59 (3H, s), 3.42 (1H, s), 6.93 (1H, dd, J 4.0, 7.0), 7.39 (2H, d, J 9.0), 8.15 (2H, d, J 9.0), 8.55 (1H, dd, J 2.0, 4.0), 8.61 (1H, dd, J 2.0, 7.0). ^{13}C NMR (CDCl_3 , 100 MHz): δ 29.1, 31.7, 31.7, 57.0, 61.0, 108.2, 121.2, 122.1, 130.3, 131.3, 135.1, 139.5, 145.1, 149.3, 150.0. HRMS (ES-TOF) m/z : $[\text{M}+\text{H}]^+$ Calcd. for $\text{C}_{28}\text{H}_{26}\text{F}_{17}\text{N}_4\text{O}_3\text{S}$ 821.1454, found 821.1486.



2-(4-(Phenylthio)phenyl)-N-(2,4,4-trimethylpentan-2-yl)imidazo[1,2-a]pyrimidin-3-amine **104a.**

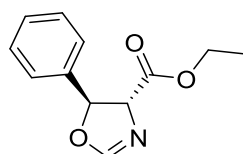
A mixture of **103a** (0.164 g, 0.2 mmol), thiophenol (0.021 g, 0.19 mmol), Cs₂CO₃ (0.130 g, 0.4 mmol) and Pd(dppf)Cl₂ (0.015 g, 0.02 mmol) in DMF was heated to 180 °C over 10 mins under microwave conditions. The reaction was maintained at this temperature for 10 mins and then cooled to room temperature. The mixture was then separated with ethyl acetate and water. The organic layer was dried over Mg₂SO₄ and concentrated at reduced pressure. The crude mixture was purified by F-SPE eluted with 80:20 MeOH: H₂O followed by Flash column chromatography on silica eluted with 1:1 ethyl acetate: petroleum ether to a yellow amorphous solid (0.04 g, 46% yield). R_f 0.8 (1:1 ethyl acetate: petroleum ether). ν_{\max} (solid)/cm⁻¹ 3252, 2954, 1611, 1477, 1366. ¹H NMR (CDCl₃, 400 MHz): δ 1.00 (6H, s), 1.05 (9H, s), 1.60 (2H, s), 3.25 (1H, s), 6.87 (1H, dd, *J* 4.0, 6.5), 7.27-7.41 (5H, m), 7.44 (2H, d, *J* 8.5), 7.91 (2H, d, *J* 8.5), 8.51-8.56 (2H, m). ¹³C NMR (CDCl₃, 100 MHz): δ 29.1, 31.8, 31.9, 57.0, 61.0, 107.9, 121.8, 127.1, 129.2, 129.3, 130.9, 131.0, 131.1, 133.6, 135.4, 135.7, 140.8, 145.2, 149.5. HRMS (ES-TOF) *m/z*: [M+H]⁺ Calcd. for C₂₆H₃₁N₄S 431.2269, found 431.2278.

7.3 Experimental Data for Chapter 4

General procedure of oxazoline synthesis

Batch - To a mixture of diisopropyl ethyl amine (0.026 mL, 0.1 mmol), aldehyde (1 mmol) and the catalyst mixture, copper(I) chloride (0.005 g, 0.05 mmol) and triphenyl phosphine (0.026 g, 0.1 mmol) in CH₂Cl₂, ethyl isocyanoacetate (0.109 ml, 1 mmol) was added. The reaction mixture was stirred at 40 °C for 2 h and then allowed to cool to room temperature. After the solvent was removed under reduced pressure the product was purified using flash column chromatography (petroleum ether/ethyl acetate, 1:1).

Flow – A stream of 1 M ethyl isocyanoacetate and 1 M diisopropylethylamine in CH₂Cl₂ was mixed with a stream of 1 M aldehyde in CH₂Cl₂ and was passed through a reactor heated to 60 °C over 20 mins. The solution was collected and concentrated at reduced pressure. The product was purified using flash column chromatography (petroleum ether: ethyl acetate, 1:1). Depending on the solubility of the aldehyde starting material a solvent system of 1:3 methanol: CH₂Cl₂ could be employed.

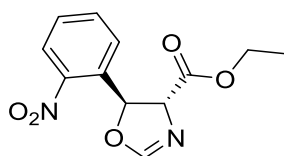


trans-4,5-Dihydro-5-phenyloxazoline-4-ethyl ester **122**⁹⁴

Batch: Benzaldehyde afforded the product as a colourless oil (0.43 g, 99% yield).

Flow: Benzaldehyde afforded the product as a colourless oil (0.32 g, 72% yield).

R_f = 0.9 (1:1 ethyl acetate: petroleum ether). ¹H NMR (CDCl₃, 400 MHz): δ 1.29 (3H, t, *J* 7.0), 4.20-4.29 (2H, m), 4.57 (1H, dd, *J* 2.0, 7.5), 5.66 (1H, d, *J* 7.5), 7.19 (1H, d, *J* 2.0), 7.35-7.47 (4H, m). ¹³C NMR (CDCl₃, 100 MHz): δ 13.5, 61.6, 75.5, 82.0, 125.8, 128.8, 129.0, 139.5, 156.3, 170.5. HRMS (ES-TOF) *m/z*: [M+H]⁺ Calcd. for C₁₂H₁₃NO₃ 220.0974, found 220.0963.

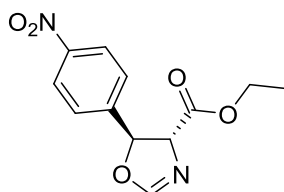


trans-4,5-Dihydro-5-(2-nitrophenyl)oxazoline-4-ethyl ester **123**

Batch: 2-Nitrobenzaldehyde afforded the product as a yellow oil (0.51 g, 97% yield).

Flow: 2-Nitrobenzaldehyde afforded the product as a yellow oil (0.34 g, 65% yield).

R_f 0.9 (1:1 ethyl acetate: petroleum ether). ^1H NMR (CDCl_3 , 400 MHz): δ 1.30 (3H, t, J 7.0), 4.21-4.35 (2H, m), 4.46 (1H, dd, J 2.0, 6.0), 6.23 (1H, d, J 6.0), 7.17 (1H, d, J 2.0), 7.48-7.55 (2H, m), 7.65-7.71 (1H, m), 8.10, (1H, d, J 8.0). ^{13}C NMR (CDCl_3 , 100 MHz): δ 14.1, 62.1, 71.3, 76.1, 128.5, 129.3, 129.3, 129.4, 134.5, 135.3, 146.2, 170.3. HRMS (ES-TOF) m/z : $[\text{M}+\text{H}]^+$ Calcd for $\text{C}_{12}\text{H}_{13}\text{N}_2\text{O}_5$ 265.0824, found 265.0832.

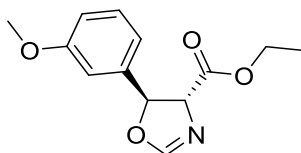


trans-4,5-Dihydro-5-(4-nitrophenyl)oxazoline-4-ethyl ester **124**⁹⁴

Batch: 4-Nitrobenzaldehyde afforded the product as a colourless oil (0.52 g, 99% yield).

Flow: 4-Nitrobenzaldehyde afforded the product as a colourless oil (0.32 g, 60% yield).

R_f 0.9 (1:1 ethyl acetate: petroleum ether). ^1H NMR (CDCl_3 , 400 MHz): δ 1.35 (3H, t, J 7.0), 4.28-4.36 (2H, m), 4.56 (1H, dd, J 2.0, 8.0), 5.78 (1H, d, J 8.0), 7.14 (1H, d, J 2.0), 7.52 (2H, d, J 8.5), 8.24 (2H, d, J 8.5). ^{13}C NMR (CDCl_3 , 100 MHz): δ 14.1, 62.4, 75.6, 80.8, 124.2, 126.2, 146.0, 148.0, 156.0, 169.8. HRMS (ES-TOF) m/z : $[\text{M}+\text{H}]^+$ Calcd. for $\text{C}_{12}\text{H}_{13}\text{N}_2\text{O}_5$ 265.0824, found 265.0814.

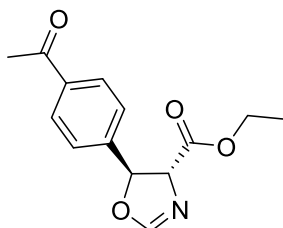


trans-4,5-Dihydro-5-(3-methoxyphenyl)oxazoline-4-ethyl ester **125**

Batch: 3-Methoxybenzaldehyde afforded the product as a colourless oil (0.41 g, 82% yield).

Flow: 3-Methoxybenzaldehyde afforded the product as a colourless oil (0.31 g, 62% yield).

R_f 0.8 (1:1 ethyl acetate: petroleum ether). $^1\text{H NMR}$ (CDCl_3 , 400 MHz): δ 1.31 (3H, t, J 7.0), 3.78 (3H, s), 4.22-4.31 (2H, m), 4.58 (1H, dd, J 2.0, 7.5), 5.63 (1H, d, J 7.5), 6.81-6.91 (3H, m), 7.08 (1H, d, J 2.0), 7.25-7.31 (1H, m). $^{13}\text{C NMR}$ (CDCl_3 , 100 MHz): δ 14.1, 55.2, 61.9, 75.4, 82.0, 111.0, 114.1, 117.6, 130.1, 140.6, 156.3, 160.0, 170.4. HRMS (ES-TOF) m/z : $[\text{M}+\text{H}]^+$ Calcd. for $\text{C}_{13}\text{H}_{16}\text{NO}_4$ 250.1079, found 250.1082.

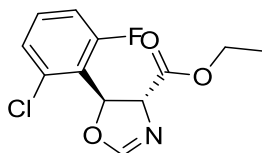


trans-4,5-Dihydro-5-(4-acetylphenyl)oxazoline-4-ethyl ester **126**

Batch: 4-Acetylbenzaldehyde afforded the product as a colourless oil (0.39 g, 74% yield).

Flow: 4-Acetylbenzaldehyde afforded the product as a colourless oil (0.33 g, 63% yield).

R_f 0.9 (1:1 ethyl acetate: petroleum ether). $^1\text{H NMR}$ (CDCl_3 , 400 MHz): δ 1.29 (3H, t, J 7.1), 2.55 (3H, s), 4.21-4.29 (2H, m), 4.52 (1H, dd, J 2.0, 8.0), 5.68 (1H, d, J 8.0), 7.08 (1H, d, J 2.0), 7.37 (2H, d, J 8.5), 7.93 (2H, d, J 8.5). $^{13}\text{C NMR}$ (CDCl_3 , 100 MHz): δ 14.1, 26.6, 62.1, 75.5, 81.4, 125.5, 129.9, 137.2, 144.0, 156.2, 170.1, 197.3. HRMS (ES-TOF) m/z : $[\text{M}+\text{H}]^+$ Calcd. for $\text{C}_{14}\text{H}_{16}\text{NO}_4$ 262.1079, found 262.1074.

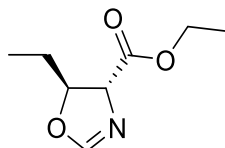


trans-4,5-Dihydro-5-(2-fluoro-6-chloro)oxazoline-4-ethyl ester **127**⁹⁴

Batch: 2-Fluoro-6-chlorobenzaldehyde afforded the product as a colourless oil (0.47 g, 87% yield)

Flow: 2-Fluoro-6-chlorobenzaldehyde afforded the product as a colourless oil (0.54 g, 99% yield).

R_f 0.8 (1:1 ethyl acetate: petroleum ether). ^1H NMR (CDCl_3 , 400 MHz): δ 1.26 (3H, t, J 7.0), 4.18-4.28 (2H, m), 4.76 (1H, dd, J 2.0, 8.5), 6.14 (1H, d, J 8.5), 6.97 (1H, d, J 2.0), 6.98-7.03 (1H, m), 7.17-7.30 (2H, m). ^{13}C NMR (CDCl_3 , 100 MHz): δ 14.0, 62.0, 73.3 (d, J 2.0), 75.9, 115.1 (d, J 22.5), 123.5 (d, J 14.5), 126.0 (d, J 3.5), 131.0 (d, J 10.0), 134.8 (d, J 5.5), 155.9, 162.0 (d, J 252.5), 170.1. HRMS (ES-TOF) m/z : $[\text{M}+\text{H}]^+$ Calcd. for $\text{C}_{12}\text{H}_{12}^{35}\text{ClFNO}_3$ 272.0490, found 272.0487.

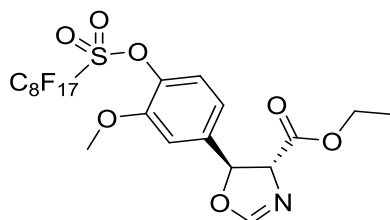


trans-4,5-Dihydro-5-ethyl oxazoline-4-ethyl ester **128**

Batch: Propanal afforded the product as a pale yellow oil (0.17 g, 49% yield).

Flow: Propanal afforded the product as a pale yellow oil (0.23 g, 67% yield).

R_f 0.9 (1:1 ethyl acetate: petroleum ether). ^1H NMR (CDCl_3 , 400 MHz): δ 1.01 (3H, t, J 7.0), 1.33 (3H, t, J 7.0), 1.75 (1H, p, J 7.0), 4.26 (2H, q, J 7.0), 4.32 (1H, d, J 7.0), 4.63 (1H, q, J 7.0), 6.96 (1H, s). ^{13}C NMR (CDCl_3 , 100 MHz): δ 8.8, 14.1, 27.9, 61.6, 71.8, 82.7, 133.6, 170.8. HRMS (ES-TOF) m/z : $[\text{M}+\text{H}]^+$ Calcd. for $\text{C}_8\text{H}_{14}\text{NO}_3$ 172.0974, found 172.0966.



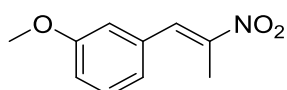
Ethyl 5-(3-methoxy-4-(perfluorooctylsulfonyloxy)phenyl)-trans-4,5-dihydrooxazole-4-carboxylate **129**

Prepared under continuous flow conditions stated above using 3-methoxy-4-perfluorooctylsulfonyloxybenzaldehyde as the starting material to provide the product as a sticky white solid (1.38 g, 92% yield). R_f 0.9 (1:1 ethyl acetate: petroleum ether). ν_{\max} (solid)/ cm^{-3} 2985, 2945, 2848, 2242, 1740, 1629, 1609, 1506, 1467, 1424, 1371, 1215. ^1H NMR (CDCl_3 , 400 MHz): δ 1.27 (3H, t, J 7.0), 3.87 (3H, s), 4.19-4.28 (2H, m), 4.53 (1H, dd, J 2.0, 8.0), 5.62 (1H, d, J 8.0), 6.89 (1H, dd, J 2.0, 8.5), 6.97 (1H, d, J 2.0), 7.06 (1H, d, J 2.0), 7.18 (1H, d, J 8.5). ^{13}C NMR (CDCl_3 , 100 MHz): δ 13.9, 56.2, 62.0, 75.5, 81.1, 110.2, 116.4, 122.7, 138.7, 140.7, 151.7, 156.0, 170.0. HRMS (ES-TOF) m/z : $[\text{M}+\text{H}]^+$ Calcd. for $\text{C}_{21}\text{H}_{15}\text{F}_{17}\text{NO}_7\text{S}$ 748.0298, found 748.0264.

7.4 Experimental Data for Chapter 5

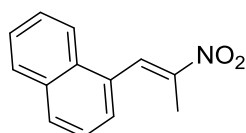
General synthesis of nitrostyrenes

To a stirred solution of NH_4OAc (2.76 g, 20 mmol) and nitroethane (0.712 mL, 10 mmol) in AcOH, aldehyde was added (10 mmol). The mixture was stirred at reflux until no starting material was present, shown by TLC. The solution was neutralised by addition of sat. aq. NaHCO_3 and the product separated with ethyl acetate. The aqueous layer was washed 3 times with ethyl acetate and the organic fractions were collected. The organic layer was dried over MgSO_4 and concentrated at reduced pressure. The residue was purified by flash column chromatography (petroleum ether: ethyl acetate 9:1) to afford the products described below.



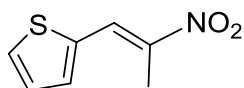
*(E)-1-Methoxy-3-(2-nitroprop-1-enyl)benzene 154*¹²³

3-Methoxybenzaldehyde afforded the product as a yellow solid (1.54 g, 82% yield). R_f 0.9 (1:9 ethyl acetate: petroleum ether). MP: 55-61 °C. ^1H NMR (CDCl_3 , 400 MHz): δ 2.48 (3H, s), 3.87 (3H, s), 6.95-7.06 (3H, m), 7.39 (1H, t, J 8.0), 8.08 (1H, s). ^{13}C NMR (CDCl_3 , 100 MHz): δ 14.1, 55.4, 115.4, 115.5, 122.3, 130.0, 133.4, 133.7, 148.0, 159.8. HRMS (ES-TOF) m/z . $[\text{M}+\text{H}]^+$ Calcd. for $\text{C}_{10}\text{H}_{12}\text{NO}_3$ 194.0817, found 194.0810.



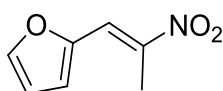
*(E)-1-(2-Nitroprop-1-enyl)naphthalene 155*¹²⁴

1-Naphthaldehyde afforded the product as a yellow solid (1.87 g, 88% yield). R_f 0.9 (1:9 ethyl acetate: petroleum ether). MP: 50-57 °C. ν_{max} (solid)/ cm^{-1} 3060, 1659, 1521, 1441, 1386, 1324. ^1H NMR (CDCl_3 , 400 MHz): δ 2.39 (3H, d, J 1.6), 7.45-7.63 (4H, m), 7.91-7.98 (3H, m), 8.66 (1H, s). ^{13}C NMR (CDCl_3 , 100 MHz): δ 14.2, 124.2, 125.2, 126.7, 127.2, 127.3, 128.9, 129.7, 128.9, 129.7, 130.3, 131.5, 131.9, 133.5, 149.3.



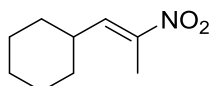
(E)-2-(2-Nitroprop-1-enyl)thiophene **156**¹²⁵

2-Thiophenecarboxaldehyde afforded the product as a brown solid (1.22 g, 72% yield). Rf 0.9. MP: 65-78 °C. ν_{\max} (solid)/ cm^{-1} 3111, 3093, 1644, 1494, 1494, 1419, 1364, 1331. ^1H NMR (CDCl_3 , 400 MHz): δ 2.53 (3H, s), 6.55 (1H, dd, J 2.0, 3.5), 6.80 (1H, d, J 3.5), 7.62 (1H, d, J 2.0) 7.79 (1H, s). ^{13}C NMR (CDCl_3 , 100 MHz): δ 13.9, 112.9, 119.4, 120.6, 144.3, 146.4, 147.9.



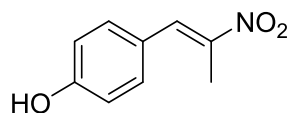
(E)-2-(2-Nitroprop-1-enyl)furan **157**¹²³

2-Furaldehyde afforded the product as a yellow solid (1.12 g, 73% yield). Rf 0.9. MP: 52-60 °C. ν_{\max} (solid)/ cm^{-1} 3130, 2931, 1798, 1654, 1508, 1384, 1308. ^1H NMR (CDCl_3 , 400 MHz): δ 2.57 (3H, s), 7.21 (1H, dd, J 3.5, 5.0), 7.45 (1H, d, J 3.5), 7.67 (1H, d, J 5.0), 8.32 (1H, s). ^{13}C NMR (CDCl_3 , 100 MHz): δ 14.2, 127.3, 128.2, 131.8, 134.8, 135.2, 144.4.



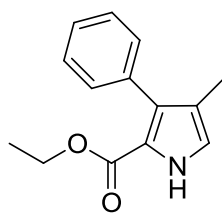
(E)-2-(2-Nitroprop-1-enyl)cyclohexane **158**¹²⁶

Cyclohexanecarboxaldehyde afforded the product as a brown oil (1.13 g, 67% yield). Rf 0.8. ν_{\max} (solid)/ cm^{-1} 2928, 2853, 1750, 1671, 1553, 1519, 1112. ^1H NMR (CDCl_3 , 400 MHz): δ 1.20-1.84 (10H, m), 2.19 (s, 3H), 2.23-2.34 (1H, m), 6.99 (1H, d, J 10.0). ^{13}C NMR (CDCl_3 , 100 MHz): 12.6, 25.3, 25.6, 31.7, 37.6, 140.9, 146.3. HRMS (ES-TOF) m/z : $[\text{M}+\text{H}]^+$ Calcd. for $\text{C}_9\text{H}_{15}\text{NO}_2$ 169.1103, found 169.1095.



(E)-4-(2-Nitroprop-1-enyl)phenol **165**¹²³

4-Hydroxybenzaldehyde afforded the product as a yellow solid (1.36 g, 67% yield). R_f 0.7 (1:4 ethyl acetate: petroleum ether). MP: 75-82 °C. ¹H NMR (CDCl₃, 400 MHz): δ 2.41 (3H, s), 6.90 (2H, d, *J* 8.5), 7.51 (2H, d, *J* 8.5), 8.05 (1H, s), 10.23 (1H, s). ¹³C NMR (CDCl₃, 100 MHz): δ 14.4, 116.4, 123.1, 133.4, 134.3, 145.0, 160.2. HRMS (ES-TOF) *m/z*: [M+H]⁺ Calcd. for C₉H₈NO₃ 178.504, found 178.0507.

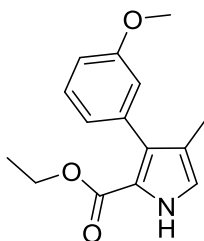


Ethyl 3-phenyl-4-methylpyrrole-2-carboxylate **150**¹¹³

Batch - To a solution of *trans*-β-methyl-β-nitrostyrene (0.17 g, 1.05 mmol) and ethyl isocynoacetate (0.11 mL, 1.2 mmol) in a mixture of 1:1 THF: *i*PrOH (5 ml) was added DBU and the resulting solution was allowed to stir at 50 °C for 3 h. The solution was poured into water and extracted with dichloromethane. The organic layer was dried over Na₂SO₄. The resulting oil was purified using flash column chromatography with dichloromethane as the eluent to provide the product as a yellow solid (0.18 g, 79 % yield).

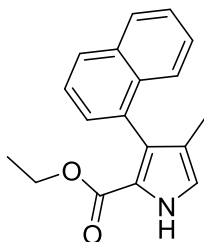
Flow – A stream of 0.5 M ethyl isocynoacetate and 0.5 M DBU in a mixture of 1:1 THF: *i*PrOH was mixed with a stream of 0.57 M in a mixture of 1:1 THF: *i*PrOH and passed through a reactor heated to 70 °C over 10 mins. The solution collected was concentrated at reduced pressure and the crude oil obtained was dissolved in dichloromethane. The mixture was washed with 10 mL of 1 M HCl followed by 10 mL brine and the organic layer was dried with magnesium sulphate and the solution was concentrated at reduced pressure. The crude oil was purified by column chromatography eluted with dichloromethane to yield a yellow solid (0.22 g, 96% yield). R_f 0.9 (CH₂Cl₂). Mp: 60-62 °C. ¹H NMR (CDCl₃, 400 MHz): δ 1.17 (3H, t, *J* 6.0), 2.02 (3H, s), 4.19 (2H, q, *J* 6.0), 6.80 (1H, s), 7.27-7.43 (5H, m), 8.94 (1H, s). ¹³C NMR (CDCl₃, 100 MHz): δ 10.6, 14.1, 60.1,

118.9, 120.3, 120.6, 120.9, 126.6, 127.4, 130.5, 135.0, 161.6. HRMS (ES-TOF) m/z : $[M+H]^+$ Calcd. for $C_{14}H_{16}NO_2$ 230.1181, found 230.1189.



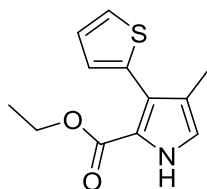
Ethyl 3-(3-methoxyphenyl)-4-methyl-1H-pyrrole-2-carboxylate 159

(E)-1-Methoxy-3-(2-nitroprop-1-enyl)benzene afforded the product as a yellow solid (0.22 g, 86% yield). R_f 0.9 (CH_2Cl_2). MP: 64-68 °C. Purity (HPLC): 83%. ν_{max} (solid)/ cm^{-1} 3318, 3064, 2980, 2938, 2870, 2834, 1670, 1610, 1581, 1563, 1519, 1477, 1465, 1379, 1312, 1288. 1H NMR ($CDCl_3$, 400 MHz): δ 1.17 (3H, t, J 7.0), 2.03 (3H, s), 3.85 (3H, s), 4.19 (2H, q, J 7.0), 6.80 (1H, s), 6.87-6.97 (3H, m), 7.30-7.34 (1H, m), 9.10 (1H, s). ^{13}C NMR ($CDCl_3$, 100 MHz): δ 10.6, 14.1, 55.2, 60.0, 112.3, 116.0, 119.0, 120.4, 120.5, 122.9, 128.4, 130.9, 136.1, 158.9, 161.2. HRMS (ES-TOF) m/z : $[M+H]^+$ Calcd. for $C_{15}H_{18}NO_3$ 260.1287, found 260.1292.



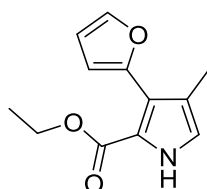
Ethyl 4-methyl-3-(naphthalen-1-yl)-1H-pyrrole-2-carboxylate 160

(E)-1-(2-Nitroprop-1-enyl)naphthalene afforded the product, a white solid (0.23 g, 83% yield). R_f 0.9 (CH_2Cl_2). MP: 58-64 °C. Purity (HPLC): 96%. ν_{max} (solid)/ cm^{-1} 3307, 3055, 2926, 2890, 2869, 1928, 1814, 1669, 1594, 1562, 1517, 1503, 1466, 1405, 1379, 1284, 1258. 1H NMR ($CDCl_3$, 400 MHz): δ 0.79 (3H, t, J 7.0), 1.98 (3H, s), 4.07 (2H, q, J 7.0), 6.94 (1H, s), 7.47-8.03 (7H, m), 10.06 (1H, s). ^{13}C NMR ($CDCl_3$, 100 MHz): δ 10.5, 13.6, 59.9, 120.5, 121.2, 121.5, 125.3, 125.5, 125.7, 126.5, 127.3, 127.9, 128.2, 129.1, 133.1, 133.6, 133.7. HRMS (ES-TOF) m/z : $[M+H]^+$ Calcd. for $C_{18}H_{18}NO_2$ 280.1338, found 280.1350.



Ethyl 4-methyl-3-(thiophen-2-yl)-1H-pyrrole-2-carboxylate 161

(E)-2-(2-Nitroprop-1-enyl)thiophene afforded the product as an oily red solid (0.18 g, 75% yield). Rf 0.8 (CH₂Cl₂). Purity (HPLC): 85%. ν_{max} (solid)/cm⁻¹ 3310, 2980, 2925, 2350, 1678, 1495, 1462, 1408, 1381. ¹H NMR (CDCl₃, 400 MHz): δ 1.24 (3H, t, *J* 7.0), 2.10 (3H, s), 4.24 (2H, q, *J* 7.0), 6.80 (1H, d, *J* 2.5), 7.08-7.13 (2H, m), 7.37 (1H, dd, *J* 1.5, 5.0), 8.98 (1H, s). ¹³C NMR (CDCl₃, 100 MHz): δ 11.0, 14.2, 60.2, 119.8, 120.3, 121.6, 123.1, 125.2, 126.4, 127.7, 135.1, 160.8. HRMS (ES-TOF) *m/z*: [M+Na]⁺ Calcd. for C₁₂H₁₃NNaO₂S 258.0565, found 258.0558.



Ethyl 3-(furan-2-yl)-4-methyl-1H-pyrrole-2-carboxylate 162

(E)-2-(2-Nitroprop-1-enyl)furan afforded the product as an oily red solid (0.17 g, 78% yield). Rf 0.8 (CH₂Cl₂). Purity (HPLC): 78%. ν_{max} (solid)/cm⁻¹ 3315, 3148, 2981, 2932, 2904, 1688, 1552, 1515, 1479, 1445, 1405, 1377, 1355, 1326, 1276, 1220. ¹H NMR (CDCl₃, 400 MHz): δ 1.33 (3H, t, *J* 7.0), 2.23 (3H, s), 4.32 (2H, q, *J* 7.0), 6.51 (1H, dd, *J* 2.0 and 3.5), 6.76 (1H, d, *J* 3.0), 6.81 (1H, d, *J* 3.5), 7.51 (1H, d, *J* 2.0), 9.02 (1H, s). ¹³C NMR (CDCl₃, 100 MHz): δ 11.7, 14.3, 60.4, 109.8, 110.8, 118.9, 120.0, 121.0, 141.3, 145.2, 148.6, 160.8. HRMS (ES-TOF) *m/z*: [M+H]⁺ Calcd. for C₁₂H₁₄NO₃ 220.0974, found 220.0978.

References

1. C. P. Adams and V. V. Brantner, *Health Aff.*, 2006, **25**, 420–428.
2. Switchbiotech (2011), Switchbiotech-Drug Discovery, <http://www.switchbiotech.com/drug%20discovery.html> [1st June 2011] .
3. M. Stocks, L. Alcaraz, and E. Griffen, *On Chemistry Series4, On Medicinal Chemistry*, Sci-Ink Ltd, 2007.
4. D. N. Breslauer, P. J. Lee, and L. P. Lee, *Mol. Biosyst.*, 2006, **2**, 97–112.
5. C. Wiles and P. Watts, *Expert Opin. Drug Discov.*, 2007, **2**, 1487–1503.
6. H. Salimi-moosavi, T. Tang, and D. J. Harrison, *J. Am. Chem. Soc.*, 1997, **119**, 8716–8717.
7. B. D. a Hook, W. Dohle, P. R. Hirst, M. Pickworth, M. B. Berry, and K. I. Booker-Milburn, *J. Org. Chem.*, 2005, **70**, 7558–7564.
8. R. D. Chambers, D. Holling, R. C. Spink, and G. Sandford, *Lab Chip*, 2001, **1**, 132–137.
9. R. E. Banks, B. E. Smart, and J. C. Tatlow, *Organofluorine Chemistry: Principles and Commercial Applications*, Springer, New York, 1994.
10. C. Wiles and P. Watts, *European J. Org. Chem.*, 2008, **2008**, 1655–1671.
11. M. Irfan, T. N. Glasnov, and C. O. Kappe, *Org. Lett.*, 2011, **13**, 984–987.
12. K. Terao, Y. Nishiyama, H. Tanimoto, T. Morimoto, M. Oelgemöller, and T. Morimoto, *J. Flow Chem.*, 2012, **2**, 73–76.
13. I. R. Baxendale, C. M. Griffiths-Jones, S. V Ley, and G. K. Tranmer, *Chemistry*, 2006, **12**, 4407–4416.
14. P. W. Miller, N. J. Long, A. J. de Mello, R. Vilar, J. Passchier, and A. Gee, *Chem. Commun.*, 2006, 546–8.
15. P. W. Miller, N. J. Long, A. J. de Mello, R. Vilar, H. Audrain, D. Bender, J. Passchier, and A. Gee, *Angew. Chem. Int. Ed. Engl.*, 2007, **46**, 2875–2878.
16. S. V. Ley, J. Sedelmeier, I. Baxendale, and M. Baumann, *Org. Lett.*, 2010, **12**, 3618–3621.
17. C. Amador, a. Gavriilidis, and P. Angeli, *Chem. Eng. J.*, 2004, **101**, 379–390.

18. D. L. Browne, B. J. Deadman, R. Ashe, I. R. Baxendale, and S. V. Ley, *Org. Process Res. Dev.*, 2011, **15**, 693–697.
19. W. Zhang, *Tetrahedron*, 2003, **59**, 4475–4489.
20. D. W. Zhu, *Synthesis*, 1993, 953–954.
21. I. T. Horvath and J. Rabai, *Science*, 1994, **266**, 72–75.
22. A. Studer, S. Hadida, R. Ferritto, S. Y. Kim, P. Jeger, P. Wipf, and D. P. Curran, *Science*, 1997, **275**, 823–826.
23. W. Zhang and D. P. Curran, *Tetrahedron*, 2006, **62**, 11837–11865.
24. D. P. Curran, J. A. Gladysz, and I. T. Horvath, *Handbook of Fluorous Chemistry*, Wiley-VCH Verlag GmbH and Co. KGaA, Weinheim, 2004.
25. D. P. Curran, S. Hadida, and M. He, *J. Org. Chem.*, 1997, **62**, 6714–6715.
26. Fluorous Technologies Inc. (2011), *Product Application Note: Fluorous solid phase extraction*, http://fluorous.com/download/FTI_Appnote_F-SPE.pdf [17th March 2011].
27. M. Matsugi and D. P. Curran, *Org. Lett.*, 2004, **6**, 2717–2720.
28. I. Ryu, S. Kreimerman, T. Niguma, S. Minakata, and M. Komatsu, *Tetrahedron Lett.*, 2001, **42**, 947–950.
29. C. del Pozo, A. I. Keller, T. Nagashima, and D. P. Curran, *Org. Lett.*, 2007, **9**, 4167–4170.
30. F. Millich, *Chem. Rev.*, 1972, **72**, 101–113.
31. I. Ugi, U. Fetzer, U. Eholzer, H. Knupfer, and K. Offerman, *Angew. Chemie*, 1965, **77**, 492–504.
32. V. R. Pinney (1999), Non-lethal low toxicity malodorous compositions composed of carrier fluid with malodorous compounds, PCT International Applications, 9965847 A2 19991223.
33. W. Lieke, *Justus Liebigs Ann. Chem.*, 1859, **112**, 316.
34. I. Ugi and R. Meyr, *Angew. Chemie*, 1958, **70**, 702–703.
35. G. M. A. Jr and E. M. Burgess, *J. Am. Chem. Soc.*, 1968, **90**, 4744–4745.
36. S. M. Creedon, H. K. Crowley, and D. G. McCarthy, 1998, **16**, 1015–1017.

37. E. M. Burgess, H. R. Penton, and E. A. Taylor, *J. Org. Chem.*, 1973, **38**, 26–31.
38. D. A. Claremon and B. T. Phillips, 1988, **29**, 2155–2158.
39. A. Porcheddu, G. Giacomelli, and M. Salaris, *J. Org. Chem.*, 2005, **70**, 2361–2363.
40. A. Strecker, *Liebigs Ann. Chem.*, 1850, **75**, 27.
41. M. Passerini and L. Simone, *Gazz. Chim. Ital.*, 1921, **51**, 126–129.
42. I. Ugi, R. Meyr, U. Fetzer, and C. Steinbruckner, *Angew. Chemie*, 1959, **71**, 386.
43. I. Ugi, W. Betz, U. Fetzer, and K. Offerman, *Chem. Ber.*, 1961, **94**, 89–90.
44. A. V Gulevich, A. G. Zhdanko, R. V. a Orru, and V. G. Nenajdenko, *Chem. Rev.*, 2010, **110**, 5235–5331.
45. T. D. Owens, G.-L. Araldi, R. F. Nutt, and J. E. Semple, *Tetrahedron Lett.*, 2001, **42**, 6271–6274.
46. D. Genin, R. Z. Andriamialisoa, N. Langlois, and Y. Langlois, *J. Org. Chem.*, 1987, **52**, 353–356.
47. Fluorous Technol. Inc., *Fluorous Tags*, <http://fluorous.com/fluorous-tags.php> [21st March 2011].
48. W. Zhang, *Org. Lett.*, 2003, **5**, 1011–1013.
49. C. H.-T. Chen and W. Zhang, *Org. Lett.*, 2003, **5**, 1015–1017.
50. S. Fustero, A. García Sancho, G. Chiva, J. F. Sanz-Cervera, C. del Pozo, and J. L. Aceña, *J. Org. Chem.*, 2006, **71**, 3299–3302.
51. M. Sani, L. Bruché, G. Chiva, S. Fustero, J. Piera, A. Volonterio, and M. Zanda, *Angew. Chem. Int. Ed. Engl.*, 2003, **42**, 2060–2063.
52. M. Sani, A. Volonterio, G. Chiva, S. Fustero, J. Piera, R. M. Sanchez, and M. Zanda, *Tetrahedron Lett.*, 2003, **44**, 7019–7022.
53. W. Zhang and Y. Lu, *Org. Lett.*, 2003, **5**, 2555–2558.
54. W. Zhang, Y. Lu, and C. H.-T. Chen, *Mol. Divers.*, 2003, **7**, 199–202.
55. B. Piqani and W. Zhang, *Beilstein J. Org. Chem.*, 2011, **7**, 1294–1298.

56. A. Kadam, S. Buckley, T. Dinh, R. Fitzgerald, and W. Zhang, *Synlett*, 2011, **2011**, 1608–1612.
57. S. Ding, M. Le-Nguyen, T. Xu, and W. Zhang, *Green Chem.*, 2011, **13**, 847.
58. A. Liu, H. Zhou, G. Su, W. Zhang, and B. Yan, *J. Comb. Chem.*, 2009, **11**, 1083–1093.
59. J. a. Soderquist, I. Rivera, and A. Negron, *J. Org. Chem.*, 1989, **54**, 4051–4055.
60. Organic Chemistry Portal (2004), Peterson Olefination, <http://www.organic-chemistry.org/namedreactions/peterson-olefination.shtml> [2nd May 2011].
61. J. M. Aizpurua and C. Palomo, *Synth. Commun.*, 1983, **13**, 745–752.
62. S. Fustero, V. Rodrigo, M. Sanchez-Rosello, J. F. Sanz-Cervera, J. Piera, A. Simon-Fuentes, and C. del Pozo, *Chem. A Eur. J.*, 2008, **14**, 7019–7029.
63. C. Hulme and Y.-S. Lee, *Mol. Divers*, 2008, 1–15.
64. C. Sablayrolles, G. H. Cros, J. J. C. Milhavet, E. Rechenq, J. Chapat, M. Boucard, J. J. Serrano, and J. H. M. J, 1984, **27**, 206–212.
65. D. R. Gehlert, A. Cippitelli, A. Thorsell, A. D. Lê, P. a Hipskind, C. Hamdouchi, J. Lu, E. J. Hembre, J. Cramer, M. Song, D. McKinzie, M. Morin, R. Ciccocioppo, and M. Heilig, *J. Neurosci. Off. J. Soc. Neurosci.*, 2007, **27**, 2718–2726.
66. G. Sachs, J. M. Shin, and C. W. Howden, *Aliment. Pharmacol. Ther.*, 2006, **23 Suppl 2**, 2–8.
67. F. Knoflach, U. Drescher, L. Scheurer, P. Malherbe, and H. Mohler, *J. Pharmacol. Exp. Ther.*, 1993, **266**, 385–391.
68. A. Linton, P. Kang, M. Ornelas, S. Kephart, Q. Hu, M. Pairish, Y. Jiang, and C. Guo, *J. Med. Chem.*, 2011, **54**, 7705–7712.
69. C. Blackburn, B. Guan, P. Fleming, K. Shiosaki, and S. Tsai, *Tetrahedron Lett.*, 1998, **39**, 3635–3638.
70. H. Bienayme and K. Bouzid, *Angew. Chemie Int. Ed.*, 1998, **37**, 2234–2237.
71. K. Groebke, L. Weber, and F. Mehlin, *Synlett*, 1998, **1998**, 661–663.

72. M. S. Jensen, R. S. Hoerrner, W. Li, D. P. Nelson, G. J. Javadi, P. G. Dormer, D. Cai, and R. D. Larsen, *J. Org. Chem.*, 2005, **70**, 6034–6039.
73. S. Carballares, M. M. Cifuentes, and G. a. Stephenson, *Tetrahedron Lett.*, 2007, **48**, 2041–2045.
74. M. J. Thompson, J. M. Hurst, and B. Chen, *Synlett*, 2008, **2008**, 3183–3187.
75. S. Guchhait and C. Madaan, *Synlett*, 2009, **2009**, 628–632.
76. P. Maydom, Thesis submitted for the completion of MChem degree, University of Sheffield, 2009.
77. M. Thompson, J. Hurst, and B. Chen, *Synlett*, 2008, **2008**, 3183–3187.
78. Y. Lu and W. Zhang, *QSAR Comb. Sci.*, 2004, **23**, 827–835.
79. R. Andreasch, *Monatsh.*, 1884, **5**, 33–46.
80. R. H. Wiley and L. L. Bennett, *Chem. Rev.*, 1948, **44**, 447–476.
81. S. Gabriel, *Ber.*, 1889, **22**, 1139–1154.
82. D. Armesto, M. J. Ortiz, and R. Perez-Ossorio, *Tetrahedron Lett.*, 1983, **24**, 1197–1200.
83. E. Vedejs and J. W. Grissom, *J. Am. Chem. Soc.*, 1988, **110**, 3238–3246.
84. K. Fukushima and T. Arai, *J. Antibiot. (Tokyo)*, 1983, **36**, 1613–1630.
85. H. Hinoo, T. Hattori, Y. Kimura, T. Yoshida, J. Shoji, and K. Hirooka, *J. Antibiot. (Tokyo)*, 1989, **42**, 1460–1464.
86. A. a. Tymiak, T. J. McCormick, and S. E. Unger, *J. Org. Chem.*, 1989, **54**, 1149–1157.
87. K. Matsumoto, Y. Ozaki, M. Suzuki, and M. Miyoshi, *Agric. Biol. Chem.*, 1976, **40**, 2045.
88. Y. Ito, M. Sawamura, and T. Hayashi, *J. Am. Chem. Soc.*, 1986, **108**, 6405–6406.
89. V. A. Soloshonok, A. D. Kacharov, D. V Avilov, K. Ishikawa, N. Nagashima, and T. Hayashi, *J. Org. Chem.*, 1997, **3263**, 3470–3479.
90. D. Hoppe and U. Schoellkopf, *Angew. Chem. Int. Ed. Engl.*, 1970, **9**, 300–301.

91. P. Kisanga, J. Verkade, and R. Schwesinger, *J. Org. Chem.*, 2000, **65**, 5431–5432.
92. P. Kisanga, J. G. Verkade, and P. Ilankumaran, *Tetrahedron Lett.*, 2001, **42**, 6263–6266.
93. T. Saegusa, Y. Ito, H. Kinoshita, and S. Tomita, *J. Org. Chem.*, 1971, **36**, 3316–3323.
94. D. Benito-Garagorri, V. Bocokić, and K. Kirchner, *Tetrahedron Lett.*, 2006, **47**, 8641–8644.
95. F. Bonati and M. Giovanni, *Gazz. Chim. Ital.*, 1973, **103**, 373–386.
96. T. Hayashi and M. Kumada, *Acc. Chem. Res.*, 1982, **15**, 395–401.
97. V. A. Soloshonok, A. D. Kaeharov, and T. Hayashi, *Tetrahedron*, 1996, **52**, 245–254.
98. V. A. Soloshonok and T. Hayashi, *Tetrahedron Lett.*, 1994, **35**, 2713–2716.
99. Y. Ito, M. Sawamura, M. Kobayashi, and T. Hayashi, *Tetrahedron Lett.*, 1988, **29**, 6321–6324.
100. W. Zhang, C. H. Chen, Y. Lu, and T. Nagashima, *Org. Lett.*, 2004, **6**, 1473–1476.
101. R. Allerton and W. G. Overend, *J. Chem. Soc.*, 1954, 3629–3632.
102. S. K. Nayak, *Synthesis*, 2000, **2000**, 1575–1578.
103. M. S. Shashidhar and M. V. Bhatt, *J. Chem. Soc. Chem. Commun.*, 1987, **9**, 654.
104. A. E. Green, V. Agouridas, and E. Deniau, *Tetrahedron Lett.*, 2013, **54**, 7078–7079.
105. J. A. Joule and K. Mills, *Heterocyclic Chemistry*, Blackwell Publishing Ltd, Chichester, Fifth edit., 2010.
106. C. T. Walsh, S. Garneau-Tsodikova, and A. R. Howard-Jones, *Nat. Prod. Rep.*, 2006, **23**, 517–531.
107. R. S. Gordee and T. R. Matthews, *Appl. Microbiol.*, 1969, **17**, 690–694.
108. S. C. Pan and F. L. Weisenborn, *J. Am. Chem. Soc.*, 1956, **80**, 4749–4750.

109. N. Ezaki, T. Shomura, M. Koyama, T. Niwa, M. Kojima, S. Inouye, T. Ito, and T. Niida, *J. Antibiot. (Tokyo)*, 1981, **34**, 1363–1365.
110. M. Suzuki, M. Miyoshi, and K. Matsumoto, *J. Org. Chem.*, 1974, **39**, 1980.
111. O. V Larionov and A. de Meijere, *Angew. Chem. Int. Ed. Engl.*, 2005, **44**, 5664–7.
112. A. V Lygin, O. V Larionov, V. S. Korotkov, and A. de Meijere, *Chemistry*, 2009, **15**, 227–236.
113. D. H. R. Barton and S. Z. Zard, *J. Chem. Soc. Chem. Commun.*, 1985, 1098–1100.
114. P. Kumar, S. Ghalasasi, R. C. Gupta, S. Deshpande, A. Mohanah, A. Chaudhari, C. Dutt, V. Chauthaiwale, and A. B. Mandhare, 2011.
115. H. Kawamura, M. Bougauchi, N. Ono, and K. Maruyama, *J. Chem. Soc. Chem. Commun.*, 1989, 1580–1581.
116. S. Fioravanti, L. Pellacani, and M. C. Vergari, *Org. Biomol. Chem.*, 2012, **10**, 524–528.
117. J. Boelle, R. Schneider, P. Gerardin, and B. Loubinoux, *Synthesis*, 1997, 1451–1456.
118. P. Mirtschink, S. N. Stehr, H. J. Pietzsch, R. Bergmann, J. Pietzsch, G. Wunderlich, A. C. Heintz, J. Kropp, H. Spies, W. Kraus, A. Deussen, and M. Walther, *Bioconjug. Chem.*, 2008, **19**, 97–108.
119. M. L. Kantam and P. Sreekanth, *Catal. Letters*, 1999, **57**, 227–231.
120. A. Alizadeh, M. M. Khodaei, and A. Eshghi, *J. Org. Chem.*, 2010, **75**, 8295–8298.
121. L. Rokhum and G. Bez, *Tetrahedron Lett.*, 2013, **54**, 5500–5504.
122. E. J. Jacobsen, L. S. Stelzer, K. L. Belonga, D. B. Carter, W. Bin Im, V. H. Sethy, A. H. Tang, P. F. Vonvoigtlander, and J. D. Petke, *J. Med. Chem.*, 1996, **3**, 3820–3836.
123. S. Yan, Y. Gao, R. Xing, Y. Shen, Y. Liu, P. Wu, and H. Wu, *Tetrahedron*, 2008, **64**, 6294–6299.
124. M. Vilches-Herrera, J. Miranda-Sepúlveda, M. Rebolledo-Fuentes, A. Fierro, S. Lühr, P. Iturriaga-Vasquez, B. K. Cassels, and M. Reyes-Parada, *Bioorg. Med. Chem.*, 2009, **17**, 2452–2460.

125. D. Angelov, J. O'Brien, and P. Kavanagh, *Drug Test. Anal.*, 2013, **5**, 145–149.
126. T. Le Gall, C. Mioskowski, and M. Leroux, *Tetrahedron: Asymmetry*, 2001, **12**, 1817–1823.

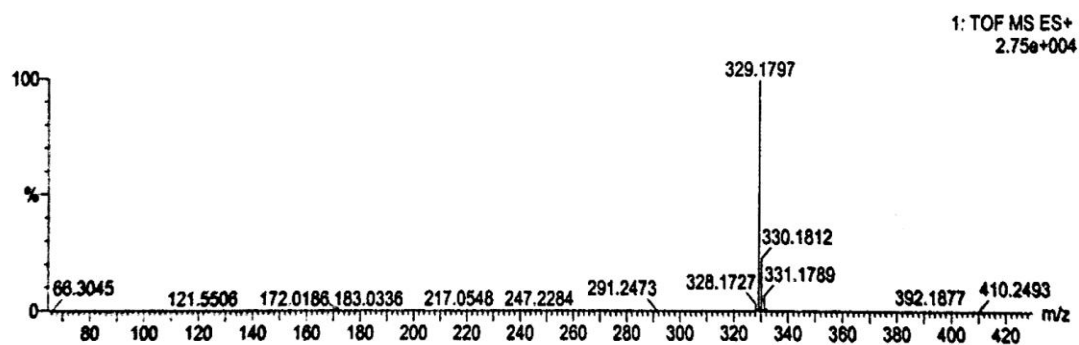
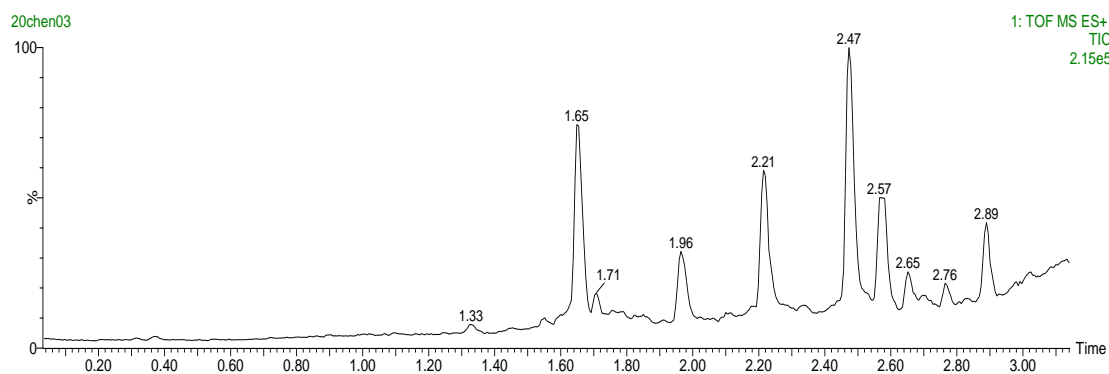
Supplementary Data

LCMS data chapter 3.....	178
NOE experimental data chapter 3.....	183

LC-MS data chapter 3

For cases in Table 7 where only a trace of the 2-amino product (**b** isomer) was detectable, its presence was confirmed by LC-MS.

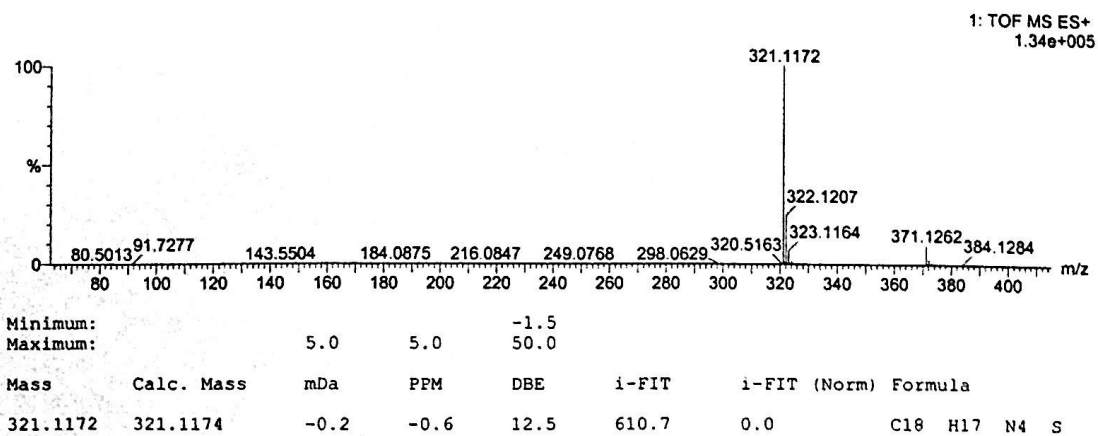
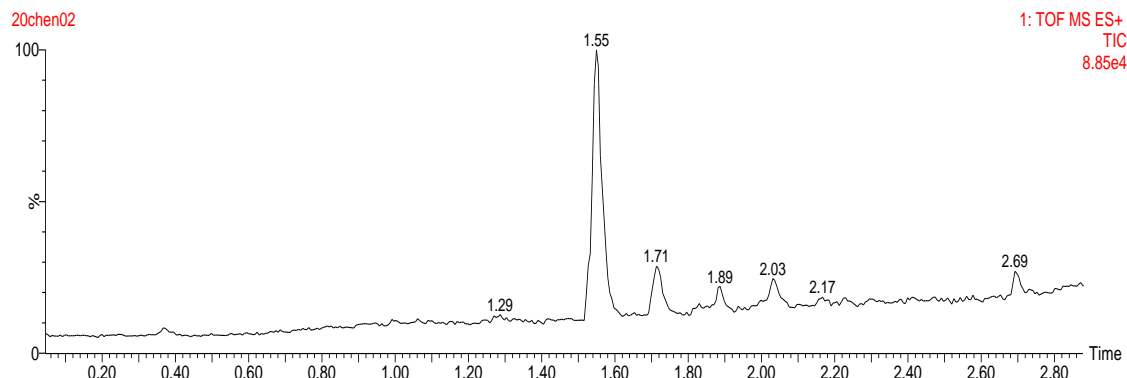
95b 3-(thiophen-2-yl)-*N*-(2,4,4-trimethylpentan-2-yl)imidazo[1,2-*a*]-pyrimidin-2-amine.



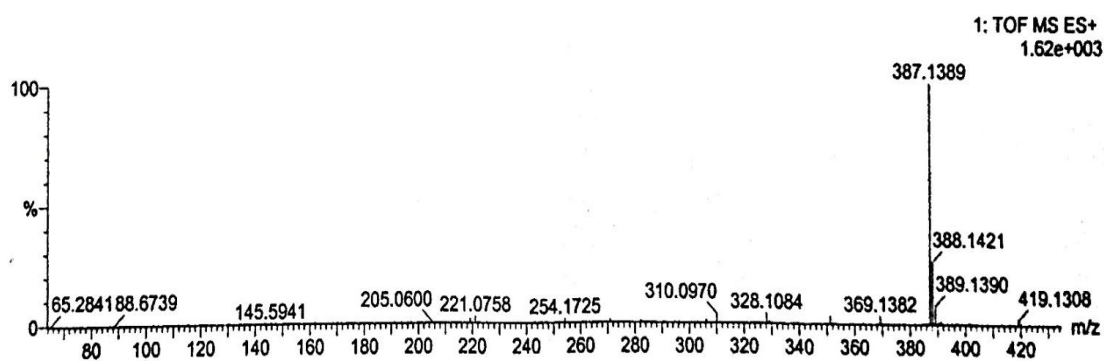
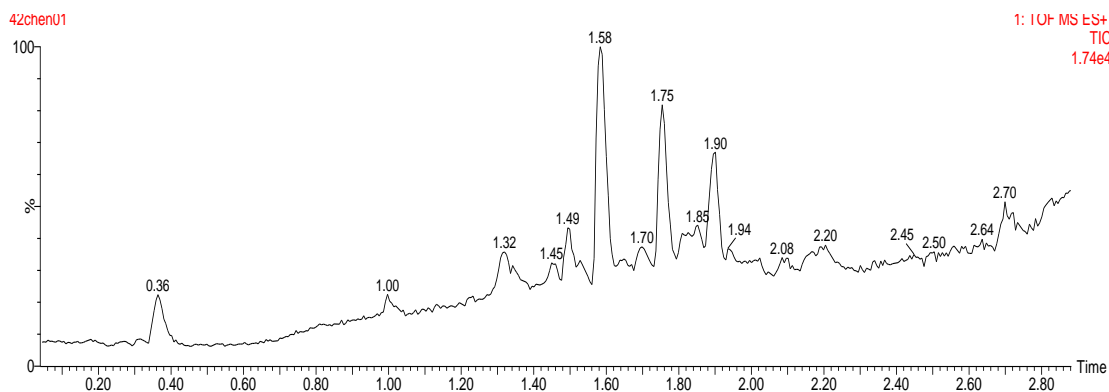
Minimum: -1.5
Maximum: 5.0 5.0 50.0

Mass	Calc. Mass	mDa	PPM	DBE	i-FIT	i-FIT (Norm)	Formula
329.1797	329.1800	-0.3	-0.9	8.5	422.1	0.0	C18 H25 N4 S

96b 3-phenyl-*N*-(2-(thiophen-2-yl)ethyl)imidazo[1,2-*a*]pyrimidin-2-amine



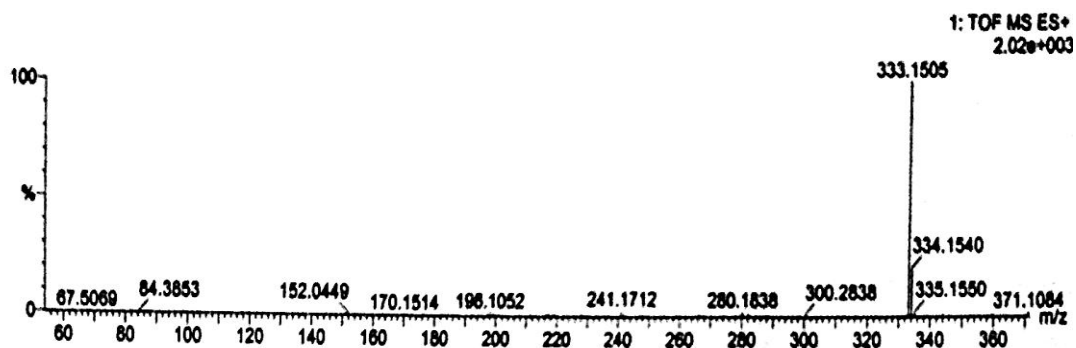
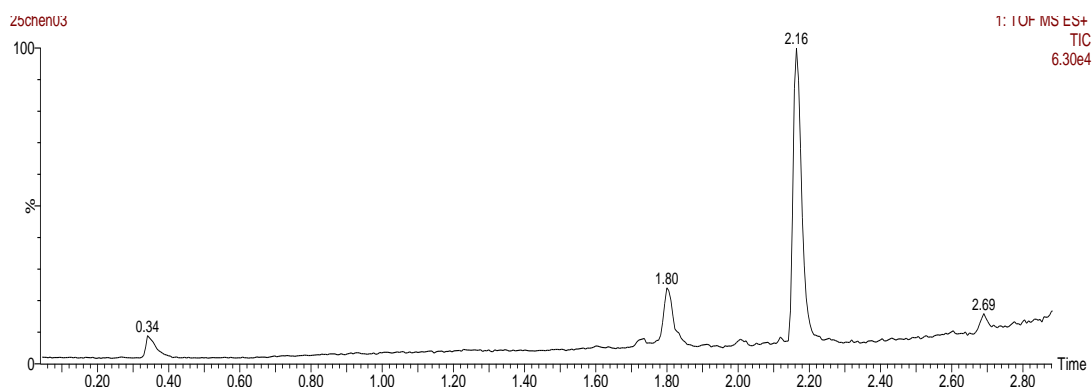
97b N-(2-(thiophen-2-yl)ethyl)-3-(4-(1*H*-pyrazol-1-yl)phenyl)imidazo[1,2-*a*]pyrimidin-2-amine



Minimum: -1.5
Maximum: 5.0 5.0 50.0

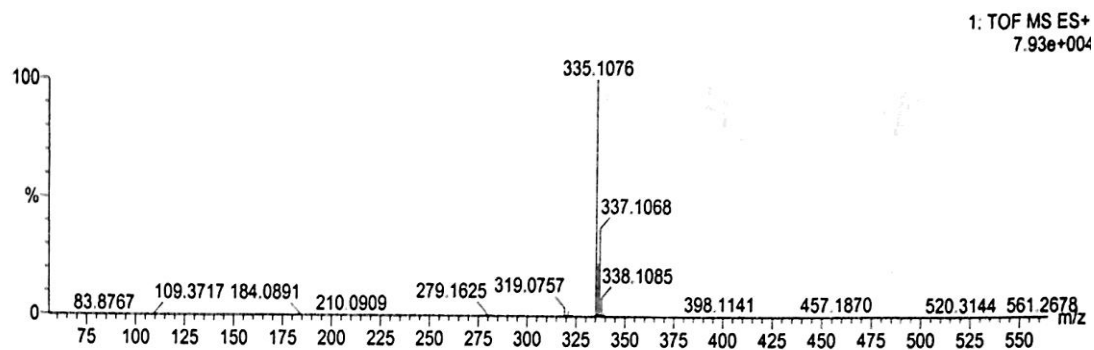
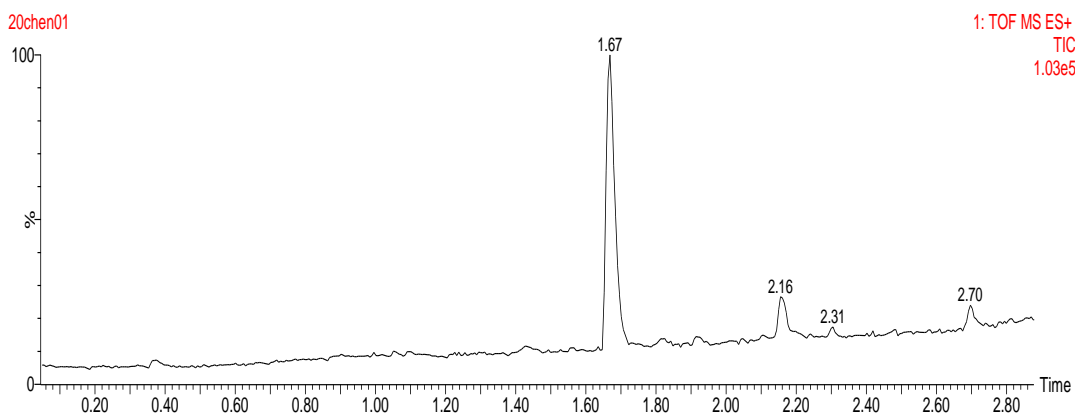
Mass	Calc. Mass	mDa	PPM	DBE	i-FIT	i-FIT (Norm)	Formula
387.1389	387.1392	-0.3	-0.8	15.5	101.4	0.0	C21 H19 N6 S

98b *N*-(3-fluoro-4-methylphenyl)-3-*p*-tolylimidazo[1,2-*a*]pyrimidin-2-amine



Mass	Calc. Mass	mDa	PPM	DBE	i-FIT	i-FIT (Norm)	Formula
333.1505	333.1516	-1.1	-3.3	13.5	109.9	0.0	C ₂₀ H ₁₈ N ₄ F

100b *N*-(4-chlorobenzyl)-3-phenylimidazo[1,2-*a*]pyrimidin-2-amine



Mass	Calc. Mass	mDa	PPM	DBE	i-FIT	i-FIT (Norm)	Formula
335.1076	335.1063	1.3	3.9	13.5	553.4	0.0	C19 H16 N4 Cl

Minimum: -1.5
Maximum: 50.0

NOE experimental data chapter 3

